Evaluation of corrosion performance for D-Gun sprayed T91 steel under simulated and actual bio-fuel fired boiler environment

A dissertation submitted
In partial fulfilment of requirements
for the degree of

Master of Engineering

in

Production Engineering

Submitted by

MANOJ KUMAR

Roll No.: 801585017

Under the Supervision of

Dr. DEEPA MUDGAL

Assistant Professor

DEPARTMENT OF MECHANICAL ENGINEERING

THAPAR UNIVERSITY

PATIALA (PB), INDIA, 147004
JULY, 2017

Certificate

I hereby declare that the work done in this thesis entitled "**Evaluation of corrosion performance for D-Gun sprayed T91 steel under simulated and actual bio-fuel fired boiler environment** " submitted towards partial fulfillment of requirement for award of degree of **Master of Engineering** in **Production Engineering, Thapar University, Patiala,** is an authentic record of the work carried out by me under the supervision and guidance of **Dr. Deepa Mudgal,** Assistant Professor, Mechanical Engineering Department, Thapar University, Patiala during 2015 to 2017. No part of the matter embodied in this report has been submitted to any other university or institute for the award of any degree.

Dated: 18-08-2017

Manoj Kumar

Registration No.: 801585017

This is to certify that above declaration made by the student concerned is correct to the best of our knowledge and belief.

Dr. Deepa Mudgal

Assistant Professor

Mechanical Engineering Department

Thapar University, Patiala

Dedicated to

TO

MY PARENTS

Who taught

me

everything

Acknowledgement

I would like to express my deepest sense of gratitude and a very sincere thanks to my guide **Dr. Deepa Mudgal**, Assistant Professor, Mechanical Engineering Department, Thapar University, Patiala for her sincere and invaluable guidance and full support which helped me in the accomplishment of this dissertation report in present form. Her dynamic and diligent enthusiasm has been highly instrumental in keeping my spirits high. Her flawless and forthright suggestions blended with an innate intelligent application have crowned my task with success. I would like to thank **Dr. S.K. Mohapatra,** Head of Mechanical Engineering Department and all the faculty member and staff members of Mechanical Engineering Department, Thapar University, Patiala for their boundless support.

I am also very thankful to my friends for their support during completion of the work.

Manoj Kumar

Registration No.: 801585017

ME (Production Engineering)

Abstract

The Purpose of this work is to enhance the corrosion characteristics of coatings. 80Cr_3C_2–20NiCr and 88WC-12Co coatings were deposited on T91 boiler tube steel by the process of Detonation Gun. Oxidation and hot corrosion studies were conducted on bare and D-Gun coated T91steel specimens after applying molten salt (40Na_2SO_4, 40K_2SO_4, 10NaCl & 10 KCl) at 800°C under 50 cyclic conditions respectively. Each cycle consisted 1 hour of heating in the tubular furnace and 20 min of cooling of the sample at room temerature.After each cycle weight of each sample was measured by using digital weighing balance. Study under actual biofuel fired boiler enviroment. (SEM) scanning electron microscopy, (EDS) energy dispersive spectroscopy and X ray diffraction (XRD) techniques were used to analyze the corrosion product. The bare steel specimen experienced higher weight gain, which may be due to the occurrence of unprotective Fe_2O_3 dominated oxide scales. The WC-Co also does not performed well as it delaminates from the substrate when exposed to higher temperature after few cycles, The Cr_3C_2–NiCr coating was found to be more protective than WC-Co the coating. The phases disclosed in the oxide scale of the coated specimens were mainly oxides and spinels of nickel and chromium, which are reported to be protective against corrosion.

Key words: Corrosion, D-gun, WC-Co, Cr_3C_2-NiCr coating.

International Conference

Kumar, M.; Mudgal, D.(2017). "High temperature corrosion evaluation of bare and coated T91 steel under simulated bio-fuel fired boiler environment" Paper presented in 5th International Conference on Advancement in Engineering and Technology, March 24-25, 2017 at Bhai Gurdas Institute of Engineering and Technology , Sangrur (Punjab) India.

Table of Contents

Lists of Figures

List of Tables

Nomenclature

Symbols

µ	Micro
°C	Degree Celsius

Acronyms

D-gun	Detonation gun
SEI	Secondary electron image
EDS	Energy dispersive spectroscopy
HVOF	High velocity oxy fuel
K_p	Parabolic rate constant
Min	Minimum
SEM	scanning electron microscopy
Wt.%	Weight percent
XRD	X-ray diffraction
h	hours
RE	Rare earth
VHN	Vickers hardness number
CLA	Centre line average
CPC	calcium phosphate ceramic
mpy	milli inches per year

Chapter 1

Introduction

Nowadays attention has been more focused on necessity of more amount of clean energy sources because of the reduction in non-renewable energy supplies and severe environmental constraints. Hence, the attention has been more focussed towards the use of renewable source of energy such as biomass instead fossil fuels with the highest worldwide potential (Armesto *et al.* 2002). The use of biomass fuel in place of fossil fuels is widely promoted in order to reduce emissions of the greenhouse gas CO_2. The design of biomass-fuelled boilers is more complex than those of coal and oil fuelled boilers due to the increased risk of fouling and corrosion on the heat transfer surfaces. The fuel characteristics of biomass are very different from those common fossil fuels, including moisture content, ash content, calorific value, and alkali/alkaline earth metal content, etc. compared to coal, biomass fuels usually have much higher potassium (K) concentration and moisture content, as well as a lower sulphur component (Shao *et al.* 2012).Presence of salt species such as potassium, sodium ,chlorine and sulphur while burning of bio-fuel causes the early damaging of components used in the boiler in fireside areas.

In India, where the production of rice is very high such as Haryana and Punjab, rice husk is fired boilers are become more popular. This is because of the extensive availability of rice husk that too free of cost. In fact, using rice husk as fuel can save too high transportation cost also in these areas. As, husk is present everywhere in these areas. Rice husk fired boilers have ability to produce 5MW to 50MW of electricity. It can substantially decreases the cost of boiler operation. Not in Indian, but in many part of the world, rice husk has been used as the major source of energy for producing electricity.

Despite so many advantage of using bio-fuel instead of fossil fuel. Some major problems were encountered during the working of rice husk fired boiler. One of the major problem which is generally faced by boilers is due to the release of many salt species. During burning of husk, many salt species mainly consisting of potassium, sulphur, chlorine, calcium, silicon etc were produces. These salt species got deposited on the surface of the components used at fireside. These boilers are usually operated at very high temperature that can be as high as 750°C. At this high temperature the components used in the boilers formed a protective oxide layer on its surface. When the salt species combined with the protective oxide, it dissolves the

oxide thereby leaving the component unprotective. This is known as hot corrosion. Due to this hot corrosion, the components get damage very soon. This leads to the need for replacing the components very soon. Such problem occurred due to corrosion causes unwanted shutdown, repair and maintenance. Some time causes accidents also. To overcome this problem, the material used in the boilers wither can be replaced by different alloys or a coating can be deposited on these components which can help in saving the material for longer hours thereby increasing the life of the components.

Thermal spray coating technology is becoming very popular for depositing metallic, ceramic and cermet coating on various different materials. Plasma spray, HVOF, Detonation gun and cold spray techniques are used to deposit coating in high temperature areas such as gas turbines, low temperature areas having hard particles or corrosive salts such as hydro turbines. Detonation gun is one of the technology which deposit coating with low porosity and high bond strength.

It is also well-known that ferritic and austenitic steels are generally used in boilers. Hence, in the present study, ferritic steel T91 has been selected for the experimentation. Oxidation and hot corrosion studies were carried out to compare the bare, Cr_3C_2-NiCr and WC-Co coated T91 steel. Coating was deposited using Detonation gun technique. To validate the results, the samples were also exposed to actual husk fired boiler environment.

Chapter 2

Literature Review

2.1 Introduction

Boilers are particularly designed to produce steam or heat water by burning fuels. Fossil fuels are widely used in these boilers to generate energy. The energy in the form of steam so produce will further used to generate electricity. However, now a days use of biomass as auxiliary fuel has been adopted in many countries. The first cause is the generation of green house gases while burning fossil fuels. Another reason is to find the alternative to non-renewable source of energy. Biomass is a renewable source of energy. Hence, biomass fuels such as wood, husk etc has been used as auxiliary fuel in boilers. It was reported that the use of rice husk as a source fuel for electric power can give extensive savings to the cooperatives of rice. Its feasibility is fundamentally linked to the ability to internalize the environmental benefits provided by it (Oliveira *et al.* 2012). There are many another advantages also of using rice as fuel. Coal demands the material handling and transportation which is more difficult than using husk (Yadav & Singh 2011). In the rice production industry, rice husk is an important by product. There is worldwide a production of 700 million tons/yr of rice-related waste, such as straw, shells, and stalk. The fuel potential of rice husk alone is near 80 million tons/yr worldwide, corresponding to an energy potential of 1.2 × 109 GJ (Skrifvars *et al.*2005).

However burning of biomass fuel in boilers creates lot of other problems. The major technical challenges associated with biomass co-firing include (Baxter 2005):

1. Ash Deposition
2. Pollutant Formation
3. Fuel Conversion
4. Fuel Preparation, Storage and Delivery
5. Formation of Striated Flows.
6. Impacts on SCR Systems
7. Fly Ash Utilization
8. Corrosion

2.2 Corrosion in biomass fuel fired boiler

In recent years, there has been a deviation from burning fossil fuels to biomass Europe, Sweden and USA in order to reduce CO emission (Henderson *et al.* 2000). However, it was opined that burning of biomass fuel such as wood etc leads to severe corrosion problem. The burning of 100% wood as bio-fuel lead to the formation of alkali chlorides instead of sulphur compounds which creates more corrosive environment. (Henderson *et al.* 2006) also studied the composition of biomass fuels. It was reported that biomass contains very high amount of alkali chlorides and alkali metals along with very little amount of sulphur. (Baxter *et al.*1998) reported the amount of chlorine, potassium and silica produces during burning of different type of fuel. From figure 2.1 and figure 2.2. It is evident that burning of rice husk emits maximum amount of silica and chloride among all the fuel. Whereas burning of almond hull produces maximum amount of potassium as shown in figure 2.3. The alkali metals of potassium are of major concern which is present in the form of KOH and KCl which released during the combustion in the form of gas. These alkali metals condense on the tubes and causes fouling which lead to the corrosion as these alkali metals and chlorides have low melting points. Also during combustion of biomass fuel, the alkali chloride particles deposited on the metallic surfaces by transported in the form of vapour phase and thus damages the protective oxide (Cha & Spiegel 2004).

Various methods were proposed to increase the efficiency of these boilers. One of them is by adding ammonium sulphate when the fuel was burning. To check the effect of adding ammonium sulphate a study was carried out in waste fired boiler in Ha¨ndelo¨ ,Sweden. One ferritic and one austenitic steel was chosen for studies. 30% of household waste and 50–70% industrial waste was burnt in the boiler. It was found that the deposits formed in the boiler contains large quantity of Cl and K along with Calcium, sulphur and sodium. Significant reduction in formation of chloride were observed after adding ammonium sulphate. Few more studies were reported by (Viklund *et al* 2009, 2010). They tested some nickel based alloys along with austenitic and ferritic steel in a waste-to-energy plant. The test were conducted in 100% wood-based bio-fuels (i.e. not co-firing with fossil fuels). It was reported that the tube at these power stations were replaced after every 20,000 h of usage.

Steels such as 13CrMo44, Super 304 and HCM12A showed unacceptably high rate of corrosion when metal mass measurements were carried out. The corrosion attack for low alloy steels was evident by the development of mixed metal oxides/metal chloride scales. However, high alloyed steels and nickel based alloys showed much better corrosion

resistance due to the formation of chromium rich oxide but these alloys also experiences localized pitting corrosion. (Viklund *et al.*2010). Table 2.1 shows presence of salt deposits using different fuel.

Table 2.1 Salts produce while burning Auxiliary Fuels

Type of fuel	Typical salt deposits	References
Waste	$ZnCl_2$,$PbCl_2$,KCl,NaCl	(Smith *et al.*2001) (Spiegel *et al.*2000)
Straw	KCl K_2SO_4	(Montgomery *et al.* 2000)
Wood	KCl,K_2SO_4,NaCl,Na_2SO_4	(Henderson *et al.*2000)
Residual oil	Na_2SO_4,V_2O_5	(Luthra *et al.* 1982)
Coal	Na_2SO_4,K_2SO_4,$(Na\ K)_2Fe(SO4)_3$	(Reichel 1988) (Viswanathan *et al.* 2006)

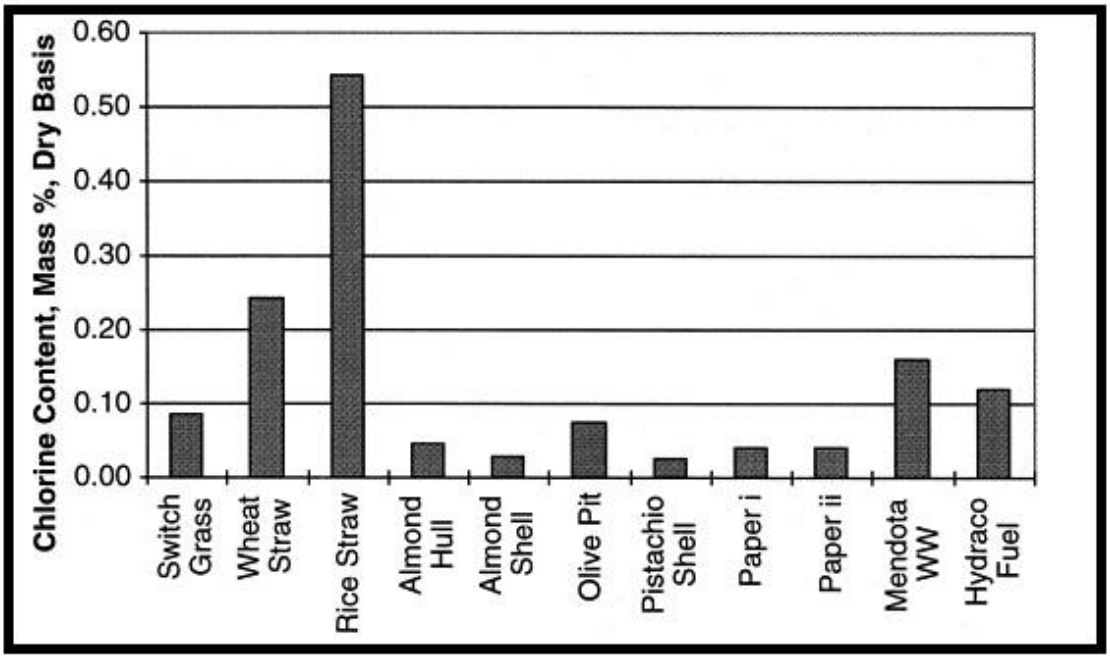

Figure 2.1 Chlorine concentration as a function of fuel type for the fuels used (Baxter *et al.*1998)

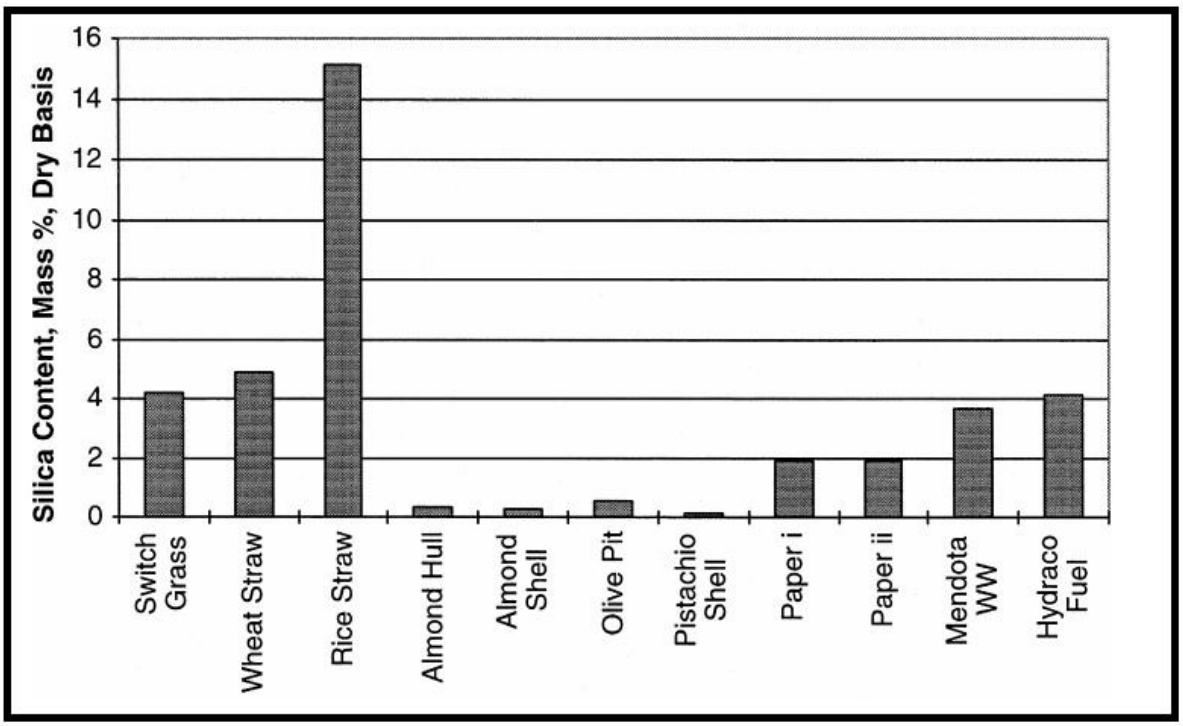

Figure 2.2 Silica concentration as a function of fuel type for the fuels used (Baxter *et al.*1998)

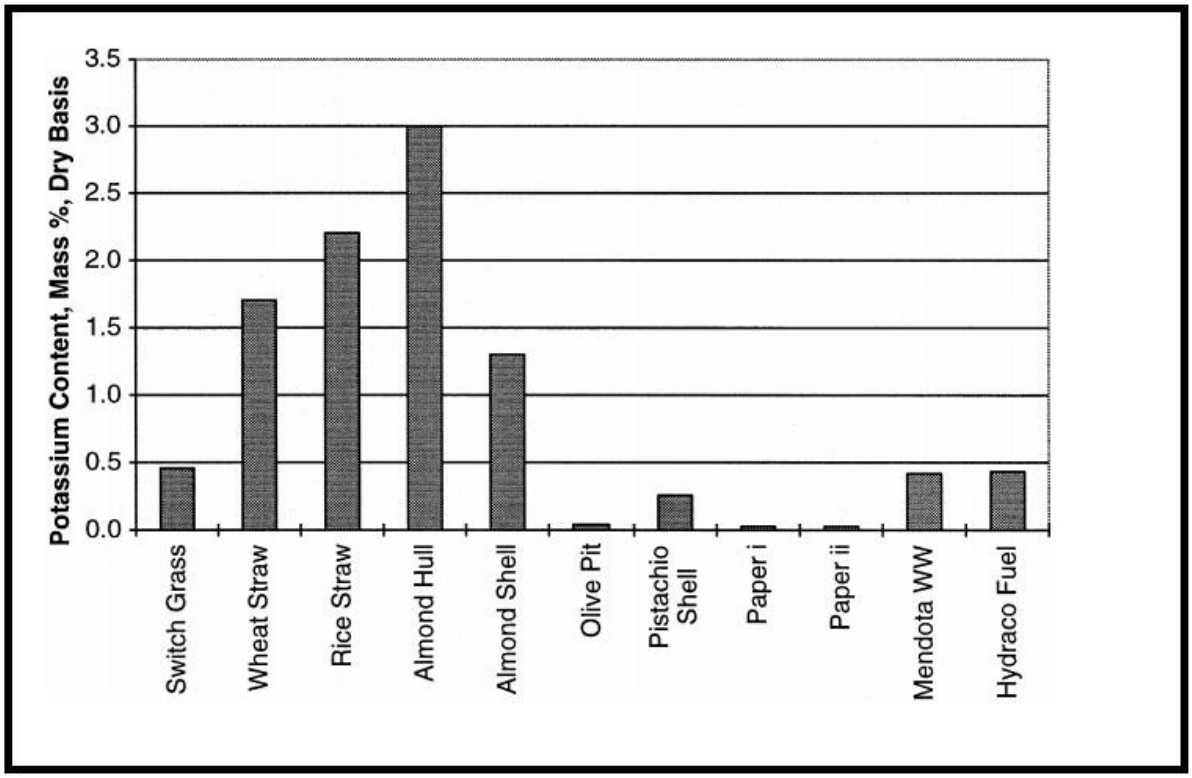

Figure 2.3 Potassium concentration as a function of fuel type for the fuels used (Baxter *et al.*1998)

2.3 Steels used in boilers

Ferritic steels which contains molybdenum and chromium are well renowned for their good mechanical properties combining high temperature strength with high thermal fatigue life, as well as with good thermal conductivity, weldability, resistance to corrosion and (Laverde *et al.* 2004). For higher temperatures work austenitic steels and Ni-based alloys are needed. Depending on the corrosives of the coal used, higher Cr steels or clad steels are used in boilers. Advanced austenitic stainless steels are used for as super and reheater tubing are up to temperatures 650 °C and possibly 750 °C. The materials with higher strength are needed for upper water walls of boilers with steam pressure of above 24 MPa (3400 psi). (Viswanathan *et al.*2001).These materials show excellent strength at higher temperatures. (Benjamin 1970). Both high temperature strength and economy must be considered in the selection of materials. **(**Masuyama 2001). Steels are alloys of iron and carbon, typically with one or more alloying elements are added to improve some properties of the of the material according to the need of purpose (Chattopadhyay 2004). Thus, basically all of the materials which are used in the repair of pressure parts of boilers fall into this classification. Some high temperature, corrosion resistant alloys of nickel and chromium with less than 50% iron are not, directly speaking, steels, but are still occasionally used. Further, steels are divided into two subcategories: ferritic steels and austenitic steels, depending on the arrangement of atoms with in the solid (French 1992). Tungsten strengthened ferritic steels 12Cr-0.4Mo-2W-V-Nb-Cu and 2.25Cr-1.6W-V-Nb have been approved by the ASME Boiler and Pressure Vessels Code Committee for use in Section construction, nominate as T23 and T122. A steel tube install in field test in service along with comparative materials in the tertiary super heater and secondary reheater of a 156 MW utility power boiler has been conducted since April 1993. The tubes were removed after the test to confirm and check their material properties of material and corrosion/steam oxidation behaviours after 1-year, 3-year, 6-year, and 10-year periods of service. The tensile strength of the steels showed no noticeable change during service (Komai *et al.* 2005).

2.4 Factors affecting corrosion problems

Corrosion of furnace-wall panel tubes with fireside metal temperatures of 500-600°F (260-316°C) in refuse-fired boilers is frequently localized, occurring above the fuel feed points, along sides, or in corners of the furnace. The severity of the corrosion' generally increases with increasing proximity to the flame zone. The corrosion kinetics are usually linear, with the corrosion rate showing little tendency to decrease with the passage of time. Corrosion rates .increase rapidly with increasing tube metal temperatures (Miller *et al.*1972). Strong correlation of wastage problems with a number of boiler operating conditions. Conditions that aggravate the problems include: (a) refuse fuel rich in PVC plastics and, hence, in organic chlorides (b) higher fuel values and higher gas temperatures (c) higher tube temperatures and waterside deposition which interferes with heat removal (d) flame impingement and stratification of air flow (e) frequent and thorough fireside deposit and scale removal Several approaches have been taken to ameliorate the furnace-wall corrosion problems: (a) covering the wall with silicon carbide (b) controlling the fuel chemistry (e.g. burning a mixture of coal and refuse) (c) lowering the steam pressure and thereby lowering the saturation and tube-metal temperatures (d) decreasing the amount of flame contact with the furnace wall Each of these ameliorative actions costs a penalty in terms of unit operating load, efficiency, and flexibility. Maximum steam temperatures and pressures, and boiler efficiencies are limited by the danger of corrosion (Daniel *et al*.1986) Today biomass contributes about 15 to 18% of this demand. On Average, in the industrialized countries biomass contributes some 10 to 15% to the total energy being supplies, but in developing countries the demand of biomass is as high as one-fifth to one-third (Khan *et al.* 2009)

2.5 Thermal spray coatings

2.5.1 Thermal spraying

Thermal spraying is the most adaptable techniques use for the coating of materials that is used to secure materials from adhesive wear, abrasive wear, erosive wear and corrosion **(**Herman 2000) . Commonly, any metal which does not vaporize, breakdown or disperse on heating, can be used for thermal spraying. Therefore a huge class of non metallic and metallic materials alloys, metals and polymers can be deposited by this technique. **(**Chawla *et al.* 2011)

2.5.2 Advantages of thermal spray processes

- As Compare to other coating like painting, applying film, thermal spraying gives more duration protection and long lasting (upto 35-45 years).
- Thermal spraying gives huge bond strength (above 10,000 psi) which is more times greater than properties of other coatings applied for providing corrosion conservation.
- Thermal spray process treat the low level of porosity of coatings (< 1%) .slight porosity gives an good base for applying paint coatings for example for providing decorative features.
- As anticorrosion safety term depends upon thickness of coating applied the selection of various variants of applying is available.

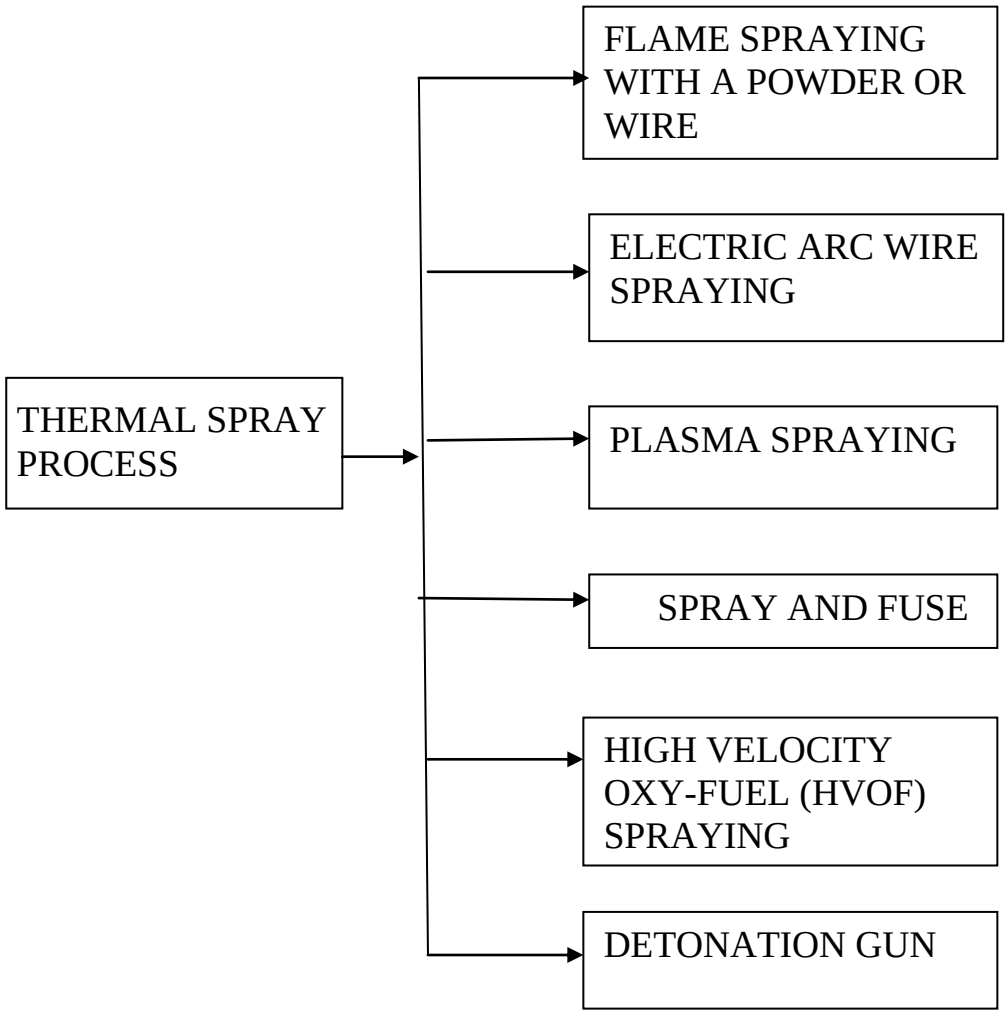

Figure 2.4 Types of Thermal spray technique

2.5.2.1 Flame spraying with a powder or wire

It is an coating process that consists of a heat source and the coating material in a powder or wire form which is melted into very small droplets and deposited onto surfaces with high velocity (Le Page 2016). Oxy-fuel flame is used for Flame spraying gun for the thermal spraying. Action and safety are guaranteed through a gas mixture system using the injector principle. The following fuel gases can be used: propane, acetylene, (for zinc and plastic powders) and For cooling purpose hydrogen in combination oxygen as well as compressed air used. (Herman *et al.* 2000).

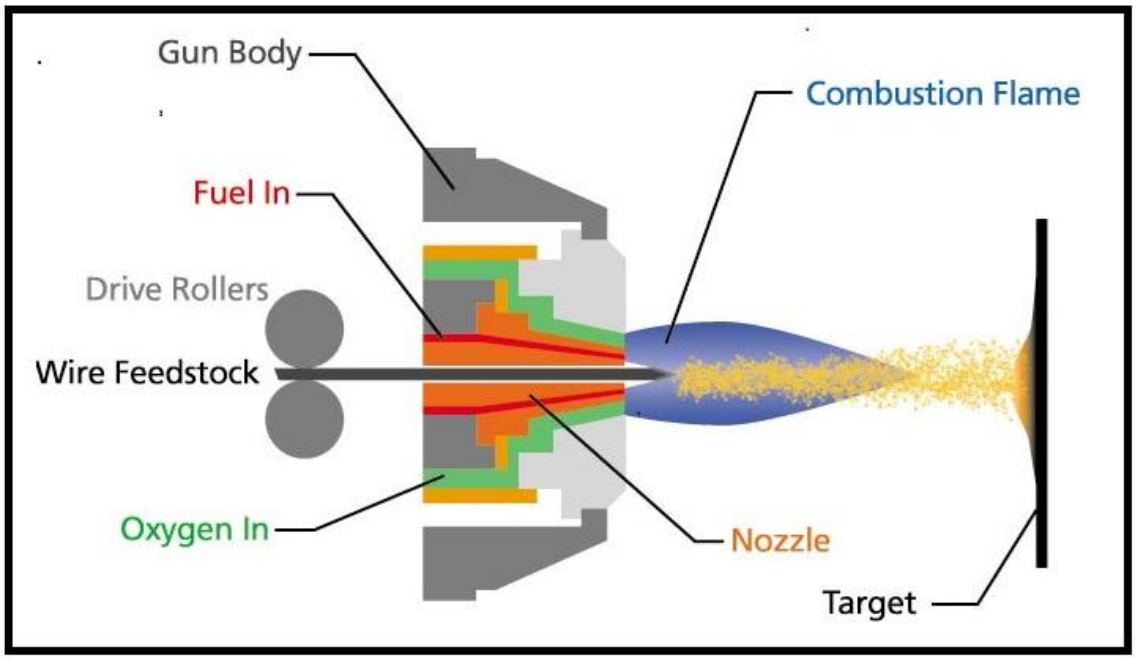

Figure 2.5 Schematic of the flame spraying with powder or wire (web reference 2)

2.5.2.2 Electric arc wire spraying

A high velocity arc spray apparatus includes a transferred-arc-plasma torch assembly which forms a transferred-arc column. A metal feedstock is fed into the transferred-arc column at an angle such that no portion of the metal feedstock is closer to the transferred-arc-plasma torch assembly than the leading edge of the metal feedstock in the feeding direction. A power source is coupled to both the metal feedstock and transferred-arc-plasma torch assembly for creating an electrical potential difference between the metal feedstock and the transferred torch assembly. **(**Marantz *et al.*1995) Inert gas, preferably nitrogen, is supplied to the arc spray gun such that the mass ratio of the wire feed rate to the gas feed rate is preferably between about 0.07 and about 0.11. **(**Kaiser *et al.*1994)

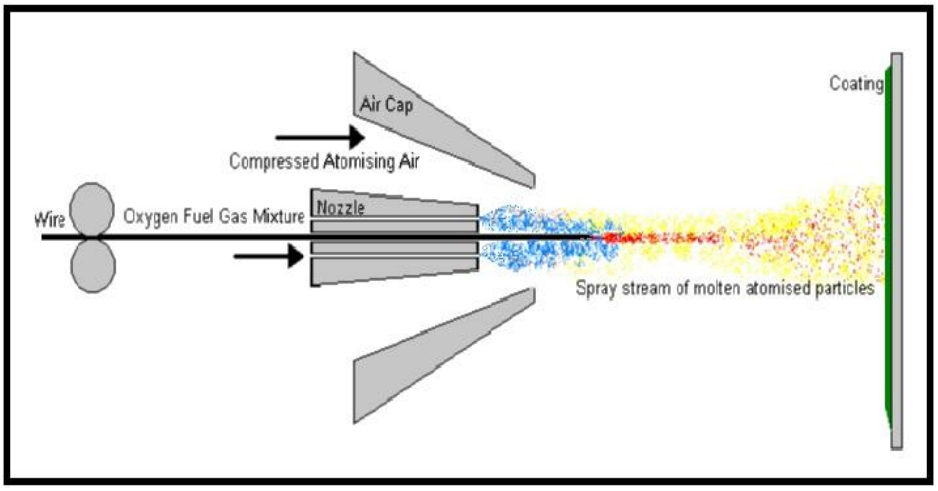

Figure 2.6 schematic of electric arc wire spraying process. (Web reference 1)

2.5.2.3 Plasma Spraying

Plasma Spraying plasma spraying technique, the molten material is sprayed onto a surface to be coated. Powdered material is infused into a high temperature plasma flame to be continuously heated and accelerated to a greater velocity. This process is generally used to apply a thin coating. Special consideration are taken to retain the original structure of CPC (Calcium phosphate ceramic) particles. This study focused on plasma spraying induced changes in material property of commercial coatings. Major plasma spraying influenced changes can be observed in all analysed coatings, like phase composition, crystal structure and specific surface area. Starting particle of the materials affected the phase transformations. (Radin 1992) The flattening, solidifying, layering to form the coatings following formation of splats are some latest developments that can be seen in the area of production of plasma sprayed finely structured coatings. (Fauchais 2004)

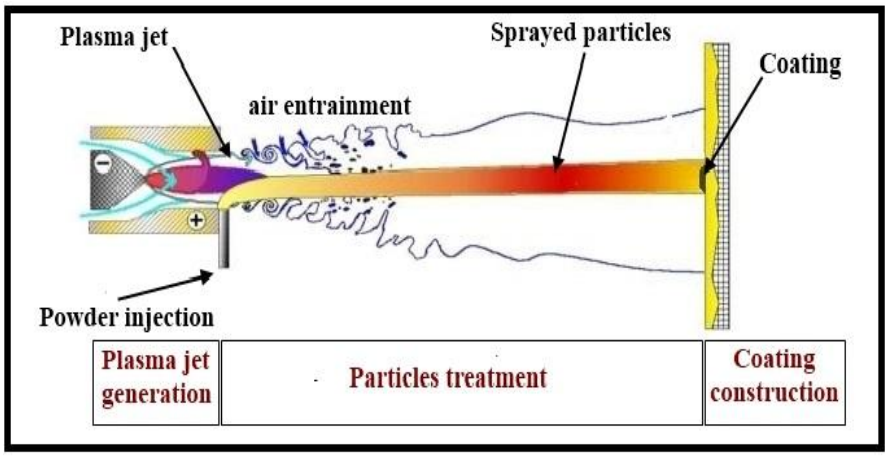

Figure 2.7 Schematic of the plasma spraying process (Web reference 3)

2.5.2.4 Spray and Fuse process

The materials that undergo spray and fuse coating are an example of self fluxing materials i.e, oxygen reacts with the constituting elements to form low density oxides which improve the density and bonding by floating to the surface. Commonly, nickel or cobalt-base alloys that use boron, phosphorus, or silicon, (either individually or in addition to another such element, , as melting-point depressants) and fluxing agents are used. Depending on its composition, the alloys are fused at high temperatures of around 1010 to 1175 degree Celsius. In order to make certain that the coating is clean and well-bonded, reducing atmosphere flames are most commonly used. Micro structural development of these coatings before and after fusing treatment is discussed to identify the precipitates in the coatings (Kim *et al*. 2003)

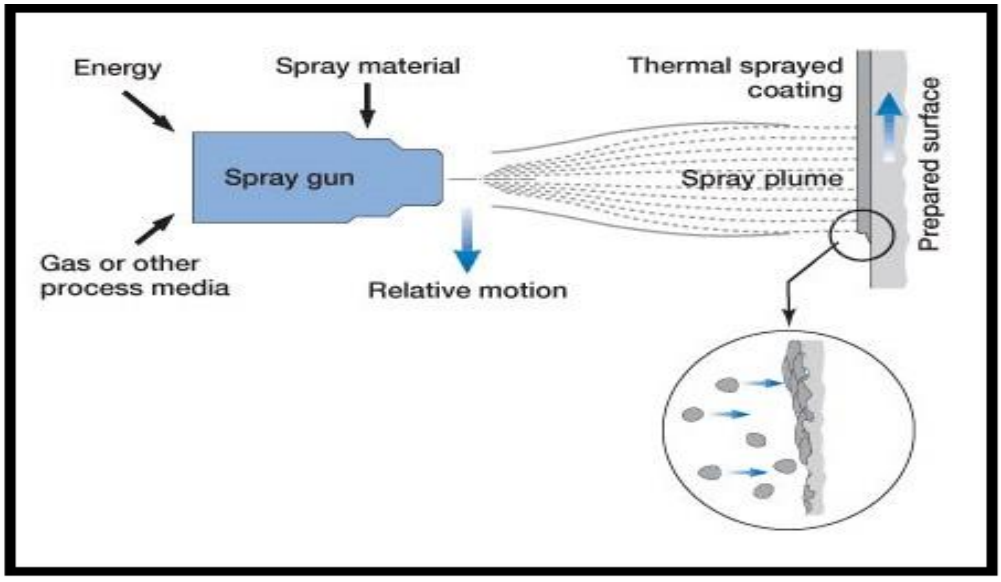

Figure 2.8 Schematic of spray and fuse coating process (web reference 4)

2.5.2.5 High velocity oxy-fuel spraying

High Velocity Oxy Fuel Spray (H.V.O.F) systems are relatively new modifications from the thermal spray industry. Improved powder particle heating and melting characteristics and supersonic spray velocities are combined in the HVOF process propylene, hydrogen, acetylene, propane, MAPP and various other fuel gases can be used. The pistol, powder feeder and operator interface can be observed as some latest advancements in this field. The result is a high quality, compact and easy to use HVOF system. One additional advantage of this technique is the low porosity coating and high bond strength. HVOF coatings have very low porosity, increased hardness, high abrasive resistance, good wear resistance

accompanying a strong ability to resist high-temperature corrosion resistance. The purpose here is to summarize the performance of such systems.(Sidhu *et al*. 2005)

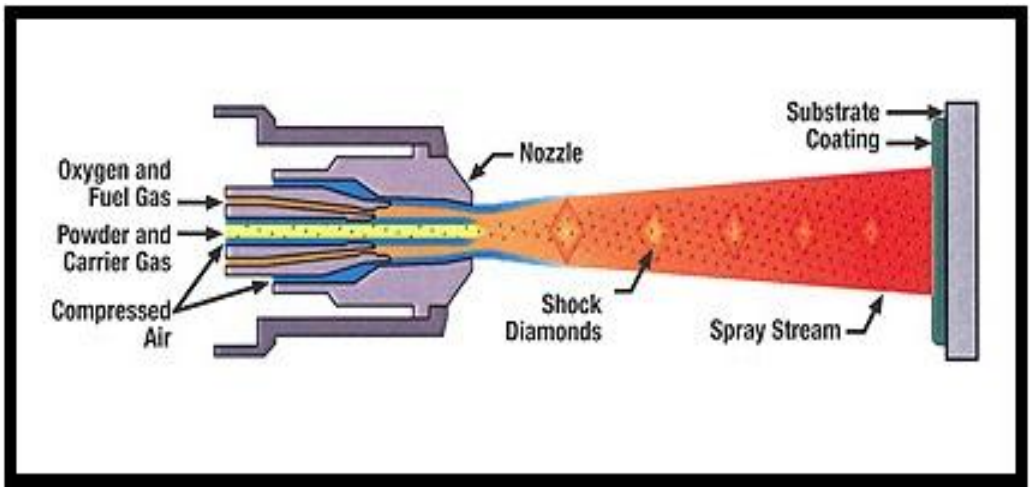

Figure 2.9 schematic of HVOF process (Web reference 5)

2.5.2.6 Detonation Gun (D-Gun)

The Detonation gun basically consists of a long water cooled barrel with inlet valves for gases and powder. Oxygen and fuel like, acetylene which is most commonly used, is fed into the barrel along with a charge of powder. The detonation resulting from the spark used to ignite the gas mixture, heats and accelerates the powder to a supersonic velocity down the barrel. Detonation gun (D-gun) spraying has proved to be one of the promising thermal spray technology for high quality wear resistant coatings. Of all the ceramic materials that can be D-gun-sprayed, WC is the most widely used and these coatings have already gained immense industrial favour for diverse applications. A precise knowledge of the influence of spraying process parameters on the coating characteristics and properties (porosity, adherence, roughness, hardness, etc.) are the prerequisites in the use of D-gun-sprayed WC–Co coating as protection against aggressive environment. In this article, structure, including surface roughness, XRD patterns and porosity, as well as adhesion strength, hardness, and fracture toughness of D-gun-sprayed WC–Co coatings as a function of spraying are presented in the experimental results (Saravanan *et al*. 2004)

Figure 2.10. Schematic of Detonation Gun process

2.6 Types of carbide coatings (Riabkina *et al*. 2001)

- Tungsten Carbide/Cobalt
- Tungsten Carbide/Cobalt/Chromium
- Chrome Carbide/Nickel-Chrome
- Tungsten Carbide/Nickel-Chrome

2.7 Advantage of Carbide Coatings (Deshpande *et al*.1994)

- High hardness, durability and toughness
- Corrosion resistance and wear
- Fretting Resistance
- Anti-galling properties
- Long Lasting Traction Surface
- Abrasion and Erosion resistance
- Fretting Resistance

2.8 Optical Microscopy for Surface Microstructure

The microstructure of the T91 steel samples, after polishing and etching with marble's reagent (Marble's Reagent = Distilled Water 50 ml, HCl 50 ml & Copper sulphate (CuSO4) 10 grams immersion or swab, etch for a few seconds) is shown in Figure 2.10 Oxidation Study of T91 Boiler Steel.

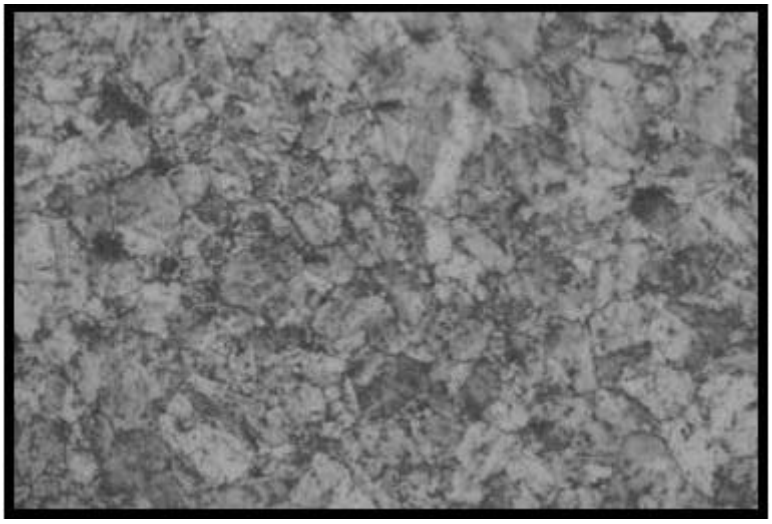

Figure 2.11 Microstructure of T91 steel (Gond *et al.* 2010)

The microstructure of T91 steel revealed ferritic structure i.e. the white spot which is seen in microstructure is ferrite and the rest is other phase. The microstructure which was found to consist of white ferrite and the rest is other phase. (Gond *et al.* 2010)

Table 2.2 Different type of thermal spray techniques with its characteristic

Types of system	Exit spray temperature (C)	Particle Impact Velocity(m/s)	Oxide content (%)	Porosity (%)	Adhesion (Bond strength)	Relative Process Cost
Detonation gun	3000	500-1200	small	0.1-3	Extremely high	Low
HVOF	2500-3100	500-800	Moderate	1-10	Very high	High
Plasma spraying	5500-8300	200-600	Moderate to course	1-10	Very high	Moderate
Wire arc	4000-6000	240	Moderate to high	10-20	High	Moderate
Flame spraying	2500-3000	30-180	High	10-30	Low	Moderate

2.9 Literature gap and Objective of work

2.9.1 Literature gap

The Aim of this work is to check the corrosion characteristics of the steel and to enhance the corrosion resistance by providing the protective coating on the surface. From the above study it can be seen that it may worthwhile to apply coatings on the heat facing steels parts so as to provide protection from aggressive environment at high temperatures. So in present work bare, Cr_3C_2-NiCr coated steel and WC-Co coated steel have been subjected to oxidation in air and simulated bio-fuel fired boiler environment (Na_2SO_4, NaCl ,K_2SO_4 and KCl) at 800°C for 50 hour (1hour of heating and 20 min cooling at room temperature) under cyclic condition in laboratory. These steel were coated by detonation gun process. All these coated alloys were subjected to corrosion test in air as well as under molten salt environments at 800°C for 50 cycles. The molten salt environment selected in the present study may simulate the environment present in the bio-fuel fired environment (Uusitalo *et al.* 2103). Moreover, the cyclic tests also provide useful information regarding the adhesion of the coatings and the spalling tendency of the oxide scale formed on the surface particularly at high temperature in catastrophic atmosphere. Therefore, the present research work is anticipate to make a detailed investigation of Detonation Gun sprayed coatings on steel subjected to oxidation, hot corrosion and also in actual boiler environment.

2.9.2 Objective

1. The present research work is aimed at studying the high temperature oxidation (air), hot corrosion in Na_2SO_4, K_2SO_4, NaCl, KCl environment in the laboratory tube furnace and actual husk fired boiler environments. Cr_3C_2-NiCr coated and WC-Co coated and bare T91 steel were used.

2. To compare the oxidation study and hot corrosion performance of the D-gun coated steel with bare one and assess its suitability for using it in the actual enviroment of the boiler.

3**.** To understand mechanism for the high temperature corrosion of the specimen bare steel and coated steel, wherever possible. As far as the testing in air environment is concerned, the study could provide useful information regarding the adhesion of the coatings and the spalling tendency of their oxide scales apart from air oxidation behaviour of coatings.

4. In order to investigate the behaviour of these coatings and bare steel in the actual working conditions in which they may be used, the coatings are to be investigated in the operational environment of the actual boiler enviroment at Derabassi, Punjab.

5. In laboratory, the experiments are planned to conduct under cyclic conditions as it provides the severest conditions for testing and represents the actual environment where breakdown and shutdown occur frequently.

6. The Cr_3C_2-NiCr coated and WC-Co coated steel were oxidized and hot corroded in the given environment. Corrosion products were characterized by the techniques such as SEM/EDS, XRD and X-ray mapping to render an insight into the corrosion mechanisms based on the morphology of the corroded products formed on the coated steel. The similar characterization studies will be performed for the corroded bare and coated specimens in actual boiler enviroment.

Chapter 3

Experimentation

3.1 Substrate Material

The substrate material was taken from Cheema Boiler which is located at Ropar, Punjab.T91 boiler steel has been selected as the substrate for this research. This type of carbon steel was recently introduced as boiler steel in the super heater zone in many regions of India. The chemical composition of the steel is shown in table 1. The dimensions of the Samples are 20mm × 15 mm ×5 mm approximately, were cut from the boiler tube steel. For polishing of the samples emery papers of 220,400 and 1000 grade were used and then polished by using velvet cloth. The samples were prepared manually. Special care was taken to avoid any structural changes in the specimen.

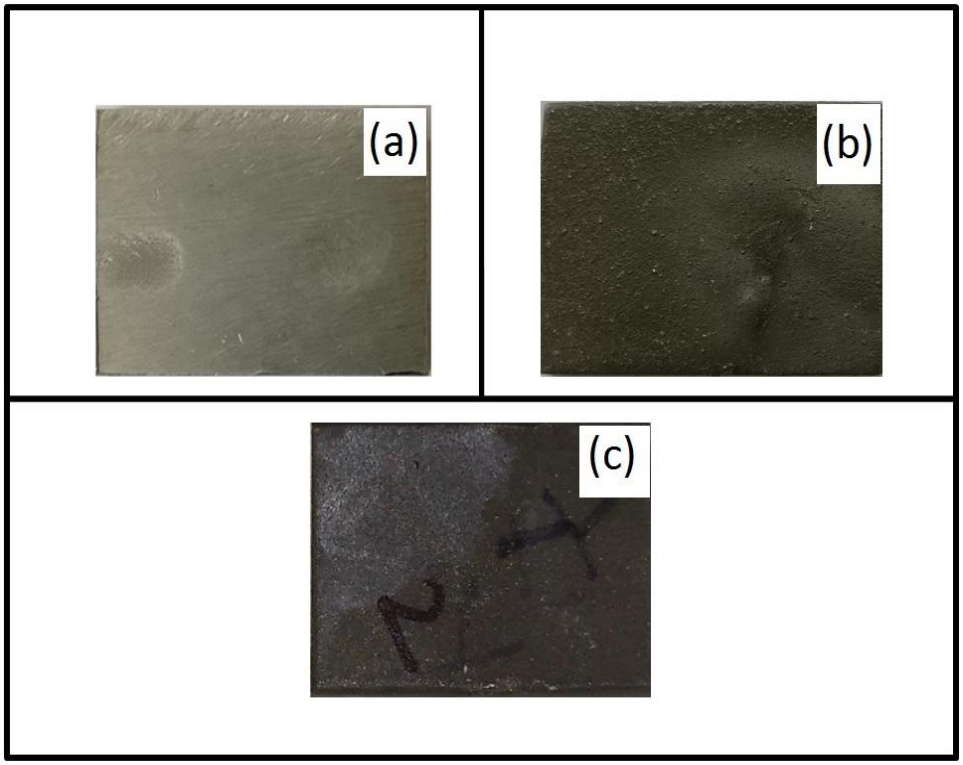

Figure 3.1 Macro photos of uncorroded (a) Bare T91 steel (b) Cr_3C_2-NiCr coated T91 steel (c) WC-Co coated T91

Table 3.1 The Chemical composition of T91 steel (weight % age)

Elements	Weight
C	.05-.15
Mn	0.3-0.6
P	0.025
Fe	Balance
S	0.025
Mo	.87-1.13
Cr	1.9-2.6
Si	.50

3.2 Development of Coating

The Cr_3C_2-NiCr and WC-Co powders were coated on T91 boiler steel specimens using the commercially available Detonation Gun process at SVX POWDER M SURFACE ENGINEERING PRIVATE LIMITED Greater Noida (UP). The Samples were grit-blasted with alumina powder (grit size 20). The Detonation Gun technique was used for the deposition of coating. The parameters of the process including the shot distance were kept constant throughout the entire coating process. Approximately 40μm to 45μm thickness was deposited on the surface of specimen during each shot of the D- Gun and so around 200-250μm thickness was deposited on the surface of each specimen. The coating was deposited on all six sides of the specimen. The thickness of the coatings was 200 to250 μm. The thickness of the coating were measured by the instruments known as Electro thickness gauge meter.

Table 3.2 Parameters for the deposition of the coating

Parameters	Details
Working Gases	Oxygen, Acetylene, Nitrogen, Air
Pressure of working Gases ((MPa)	
Oxygen	0.2
Nitrogen	0.4
Acetylene	0.14
Air	0.4
Consumption of gases/shot	
Oxygen	27×10^{-5} m^3
Nitrogen	5×10^{-5} m^3
Acetylene	23×10^{-5} m^3
Air	5×10^{-5} m^3
Firing rate	1-10 Hz
Water consumption rate	15-25 lit/min
Sound Pressure level	150 dB

3.3 Preparation of experimentaion in laboratory

3.3.1 Heat treatment of boat

The High temperature Alumina boats were heat treated at a temperature 1050˚C for 12 hours. The aim of heat treatment of boats before experimentation is to remove moisture if present in the boats so that a constant weight of boat can be achieved for the experimentation.

3.3.2 Specimen preparation for high temperature Oxidation test

The bare, Cr_3C_2-NiCr coated T91 and WC-Co Coated T91 steel specimen were polished in order to remove eliminate the impurities and to get the uniform surface of the substrate. The

dimensions of the each substrate were noted down by using digital vernier calliper before experiments After that the specimen were put in furnace at 300˚C for 1 hour for pre heating.

3.4 Oxidation Study

High temperature cyclic oxidation tests were carried out in Tubular furnace for 50 cycles each at 800˚C. Every oxidation cycle consists of heating of the specimen at 800°c temperature in furnace and then cooling for 20 minutes in at room temperature. The Weight of the specimen was noted after each cycle of the experiment to calculate K_p values and approximate the rate of oxidation.

3.5 Hot Corrosion Study

High temperature corrosion study were performed in a molten salt environment (Na_2SO_4, K_2SO_4, NaCl and KCl) for 50 cycles under the cyclic condition. Hot corrosion may be defined as an accelerated corrosion, resulting from the presence of salt contaminants such as Na_2SO_4, K_2SO_4 NaCl that combine to form molten deposits, which damage the protective surface oxides. Hot corrosion can starts when materials are heated in the temperature range between 700 to 900°C in the existence of sulphates deposits formed as a result of the reaction between sulphur compounds and sodium chloride in the gas phase surrounding the materials. At very high temperatures, deposits of Na_2SO_4 are molten salt can cause accelerated attack on metal. In the present study, the environment was simulated for bio-fuel fired environment by using 40%Na_2SO_4-10%NaCl-40%K_2SO_4-10KCl. For hot corrosion the cycles consist of 1 hour heating of the samples in the furnace and 20 minutes of the cooling of the samples at room temperature.

3.6 Study under Actual Biomass fuel fired boiler

High temperature corrosion study is also carried out in actual fuel fired boiler .The plant is located at Derrabassi Punjab. All specimen were hanged inside boiler at temperature 778°C±50° with the help of A grade kanthal wire which is good heat resistant. Substrate has been taken out after 48 hours, after that SEM/EDS, XRD analysis done to know the various change on the samples.

3.7 Characterization of the substrate

3.7.1 SEM/EDS analysis

SEM/EDS analysis is done to know the surface morphology of the coated as well as the bare specimen. In addition, EDS is also carried out to know the elemental composition at different region on the surface of substrate. Secondary electron images (SEI) were recorded for surface analysis while X-Ray mapping were recorded for cross sectional surfaces.

Figure 3.2 Scanning electron Microscope
(Courtesy: SAI Lab, Thapar University, Patiala)

3.7.2 XRD analysis

X-ray diffraction (XRD) analysis was done to know the phases and various compounds formed during the Experimentation at a particular areas of the specimen . XRD analysis was carried out for the bare, Cr_3C_2-NiCr coated T91 and WC-Co Coated T91 steel specimens to determine the various phases present on their surfaces. The substrate were scanned in 2θ range of 20º to 80º and the intensities were recorded. This analysis is done for determination of various phases with the help of JCPDS cards and X–pert hi score.

Figure 3.3 X-RAY Diffraction

(Courtesy: SAI Lab, Thapar University, Patiala)

3.7.3 Microhardness test

Micro hardness test is performed on the uncorroded Cr_3C_2-NiCr coated T91 and WC-Co Coated T91 steel. from the test Vickers No. for Cr_3C_2-NiCr coated T91 was 690.84 and for WC-Co Coated T91 steel Vickers No. was 952.55. More the Vickers no. more the hardness of the material. Micro hardness test machine is available at Thapar university.

Figure 3.4 Micro hardness testing machine

(Courtesy :Mechanical Workshop, Thapar University)

3.7.4 Surface Roughness test

To determine the surface roughness of specimens, surface roughness tester was used. The Surface Roughness test was done at Thapar University, Patiala. The Surface Roughness tester machine was made by Mitutoyo (Japan). 0.01µm is the least count of the Surface roughness. It is calibrate by the vertical deviations of a real surface from its ideal form. If the deviations are broad, then this mean the surface is rough; if these deviation are less then the surface is smooth. Roughness is typically consider to be the, short wavelength, high frequency component of a measured surface. Surface roughness is generally a good predictor of the performance of a mechanical component.

Figure 3.5 Surface roughness tester

(Courtesy: Metrology Lab, Thapar University, Patiala)

3.7.5 Weight change measurements

After each cycle of oxidation and hot corrosion the weight of substrate were measured, This is carried out to analyze the kinetics of oxidation. The weight change graph was plotted against number of cycles for each substrate at particular temperature.

3.8 Precautions

- Furnace calibration should be done in order remove the thermo-couple error if present
- In order to make the weight of boats constant, proper heating of the boats must be done so as to remove variables like volatile materials, moisture, impurities etc.
- During the high temperature test the boats should be handle with carefully .The samples should be polished on emry paper (320,800,1000,2000) so as to achieve uniform coating before conducting experiments.

Chapter 4

Characterization of Coatings

4.1 Two types of coating was deposited on substrate

4.1.1 Chrome carbide Coating ($80Cr_3C_2$-20NiCr): Chromium carbide is a ceramic compound which can have different chemical compositions like Cr_3C_2, Cr_7C_3 and $Cr_{23}C_6$. According to standard chrome carbide exists as a gray solid and is found to very hard and corrosion resistant (Teng *et al*.2004). It is also a refractory compound, which means that it retains its strength at high temperature .These properties make it useful as an additive to metal alloys. When chromium carbide crystals are coated into the surface of the substrate it improves the wear resistance and corrosion resistance of the metal, and maintains these properties at high temperatures. Cr_3C_2 is the hardest and most commonly used composition for the coating.

There are three different types of crystal structures for chromium carbide corresponding to the three different chemical compositions (Bowman *et al*.1972).

- $Cr_{23}C_6$ has a cubic crystal structure and a Vickers hardness of 976 kg/mm^2.
- Cr_7C_3 has a hexagonal crystal structure and a micro hardness of 1336 kg/mm^2.
- Cr_3C_2 is the most durable of the three compositions, and has an orthorhombic crystal structure with a micro hardness of 2280 kg/mm^2. (Bowman *et al*.1972)

Because of aforementioned reasons, Cr_3C_2 the primary form of chromium carbide is used in surface treatment.

4.1.2 Carbide coating (88WC-12Co): Carbide coatings are generally used in erosion, wear resistance to abrasion, galling, corrosion resistance of metals. Generally, HVOF and Detonation Gun are used to deposit carbide coatings in order to achieve the high bond strength and dense coating with low porosity (Hogmark *et al*. 2000). Melting point of tungsten carbide is very high is of 2870°C and the boiling point of 6,000°C. Tungsten carbide is extremely hard with a Vickers number of around 2600 (Ekmekci *et al*. 2009).

4.2 Powder Morphology

The meaning of the morphology is a particular shape, form, shape and structure of any particle. The morphology of a powder particle is represent by description for example

angular, spherical, circular irregular polygon, dish-shaped or quasi-quantitatively, for example, by means of geometrical shape parameters. The shape parameter identify mainly the shape, without considering the size of the particle (Kelly *et al.*2003).The powder morphology of Chrome carbide powder and tungsten carbide powder are give below. As shown in figure 4.1 The shape of the particle of chrome carbide powder are irregular or might be say polygon. The particles are embedded with each other. The particle of the tungsten carbide are spherical in nature. The size of the particle for both powders are 5 to35 µm. (Sharma *et al*. 1999)

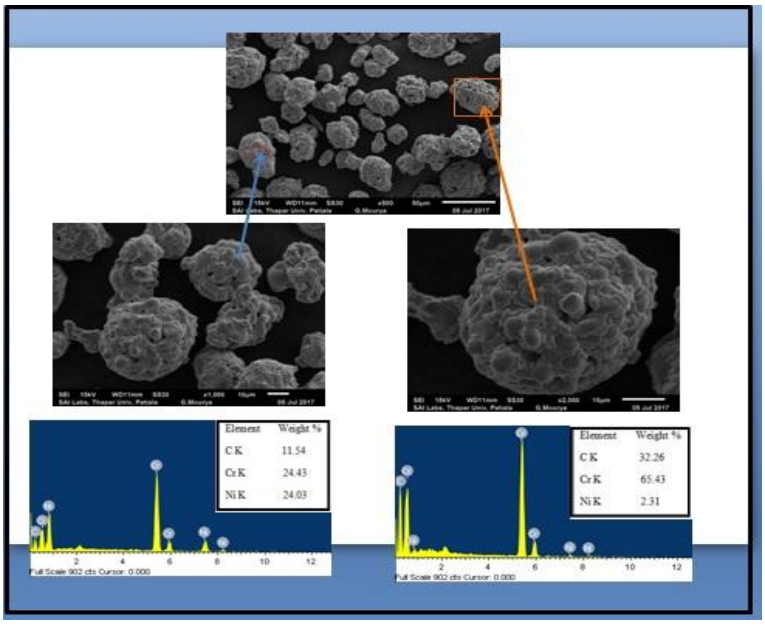

Figure 4.1 SEM micrograph along with EDS at some selected sites on Cr_3C_2-NiCr powder

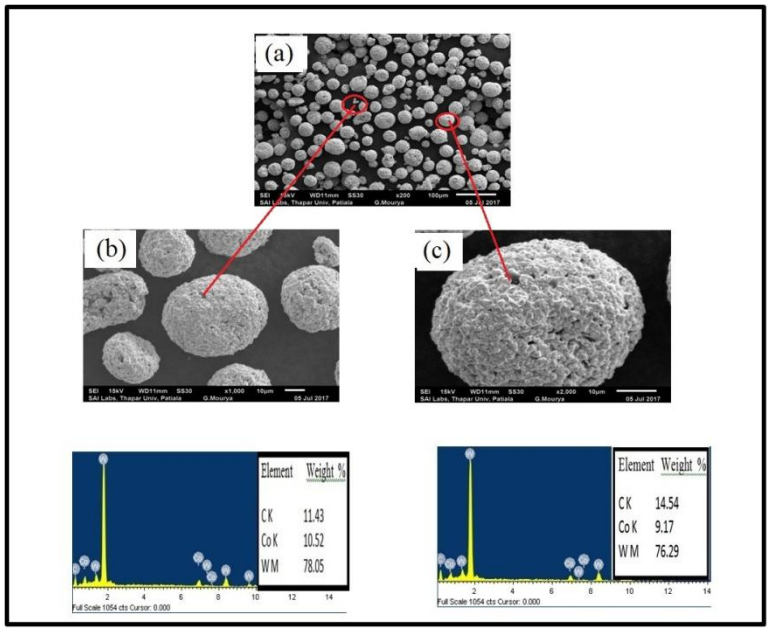

Figure 4.2 SEM micrographs along with EDS at some selected sites on WC-Co powder

4.3 Microstructural characterization of as sprayed coatings

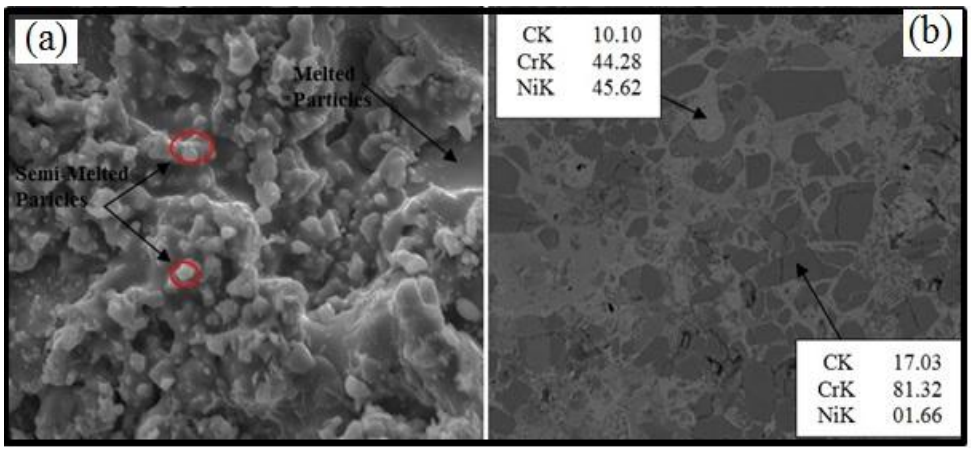

Figure 4.3 SEM/EDS of (a) as sprayed and (b) polished Cr_3C_2-NiCr coated steel

SEM micrograph along with EDS analysis of as sprayed D-gun sprayed Cr_3C_2-NiCr, coating is shown in figure 4.3(a). It can be clearly seen that the coating formed is dense and adherent with melted and semi-melted particles. Polished surface for Cr_3C_2-NiCr is shown in figure 4.3(b). Equiaxed Cr_3C_2 carbide particles (Dark grey region) were found to be distributed inside the NiCr matrix (Light grey region) in polished Cr_3C_2-NiCr coating. Similar structure of Cr_3C_2-NiCr coating was noted by (Richert *et al*.2012).

4.4 Micro hardness test

Microhardness test is carried out to know the hardness of the material. It is used as a standard method for measuring the hardness of metals, in particular, those with extremely hard surfaces. In this process, Standard pressure applied on the surface of the substrate, a pyramid shaped type of indentation seen on the surface of sample by the microscope. The diagonal of the resulting indention is measured under a microscope and a conversion table reads the corresponding Vickers Hardness. Vickers test is performed by placing the specimen on an anvil that has a screw threaded base. The indenter is thereafter pressed into the sample by an accurately controlled test force. The force is maintained for a specific dwell time, normally 20 seconds. After the completion of the dwell time, the indenter is removed and an indent is seen in the surface of the sample in the form of square shaped pyramid. The size of the indent is determined optically by measuring the two diagonals of the square indent. The average of the two diagonals is used in the following formula to calculate the Vickers hardness. The operation of applying and removing the load is controlled automatically. Several loadings

give practically identical hardness numbers on uniform material, which is much better than the arbitrary changing of scale with the other hardness machines. In case of an indentation with a tolerance of ±1/1000 of a millimeter, a microscope is used to measure the square indentation. Finally, an average is taken of all the measurements across all the diagonals. Micro hardness test is performed on the uncorroded Cr_3C_2-NiCr coated T91 and WC-Co Coated T91 steel. From the test Vickers No. for Cr_3C_2-NiCr coated T91 was 690.84 and for WC-Co Coated T91 steel vickers No. was 952.55. More the Vickers no. more the hardness of the material .Micro hardness test machine is available at Thapar university Patiala .

4.5 Surface roughness

Surface roughness can be defined as the shorter frequency of real surfaces relative to the troughs. It can be noticed in various machine parts, that their surfaces embodies a complex design constituting of a series of peaks and troughs of different height, depth and spacing. Surface roughness can also be greatly affected by the microscopic asperity of the surface of each part.

The roughness (R_a) values of the D-gun sprayed as coated specimens were measured using Surface Roughness Tester (Mitutoyo SJ-201, Japan). Each reported value of surface roughness (R_a) is the mean of the five observations taken at different locations. The centre line average (CLA) method was used to obtain the R_a value. The roughness values of Cr_3C_2-NiCr coated steel are (R_a) is 4.75µm and plain side is 0.38µm and for WC-Co coated steel the roughness is 4.36µm and plain side is 0.23µm.

4.6 Thickness loss measurements

The thickness loss is a means to express the penetration rate due to corrosion of the metal specimen. Perhaps the most common unit of corrosion penetration recognized in the United States is milli-inches per year (mpy). The formula utilized to convert mass loss or thickness loss to corrosion rate, in mpy, is as follows:

$$Corroson\,Rate\,,\,mpy = \frac{(Mass\,Loss,\,g)\times 3450000}{8760\times SA\times d} = \frac{(Thickness\,Loss,\,microns)}{25.4}$$

Where, SA is the surface area in cm^2, and d is the density in g/cm^3.

The calculation of mpy can also be done as follows: In a year there are 8730 hours and 1mm is equal to 39.37 mils. So, for "z" mm thickness loss for 1000 hours, mpy is (z) × (39.37) × (8760/1000).

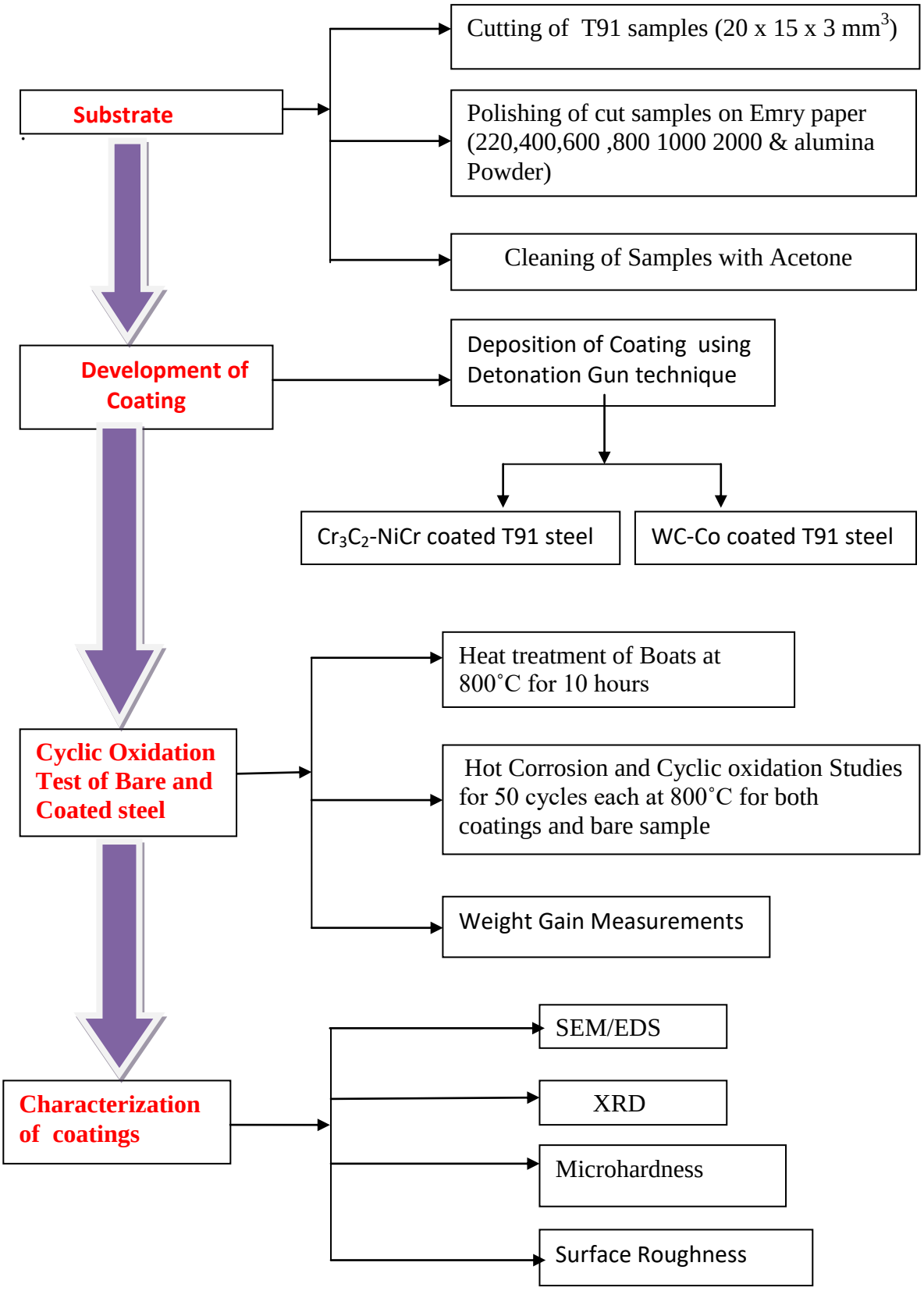

Figure 4.4 Flow chart of the methodology follow

Chapter 5

Oxidation studies in air

5.1 Introduction

There are various properties stainless steel that are desirable for construction applications (Baddoo 2008). Various grades of stainless steels which are used are austenitic, ferritic, martensitic and duplex type stainless steels. As compared to carbon steel, stainless steel have different material properties both at room and elevated temperature., stainless steel shows a more rounded stress strain response than carbon steel, at room temperature and no sharply defined yield point, together with a higher ratio of ultimate-to-yield stress and greater ductility. In comparison to carbon steel, stainless reveals better retention of strength and stiffness at high temperature (Gardner *et al.* 2010). Austenitic stainless and Ferritic steel, in particular, shows the excellent combination of strength, oxidation resistance and high temperature characteristics for long service, high temperature industrial applications and has been successfully employed for such purposes (with operating temperatures of more than 550°C) for many years. It is corrosion-resistant material which can be used for making thinner and more durable structures. Austenitic steels are more resistance to corrosion as comparison to ferritic steels. However, due to lower cost, ferritic steels are widely used at high temperature areas in boilers. (Laverde *et al.*2002) reported the cyclic an isothermal oxidation studies of T91 steel at various temperature ranging from 575°C to 700°C. They reported that under cyclic conditions the ferritic steel suffered from cracking of oxide layer with intense spallation.

5.2 Results

5.2.1 Visual Analysis

Macrophotos of bare, Cr_3C_2-NiCr and WC-Co coated T91 steel subjected to cyclic oxidation at 800°C has been show in fig 5.1, 5.2 and 5.3. In case of bare T91 steel (figure 5.1), it was observed that after the 1^{st} cycle of oxidation the colour of substrate changes from metallic silver to dark brown, no change was observed till 38^{th} cycle. However after, 39^{th} cycle the dark brown colour intensified, no spallation was observed throughout 50th cycle. In case of Cr_3C_2-NiCr coated T91 steel fig 5.2., The green colour oxide was formed on dark grey

background after the 1st cycle of oxidation, after that no change was observed till 50th cycle, in case of WC-Co coated steel (figure 5.3). The coating starts spalling from one side just after 1st cycle. The spatter intensified till 5th cycle followed by delaminated of coating in 6th cycle. The spallation of the coating was observed throughout the corrosion run.

5.2.2 Weight change measurements

Weight change if any was noted down after every cycle of exposure. A graph has been plotted between the Weight change/Surface area Vs Number of cycles and is shown in figure. 5.4. It was observed that overall weight gain is very less for T91 steel and Cr_3C_2-NiCr coated T91 after 50 cycles of exposure. For oxidation, the weight gain corresponds to the weight of oxygen and elements of substrate which reacts to form oxide. Whereas for WC-Co coated T91 steel weight gain is very starting from the initial cycles 30th cycle. After 31st cycle the weight gain became constant. Corrosion kinetic for all the specimens can be characterized by the factor K_p known as parabolic rate constant. This constant was calculated using square graph of weight change/Surface area Vs Number of cycles. From Table 5.1, it can be clearly seen that both bare and WC-Co coated T91 steel showed less résistance to the given environment. However, Cr_3C_2-NiCr coated T91 steel showed excellent resistance in the given atmosphere. Bare T91 steel and Cr_3C_2-NiCr coated T91 steel follows parabolic rate law.

Table 5.1 Parabolic rate constant (K_p) values for Bare, T91 WC-CO coated T91 and Cr_3C_2-NiCr coated T91 steel after subjected to oxidation in air at 800ºC for 50 cycles.

Substrates	$K_p \times 10^{-8} g^2 cm^{-4} s^{-1}$
Bare T91	252.1
WC-Co coated T91	598.6
Cr_3C_2-NiCr coated T91	1.095

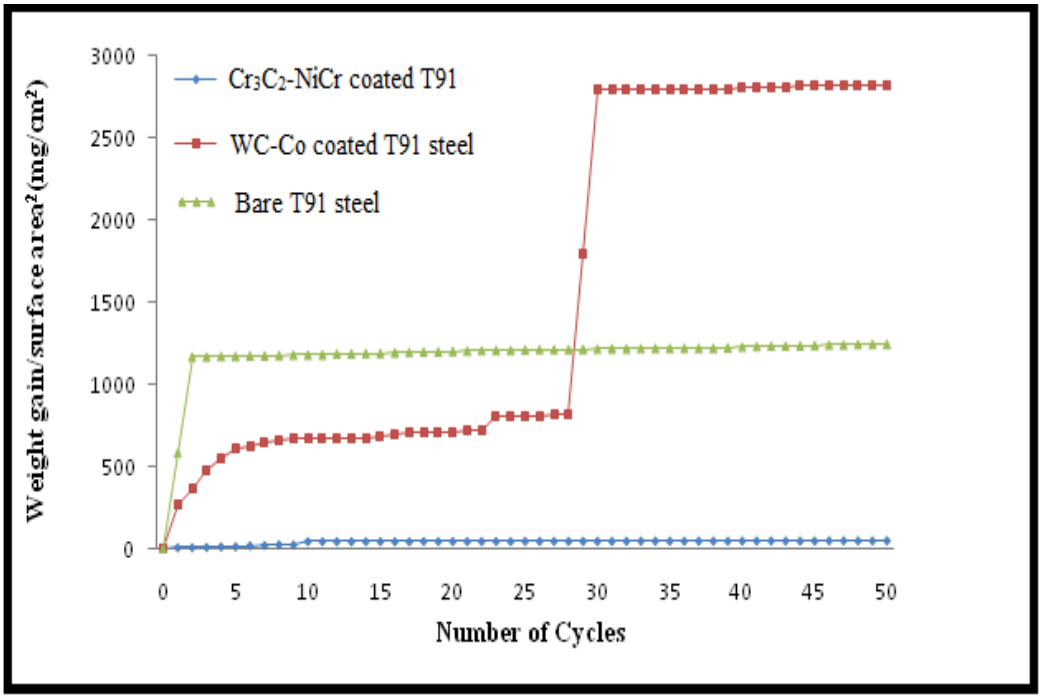

Figure 5.1 (Weight gain/Surface area) (mg/cm^2) Vs Number of cycles for Bare T91, Cr_3C_2-NiCr coated T91 steel and WC-Co coated T91 steel after oxidation in air at 800°C for 50 cycles

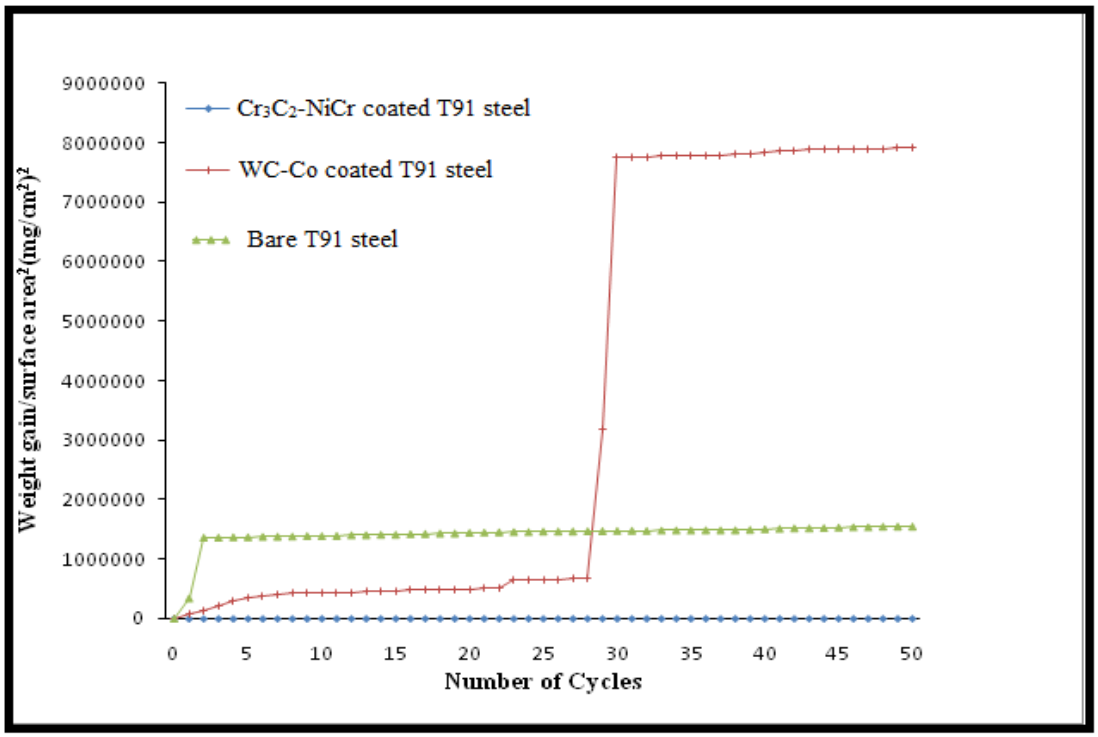

Figure 5.2 (Weight gain/Surface area) (mg/cm^2)^2 Vs Number of cycles for Bare T91, Cr_3C_2-NiCr coated T91 steel and WC-Co coated T91 steel after hot corrosion at 800°C for 50 cycles

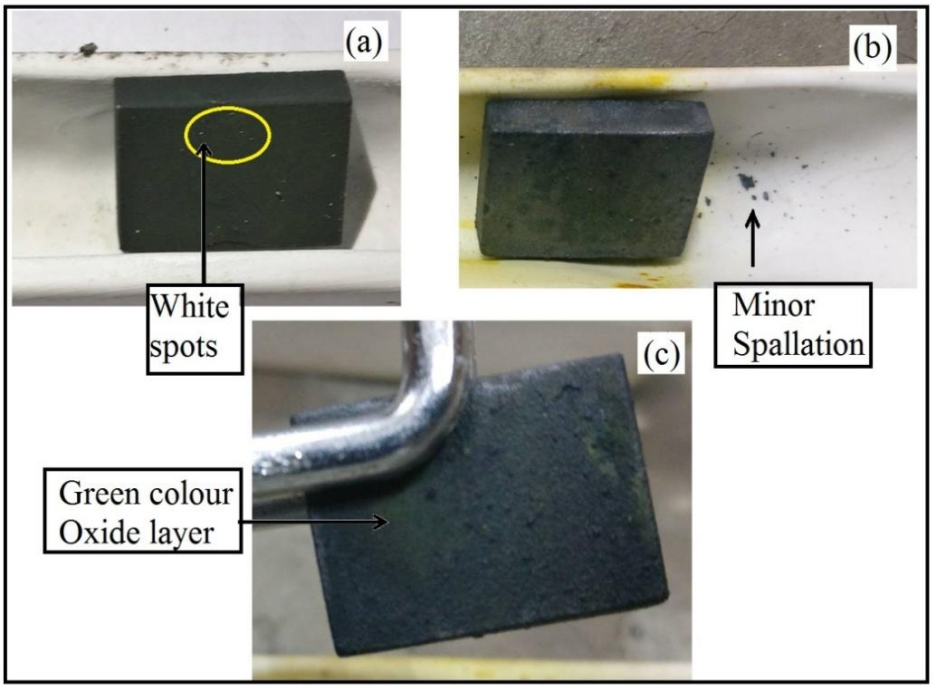

Figure 5.3 Macro photos of bare T91 steel after subjected to corrosion run for (a) 1st cycle, (b) 25th cycle and (c) 50th cycles at 800°C under simulated bio fuel fired boiler environment

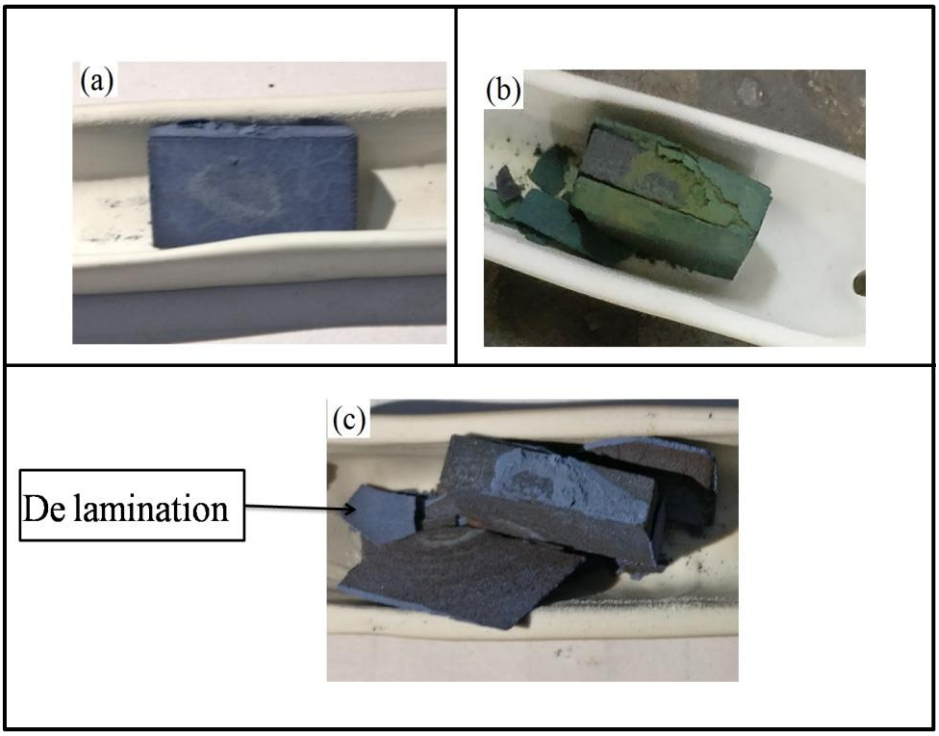

Figure 5.4 Macro photos of bare T91 steel after subjected to oxidation for (a) 1st cycle, (b) 25th cycle and (c) 50th cycles in air at 800°C

5.2.3 SEM/EDS

SEM micrograph for bare T91, Cr_3C_2-NiCr coated T91 and WC-Co coated T91 steel are shown in figure. 5.4, 5.5 and 5.6 with EDS spectrum. In case of Bare T91 steel (figure 5.4), dense oxide having rhombohedral structure along with some columnar like morphology was seen on the surface. EDS analysis depicts the presence of major amount of iron and oxygen along with minor amount of chromium and molybdenum. From the results it has been clearly observed that dense and clusters oxide was formed on the surface of Cr_3C_2-NiCr coated T91 (figure 5.5). EDS analysis shows the existence of chromium and oxygen along with minor amount of nickel. In WC-Co coated T91 (figure 5.6) steel massive and porous oxide can be observed clearly. EDS analysis were done at the point of interest on the surface of samples. Different points were taken which represents the chemical composition of that particular point on the surface of the substrate. EDS analysis showed that the dominating elements are cobalt, iron, tungsten and oxygen.

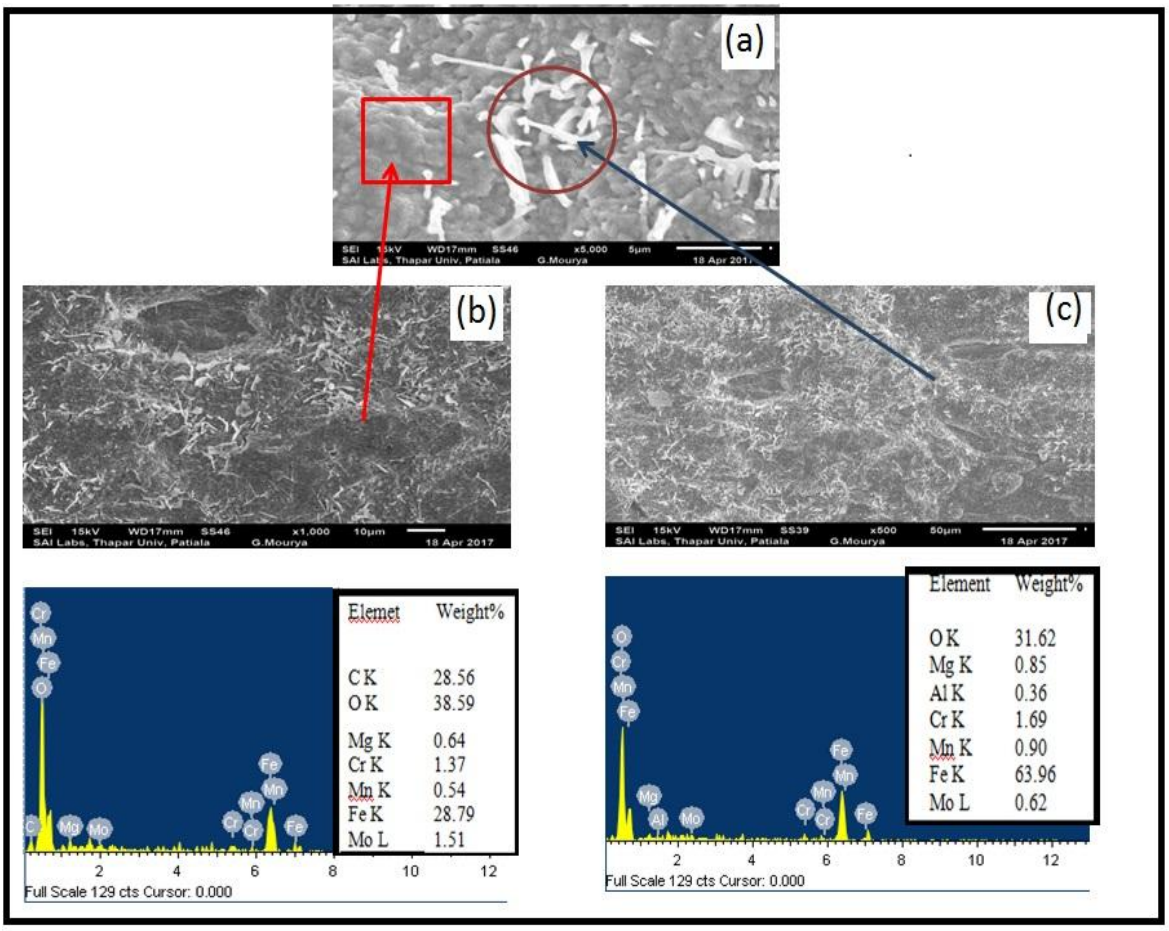

Figure 5.5 SEM Micrograph along with EDS at some selected sites on bare T91 after oxidation in air at 800°C for 50th cycle

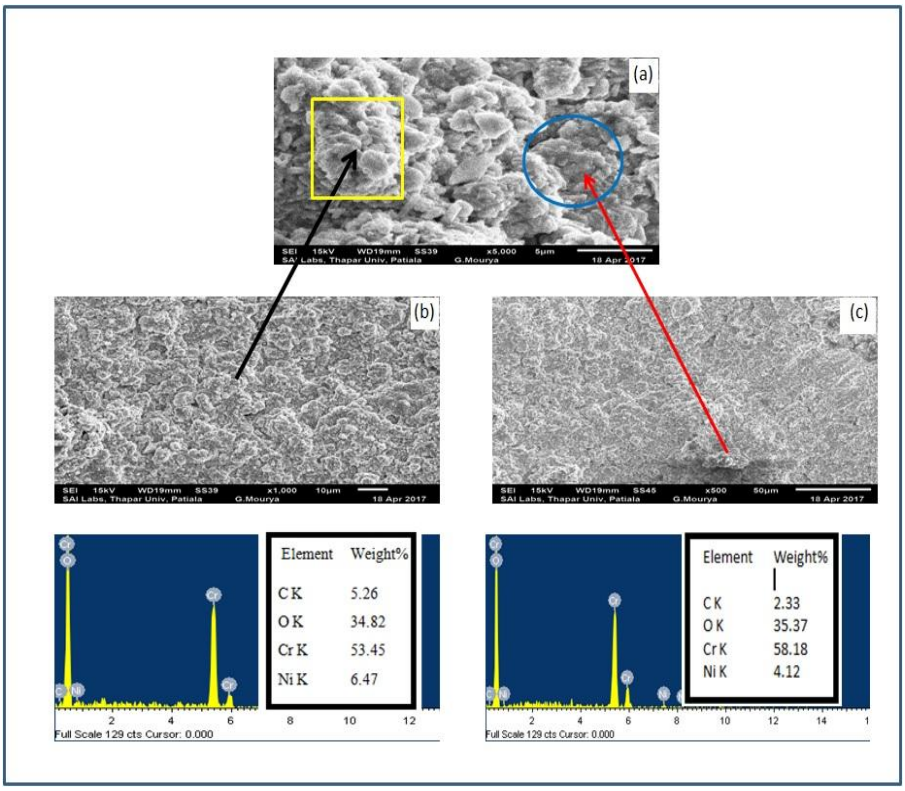

Figure 5.6 SEM micrograph along with EDS at some selected sites on Cr_3C_2-NiCr subjected to oxidation in air at 800°C after 50 cycles

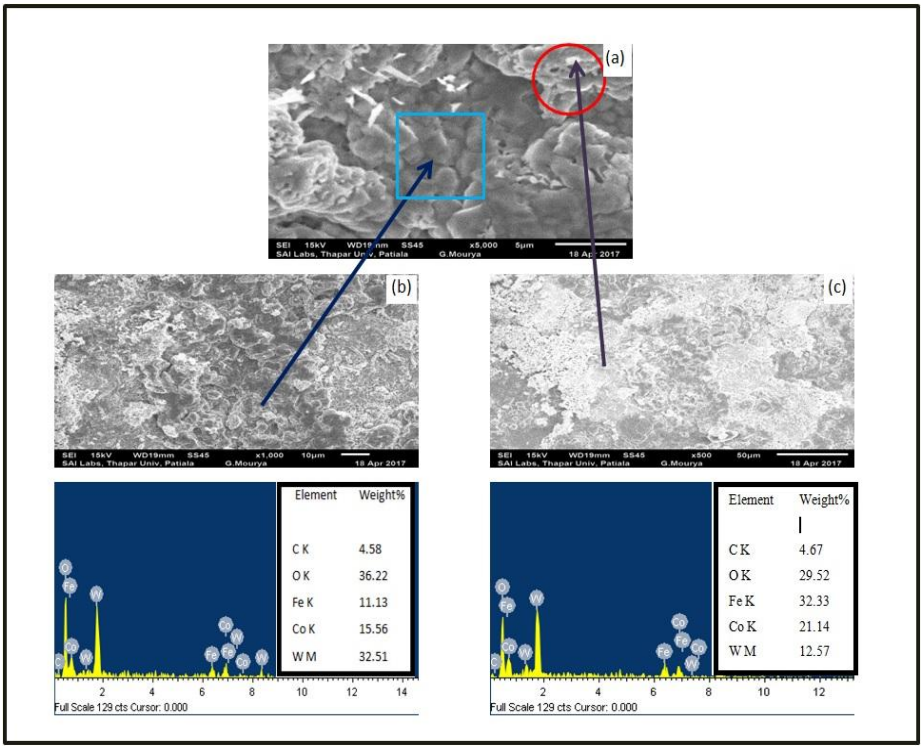

Figure 5.7 SEM micrograph along with EDS at some selected sites on WC-Co Coated T91 steel subjected to oxidation in air at 800°C after 50 cycles

5.2.4 XRD analysis

Intensity Vs Diffraction angle XRD graph were plotted to identify the phases present in the scale formed. JCPDS files can also be used to detect the phases by comparing the 'd' value of intensity peaks with the 'd' value given in files for the particular phase. X-ray diffractograms of the scale formed on the oxidized specimens are shown in figure. 5.7. In case of bare T91 steel, major phases indentified were Cr_2O_3, FeO and Fe_2O_3. Whereas in case of Cr_3C_2-NiCr coated T91 steel, main phases identified were Cr_2O_3, $Cr_{23}C_6$ and Cr_7C_3. In case of WC-Co coated T91 steel, peaks of $CoCr_2O_4$, Co_3O_4 , WO_3 and Cr_2O_3 were seen.

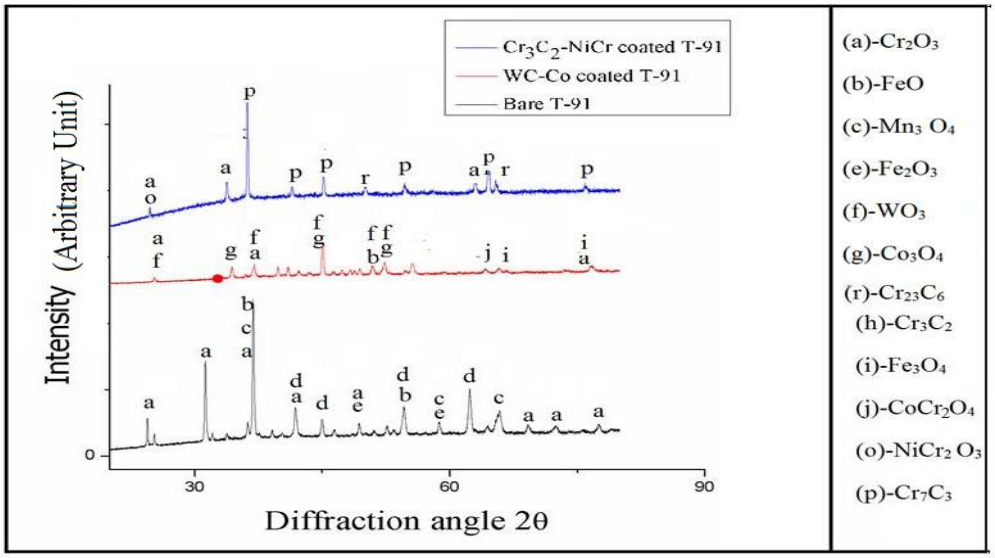

Figure 5.8 XRD analysis of bare, Cr_3C_2-NiCr and WC-Co coated T91 steel samples after cyclic oxidation in air at 800°C for 50 Cycles

5.2.5 Elemental X-Ray mapping

The elements present in the oxide layer that were found by using x ray mapping were C, O, Cr and Fe in case of bare sample. High presence of Cr and Fe can be seen in metal and oxide region from X-Ray mapping. Formation iron oxide leads to less protective behaviour of bare T91 steel. The XRD analysis also shows the presence of two main phases in bare sample that were Fe_2O_3(non protective) and Cr_2O_3(protective). In case WC-Co coated sample C, O, W and Fe were found from the X-Ray mapping. However in case of Cr_2C_3-NiCr coating the elements present are C, Fe, Ni, Cr and O. Cr_2O_3 oxide was mainly responsible for providing protection to Cr_3C_2-NiCr coated steel.

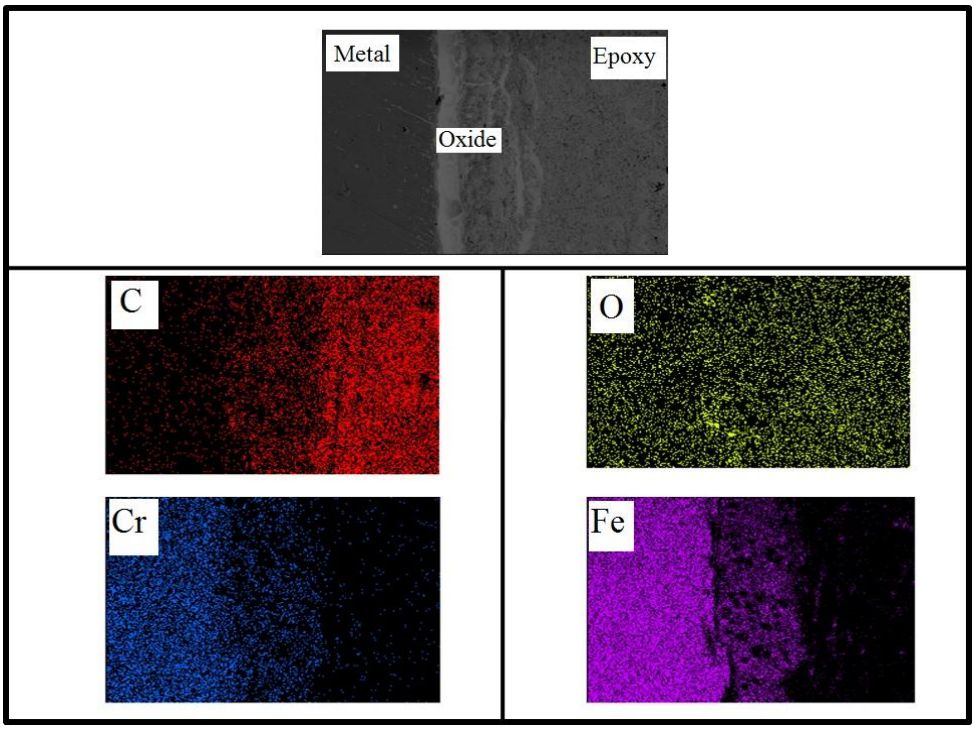

Figure 5.9 X-Ray mapping of bare T91 steel subjected to oxidation in air at 800°C after 50 cycles

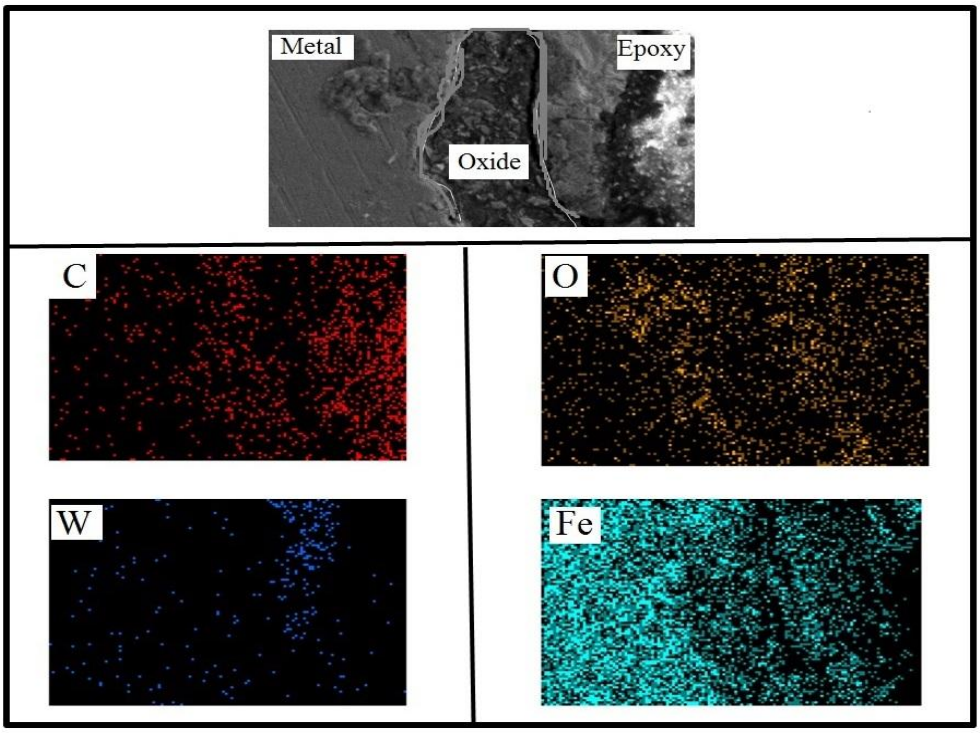

Figure 5.10 X-Ray mapping of WC-Co coated T91 steel subjected to oxidation in air at 800°C after 50 cycles

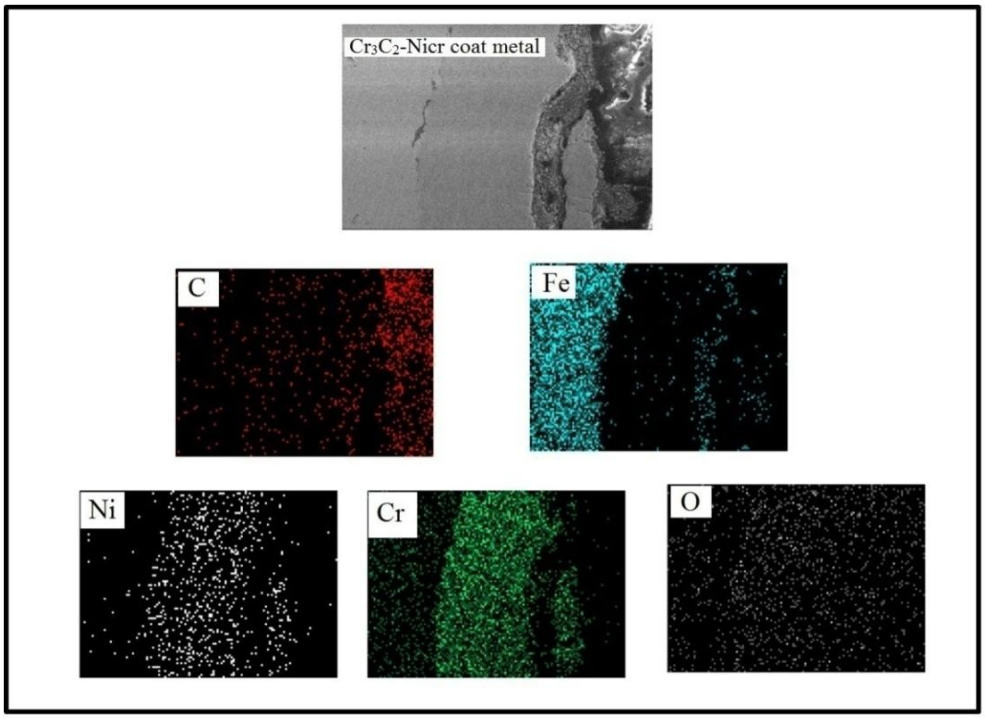

Figure 5.11 X-Ray mapping of Cr_3C_2-NiCr coated T91 steel subjected to oxidation in air at 800°C after 50 cycles

5.3 Discussion

From visual studies which has been carried out while experimentation. It can be very well seen that WC-Co coating did not sustained in the cyclic oxidation condition. Where as Cr_3C_2-NiCr coating showed best corrosion résistance by showing no spallation of sputtering throughout the experiment. Bare T91 steel again shows good corrosion résistance may be because of the presence of chromium in the substrate. It was very well documented that if chromium is present in the metal and exposed to some temperature. It has tendency to form oxide layer even in the presence of iron because of its more negative Gibbs free energy as can be noted from Ellingham diagram. As the occurrence of reaction was purely depend upon the negativity of Gibbs free energy available to carryout that reaction (Mudgal *et al.* 2012).

Weight gain analysis showed that Cr_3C_2-NiCr coated T91 steel showed lowest parabolic arte contant which again confirms its good resistance to corrosion. SEM analysis clearly showed the formation of dense oxide wheras EDS confims the presence of chormium and oxide. XRD analysis further clarify that the oxide formed is mainly chromium oxide. The chormium oxides so formed may act as a diffusion barrier against the atmosphere. This oxide mainly formed on the top of the coating and along the splat boundaries. Also , presence of Cr_7C_3 and $Cr_{23}C_6$ were also indicated in XRD analysis. This is due to decomposition of chromium

carbide when exposed to high temperature. In case of WC-Co coated T91 steel XRD analysis reveled the formtion of WO_3. This oxide if formed may leads to catastropic corrosion as this oxide is volatile in nature. Lofaz & Kaganovskii (1995) also reported the formation of brittle WO_3 while oxidation of WC-Co alloy by following reactions 5.1 and 5.2.

$$WC + \frac{5}{2}O_2 \rightarrow WO_3 + CO_2 \quad (5.1)$$

$$WC + 2O_2 \rightarrow WO_3 + CO \quad (5.2)$$

5.4 Conclusions

1. T91 steel and Cr_3C_2-NiCr coated steel showed good oxidation resistance while subjected to oxidation in air at 800°C for 50 cycles. However, WC-Co coating was totally delaminated from the substrate.

2. Cr_2O_3 oxide was mainly responsible for providing protection to Cr_3C_2-NiCr coated steel whereas formation iron oxide leads to less protective behaviour of bare T91 steel. Formation of WO_3 might have contribute to the poor corrosion resistance of WC-Co.

Chapter 6

Hot corrosion

6.1 Introduction

Accelerated oxidation which occurred because of the presence of fused salt deposits such as Na_2SO_4, NaCl, K_2So_4, KCl etc at high temperature can be named as hot corrosion (Rapp 2002). Nowadays, various auxiliary fuels has been burned in the boilers to conserved non renewable fuels such as kerosene oil etc. Burning of different fuels in the boilers creates more corrosive environment. Specific attention has been given to the burning of bio-fuels across the globe for power production because of its surplus existence such as straw and wood chips (Michelson *et al.* 1998). (Nielsen *et al.*2000) also reported problem of high temperature corrosion encountered during burning of biomass fuel in power plants. It is because of the presence of chlorine which release during burning of coal and bio fuel individually or together in boilers. Hence it is necessary to analyse the mechanism of surface degradation of various steels, alloys and coatings in such aggressive environments. (Chatha *et al.* 2012), reported that when T91 steel was exposed under molten salt environment at high 750°C, it shows intense spalling and sputtering, along with the cracking of edges. (Uusitalo *et al.* 2003) conducted experiments on HVOF coating, laser-melted HVOF coatings, ferritic and austenitic boiler steel under simulated bio fuel environment. They reported that ferritic steels showed considerably higher weight gain as compared to austenitic steel which show its less resistance to corrosion. However, HVOF coatings substantially increase the life of steels under the corrosive atmosphere. (Oksa *et al.* 2014) also reported the strong corrosion problem in biomass fuel fired boilers. It is because of the presence of chlorine which causes active oxidation even at low temperature. Active oxidation significantly degrades the components of boilers. The steel samples and HVOF coated samples were exposed under actual boiler. HVOF coating exhibits excellent resistance to corrosion as compared to steels. Hence, the present study focused on analysing the corrosion behaviour of coated and uncoated T91 ferritic steel under bio-fuel fired boiler environment. Ferritic steel has been chosen because of the considerable difference in cost of ferritic and austenitic steel. The specimen was coated with two different carbide coating using Detonation gun technique. D-gun technique has been selected due to its property of depositing coating with high bond strength and low porosity.

6.2 Results

6.2.1 Visual Analysis

Visual macro-photos were taken after each cycle of hot corrosion. Figure 6.1, 6.2 and 6.3 shows the macro-photos of bare, WC-Co coated T91 and Cr_3C_2-NiCr coated T91 steel after subjected to hot corrosion run respectively. Three different photos were shown which were taken after 1st cycle 25th cycle and 50th cycle for each specimen. Figure 6.1 shows the photos of bare T91 steel. It was observed that fragile oxide was formed just after 1st cycle. The colour of dark grey along with reddish brown patches on the surface. After 2nd cycle till 14th cycle, the corrosion was intensified which can be seen in the form of porous and fragile oxide. Some spallation and sputtering of oxide was also indicated. After 15th cycle, no significant changes were observed. Figure 6.2 shows the photos of WC-Co T91 coated steel after hot corrosion for 1st, 25th and 50th cycle. It was seen that the coating undergone major spallation just after 1st cycle. Cracks were also appeared on the surface of the coating. After that the coating starts delaminating from the steel substrate. Spallation was also intensified till 30th cycle. After 31th cycle the, coating got delaminated from the substrate. After 31st cycle, no significant changes were observed. Macro-photos of Cr_3C_2-NiCr coated T91 steel were shown in figure 6.3. It was observed that the coating undergone minor spallation just after 1st cycle. Formation of greenish oxide along with dark grey background was also indicated. No substantially changes were recorded after 2nd cycle.

6.2.2 Weight change measurements

A weight gain graph was plotted showing the Weight change/Surface area Vs Number of cycles in figure. 6.4. It can be clearly seen from the graph that WC-Co coated T91 steel showed very high weight gain starting from 1st cycle till 30th cycle. However after 31st cycle the weight gain becomes constant. Bare and Cr_3C_2-NiCr coated T91 steel both showed minor weight gain in initial cycles thereafter the weight gain becomes constant. Out of all the three specimens, Cr_3C_2-NiCr coated T91 steel showed least weight gain followed by bare T91 steel and WC-Co coated steel respectively. The comparison of K_p value allows the quantification of the corrosion rate. Hence k_p value for all the specimens have been calculated and are given in Table 6.1. The weight gain square (mg^2/cm^4) *vs.* time (number of cycles) was plotted to establish the rate law for oxidation and to calculate the K_p value. Cr_3C_2-NiCr coated T91 shows least k_p value among all the three substrate.

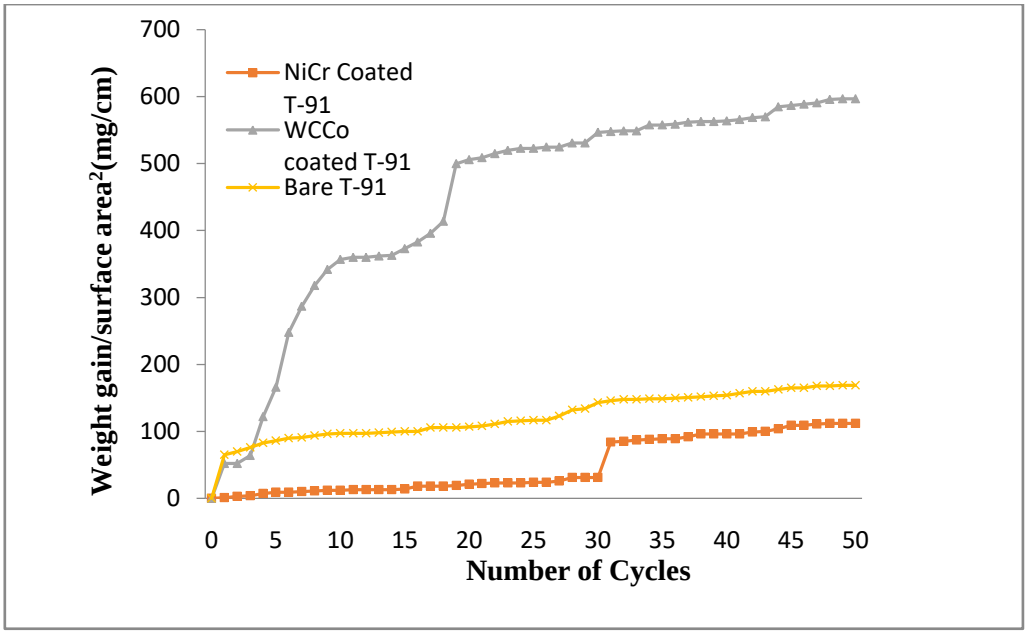

Figure 6.1 (Weight gain/Surface area) (mg/cm^2) Vs Number of cycles for Bare T91, Cr_3C_2-NiCr coated T91 steel and WC-Co coated T91 steel after corrosion under simulated bio-fuel fired boiler environment at 800°C for 50 cycles

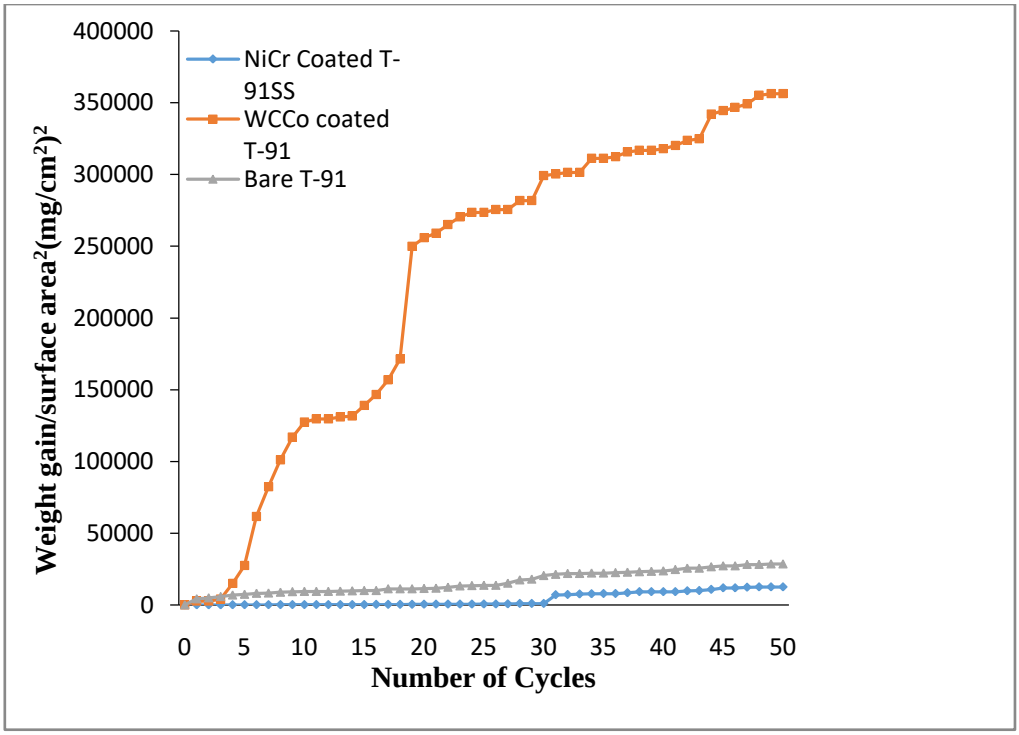

Figure 6.2 (Weight gain/Surface area) (mg/cm^2)^2 Vs Number of cycles for Bare T91, Cr_3C_2-NiCr coated T91 steel and WC-Co coated T91 steel after corrosion simulated bio-fuel fired boiler environment at 800°C for 50 cycles

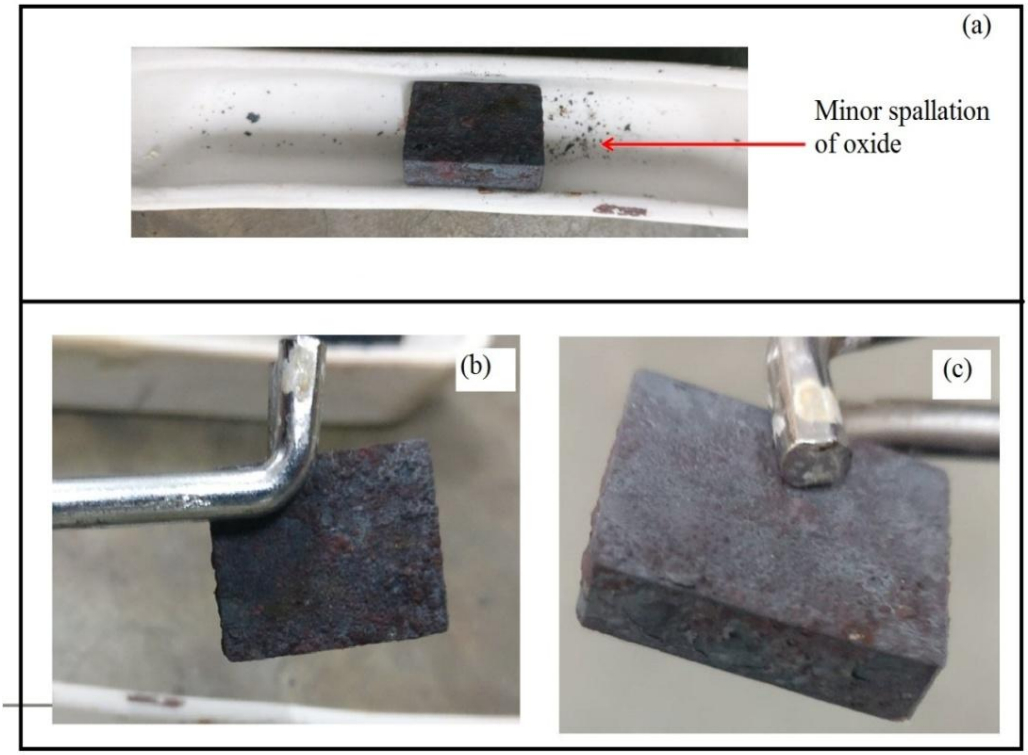

Figure 6.3 Macrophotos of bare T91 steel after subjected to corrosion run for (a) 1st cycle, (b) 25th cycle and (c) 50th cycles at 800°C under simulated bio fuel fired boiler environment

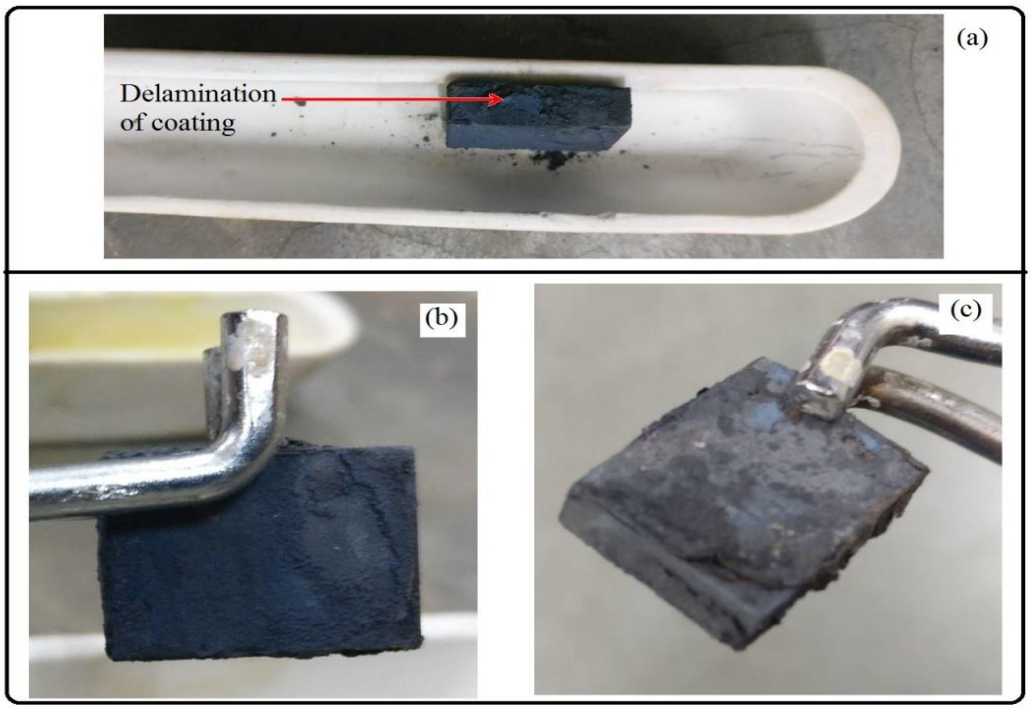

Figure 6.4 Macrophotos of WC-Co coated T91 steel after subjected to corrosion run for (a) 1st cycle, (b) 25th cycle and (c) 50th cycles at 800°C under simulated bio fuel fired boiler environment

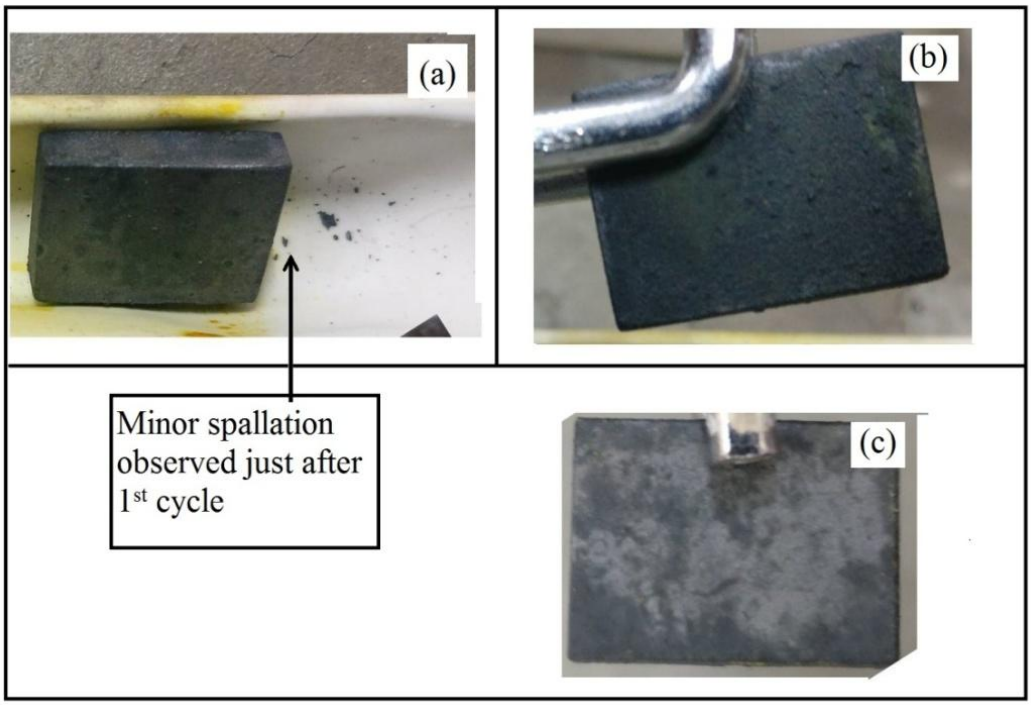

Figure 6.5 Macrophotos of Cr_3C_2-NiCr coated T91 steel after subjected to corrosion run for (a) 1st cycle, (b) 25th cycle and (c) 50th cycles at 800°C under simulated bio-fuel fired boiler environment

Table 6.1 Parabolic rate constant (K_p) values for bare T91, and WC-Co coated T91 and Cr_3C_2-NiCr coated T91 after subjected to molten salt corrosion at 800ºC for 50 cycles.

Substrates	$K_p \times 10^{-8} g^2 cm^{-4} s^{-1}$
Bare T91	15.35
WC-Co coated T91	204.1
Cr_3C_2-NiCr coated T91	8.07

6.2.3 SEM/EDS analysis

SEM micrograph for Bare T91 steel, WC-Co coated T91 steel and Cr_3C_2-NiCr coated T91 steel are shown in figure 6.6, 6.7 and 6.8 with EDS spectrum. From the results it has been clearly observed that globular and compact oxide was formed on the surface of bare T91 steel and observed porosity on the sample. Fine needle type of oxide can be seen in case of Cr_3C_2-NiCr coated T91steel and massive oxide clearly seen in WC-Co coated T91 steel. EDS

analysis showed the presence of oxygen, iron, molybdenum, sodium and potassium in bare T91 steel. In WC-Co coated T91 steel minor amount of potassium and huge amount of chromium and oxygen were present. Cobalt, chlorine, phosphorus, silicon, iron ,tungsten and oxygen are present in Cr_3C_2-NiCr coated T91 steel.

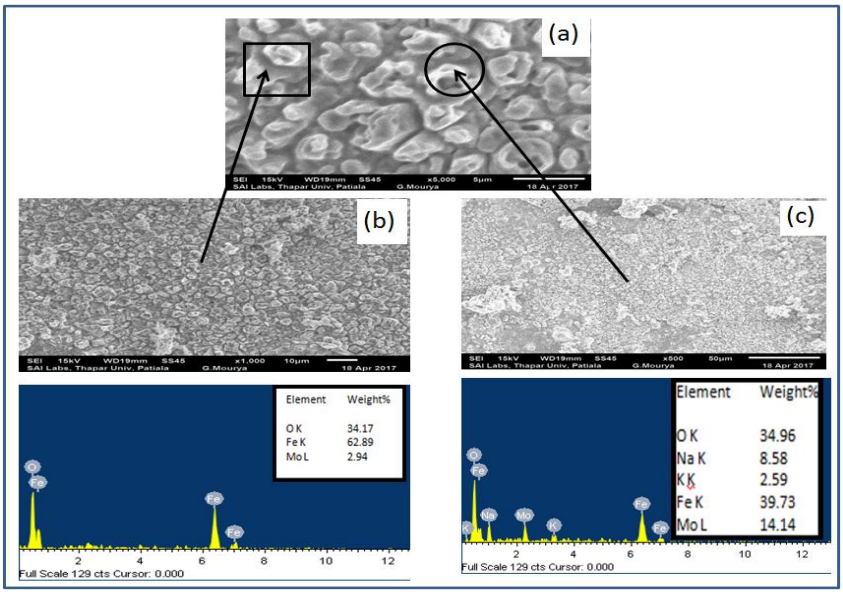

Figure 6.6 SEM Micrograph along with EDS at some selected sites on bare T91 after subjected to hot corrosion under simulated bio-fuel fired boiler environment at 800°C for 50 cycles

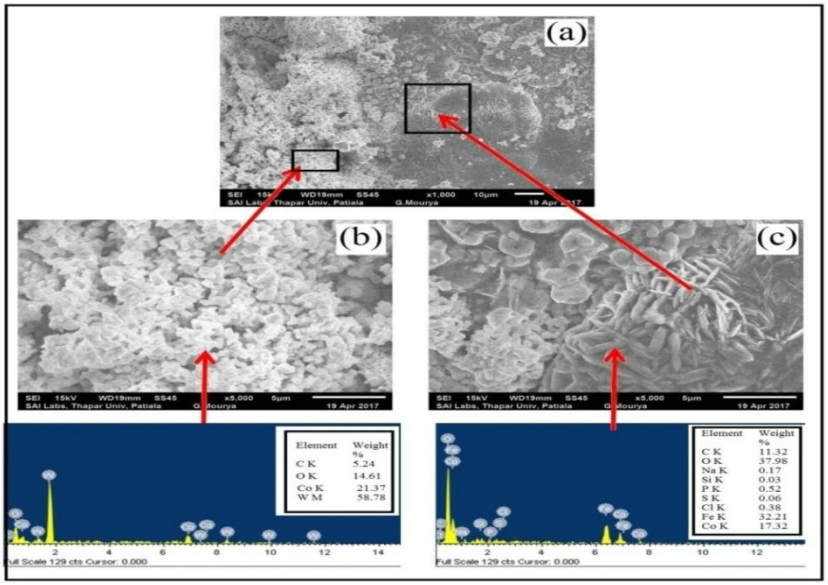

.

Figure 6.7 SEM micrograph along with EDS at some selected sites on WC-Co Coated T91 steel subjected to cyclic hot corrosion under simulated bio-fuel fired environment at 800°C for 50 cycle

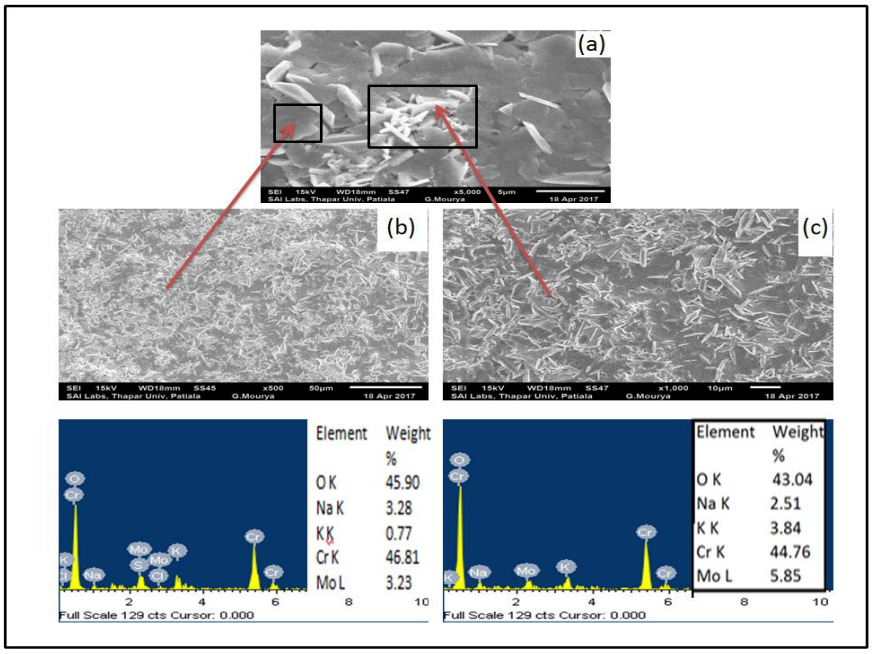

Figure 6.8 SEM micrograph along with EDS at some selected sites on Cr_3C_2-NiCr subjected to cyclic hot corrosion under simulated bio-fuel fired environment at 800°C after 50 cycles

6.2.4 XRD analysis

XRD graph has been plotted between Intensity and diffraction angle 2θ to identify the phases present in the scale formed. This can be done by comparing the 'd' value of intensity peaks. X-ray diffractograms of the scale formed on the oxidized steel are shown in figure. 6.9. The major phases indentified in case of Cr_3C_2-NiCr samples are Cr_2O_3, $CrCl_3$, Na_2SO_4 and Cr_3S_4, Whereas in case of WC-Co the major oxide are Co_3O_4, FeO, Fe_3O_4 etc. and In case of bare sample the formation of oxide are Cr_2O_3 MnO_2 and Mn_3O_4 was illustrated in the oxide.

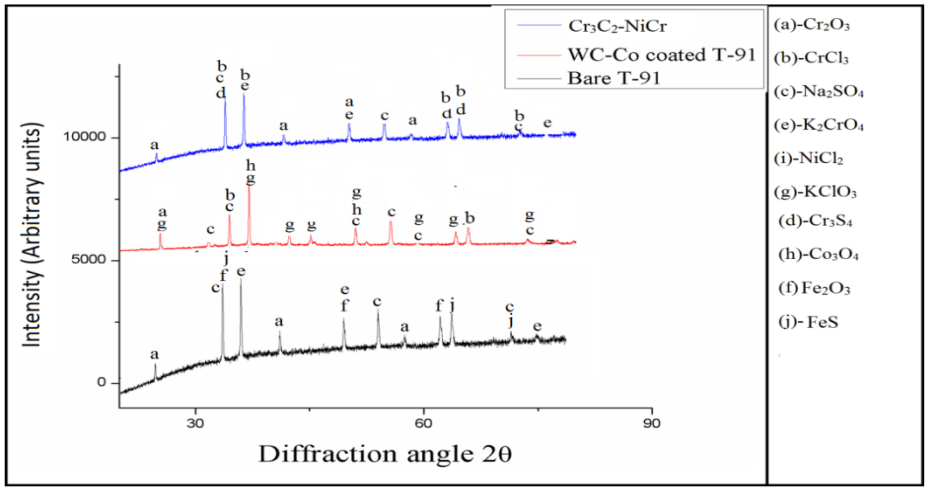

Figure 6.9 XRD analyses of bare, Cr_3C_2-NiCr and WC-Co coated T91 steel after hot corrosion under simulated bio-fuel fired boiler environment at 800°C for 50 Cycles

6.2.5 Elemental X-ray Mapping

The elements present in the oxide layer that were found by X-Ray mapping were C, O, Cr, Fe, Na, K and Mo in case of bare sample. Chromium oxide is formed on all the three substrate. This is because of the presence of chromium in base metal that is T91 steel and in Cr_3C_2-NiCr coated T91 steel Fe_2O_3 act as non protective oxide for the bare sample. Chromium have tendency to form oxide when exposed at high temperature presence of K_2CrO_4 was also seen indicated in case of Cr_3C_2-NiCr coated T91 steel. Chromium oxide formed on this coating because of the conversion of chromium carbide to chromium oxide. Elements present in Cr_3C_2-NiCr coated T91 steel are C, O, Fe, Ni and Cr. Chromium oxide was observed in WC-Co coated T91 steel also because T91 steel delaminated from the substrate. Fe_2O_3 and Co_3O_4 are the non protective oxide.

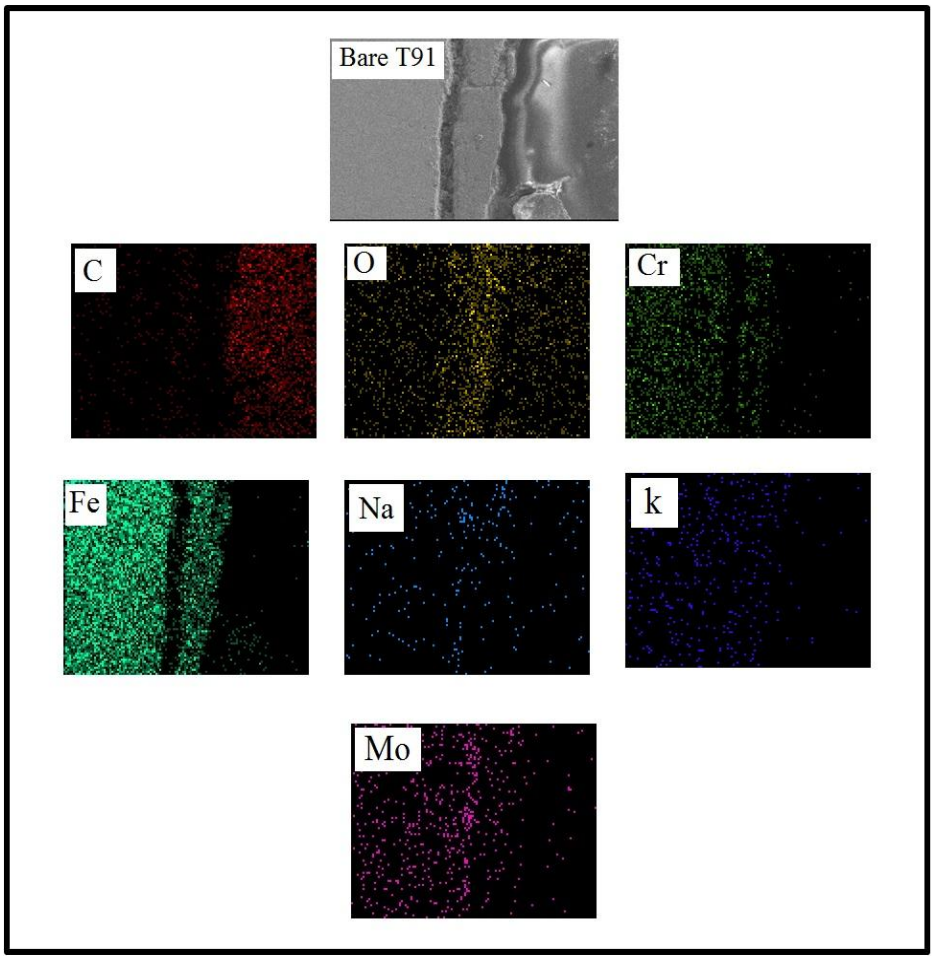

Figure 6.10 X-Ray mapping of bare T91 steel subjected to cyclic hot corrosion under molten enviroment at 800°C after 50 cycles

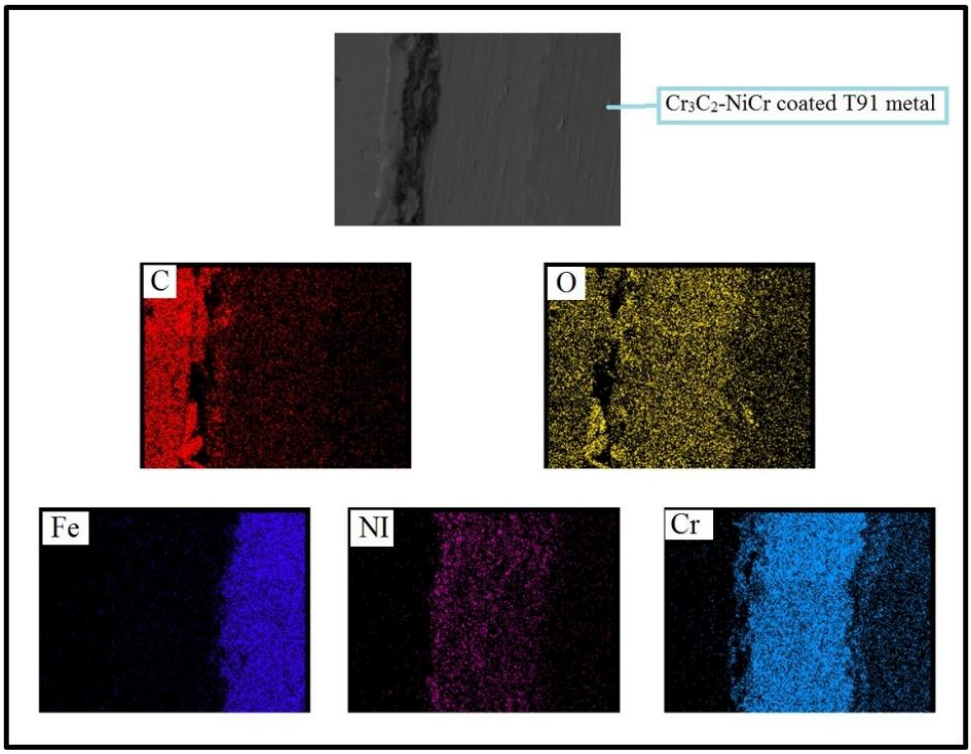

Figure 6.11 X-Ray mapping of Cr_3C_2-NiCr coated T91 steel subjected to cyclic hot corrosion under molten enviroment at 800°C after 50 cycles.

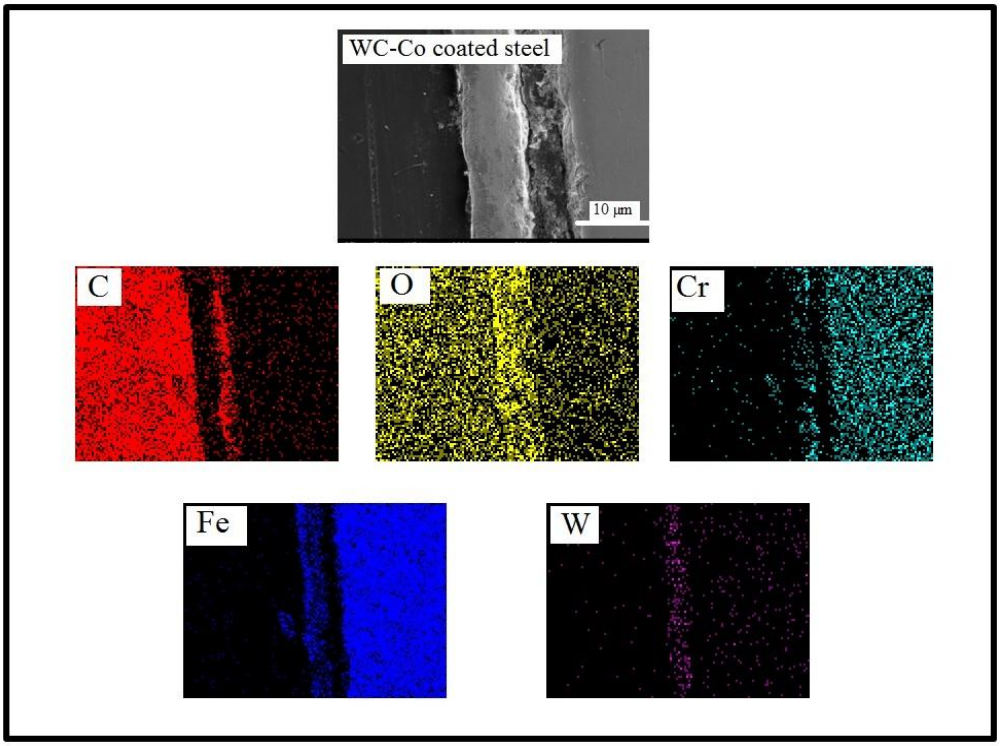

Figure 6.12 X-Ray mapping of WC-Co coated T91 steel subjected to cyclic hot corrosion under molten enviroment at 800°C after 50 cycles

6.3 Discussion

Visual analysis clearly show that Bare T91 steel and Cr_3C_2-NiCr coated T91 steel suffered from minor spallation. Presence of reddish oxide on the surface of T91 depicts the formation of iron oxide just after 1st cycle. Similar observation was also reported elsewhere (Nallan 2001). They reported that reddish colour oxide was formed due to presence of iron in the substrate. In the later cycle it was also observed that the oxide of the colour changes to dark grey which depicts the formation of chromium oxide. Figure 6.2 shows the visual macrophotos of WC-Co coated T91 steel. It can be observed that the coating got delaminated from the surface of the substrate. This might have occurred because of the co-efficient of thermal expansion mismatch between the steel substrate and the coating. Although, the coating was intact before the experimentation. However, after hot corrosion experiments, the substrate and the coating experiences sudden thermal fluctuations. This creates the sudden expansion and contraction in the substrate and coating, thereby leading to delamination of the coating from the substrate. From weight gain graph (figure. 6.4) also, it can be depicted that WC-Co coated T91 steel suffered from very high weight gain starting from the 1st cycle till 50th cycle. This might have occurred because of the formation of oxide as well as delamination of coating. Whereas, both bare T91 steel and Cr_3C_2-NiCr coated T91 steel showed initial weight gain which becomes constant after few cycles. Initial weight gain was occurred because of the formation of the oxides during exposure of the specimens at high temperature. As, these samples have tendency to form oxides if exposed to high temperature. Similar results have been discussed by (Mahesh *et al.*2012) (H Singh *et al.* 2006).However, the graph became constant after few cycle which shows that the oxide formed on the substrate is protective which does not allows any diffusion from substrate towards the environment or vice versa. It was also seen from the graph that the weight gain of Bare T91 steel is more as compare to Cr_3C_2-NiCr coated T91 steel. This shows the less protective nature of substrate as compared to Cr_3C_2-NiCr coated T91 steel. Minor spallation also causes the higher weight gain of bare substrate. Graphs shown in figure 6.5 helps in identifying the parabolic behaviour of substrates. Form parabolic rate constant it can be predicted that Cr_3C_2-NiCr coated T91 steel shows best resistance to corrosion under the given environment. Parabolic behaviours of graphs shows that the oxide formed on the substrate plays a protective role.

SEM analysis for all the three alloys has been done to know the surface morphology and is shown in figure 6.6, 6.7 and 6.8. Surface morphology of the oxide formed on WC-Co coated

T91 steel indicated the formation of different types of morphology. Needle type morphology depicts the presence of oxygen, cobalt and iron in major amount. Fe might have present because of the exposure of the base metal due to delamination of the coating. Cobalt was present because of the presence of cobalt in coating. Oxygen shows that the oxide of cobalt and iron might have formed after the exposure of specimens at high temperature. EDS analysis also confirms the presence of tungsten, cobalt and oxygen on the surface. SEM analysis of Cr_3C_2-NiCr coated T91 steel shows the formation of dense needle type oxide consisting of chromium and oxygen in major amount. Similar results of formation of needle type oxide in case of Cr_3C_2-NiCr coating has been reported elsewhere (Mudgal *et al.* 2015). EDS analysis also shows the presence of sodium and potassium which might have present from the salt deposits.

XRD (figure. 6.8) analysis predicts that chromium oxide is formed on all the three substrate. This is because of the presence of chromium in base metal that is T91 steel and in Cr_3C_2-NiCr coated T91 steel. Chromium oxide was observed in WC-Co coated T91 steel also because T91 steel delaminated from the substrate. In bare T91 steel chromium oxide was formed because chromium was present in this substrate. Chromium have tendency to form oxide when exposed at high temperature (Kumar *et al.* 2013). Existence of K_2CrO_4 was also seen indicated in case of Cr_3C_2-NiCr coated T91 steel. Chromium oxide formed on this coating because of the conversion of chromium carbide to chromium oxide as shown in reaction (6.1)(Matthews *et al.* 2009).

$$Cr_3C_2 \xrightarrow{+O_2} Cr_7C_3 \xrightarrow{+O_2} Cr_{23}C_6 \xrightarrow{+O_2} [Cr_{MET}] \xrightarrow{+O_2} Cr_2O_3 \text{.....} \quad (6.1)$$

6.4 Conclusions

1. Cr_3C_2-NiCr coating and WC-Co coating was successfully deposited on T91 steel using Detonation gun processes.

2. WC-Co coating was got delaminated from the substrate after few cycles whereas Cr_3C_2-NiCr coating remains intact throughout the experiments when subjected to cyclic hot corrosion run under simulated bio-fuel fired environment at 800°C for 50 cycles.

3. Chromium oxide was formed in all the three alloys. Chromium oxide is mainly responsible for providing protection to Cr_3C_2-NiCr coating and bare sample.

Chapter 7

Studies under actual biomass fuel fired boiler

7.1 Introduction

Biomass has become most widely used source of energy fuel. This is because of the limited availability of non-renewable source of energy such as fossil fuels. Burning of fossil fuel also causes production of green house gases. Hence, biomass such as agricultural residues and wood wastes becomes a viable substitute fuel in electricity generation units (Yoon *et al.* 2012) (Arbon 2002). As reduction in green house gases is one of the biggest advantages of using biomass fuel (Demirbas 2005) (Oliveira *et al.* 2012). Moreover, co-combustion of Biomass-coal also represents a sustainable, low-risk, low-cost, renewable energy option that assured net reduction in SOx and often NOx and CO_2 emissions (Baxter 2005) .

Rice husk is one of the bio-fuel which is being extensively used as a boiler fuel in power boilers as well as different processing industries. It is as excellent fuel with 3,000 kcal per kg of heating value (calorific value) (Web references 1). However, burning of husk produces lot of salt deposits which can contaminate the environment of the boiler. These salt species get deposited on the surface of the components used in the boilers. These deposits then react with the metal oxide formed on the components. Reactions may cause the degradation of the oxide layer by dissolving it. Due to this reactions, the oxide layer will again formed on the surface thus consuming the elements present in the component. This will further reduces the life of the component. Hence, some external protection is required to protect the component for longer hours.

To obviate this problem, the experiments has been carried out in actual husk fired boiler environment operating at 750°C for 48h. Ferritic steel T91 has been chosen for the studies as the heat exchangers installed in the boiler is made up of this particular steel only. Then, two different coating were deposited on the surface of the steel using detonation gun technique. A hole was drilled in all the three substrates. All the three samples were hung inside the boiler for 48 working hours using kanthal wire A grade. The exposed samples were then characterized using SEM/EDS and XRD analysis.

7.2 Results

7.2.1 Visual analysis

Figure 7.1 shows the sample before carrying out experimentation. After 48 h of exposure the samples were removed from the boiler for visual inspection and has shown in figure 7.2. It was observed that reddish colour oxide was formed on the surface of bare T91 steel. Oxide seems to be fragile. In case of Cr_3C_2-NiCr coated T91 steel, greenish colour oxide was formed on the surface of the coating along with the dark grey background. While, WC-Co coated T91 steel also showed erratic behaviour. It shows that the coating was delaminated from one of the corner.

7.2.2 SEM/EDS analysis

Surface morphology of the specimens exposed under boiler environment was observed using SEM analysis. The elemental analysis was done using EDS spectrum. From fig 7.4, it was observed that the oxide formed on the surface of Cr_3C_2-NiCr coated T91 steel was porous. Two different type of morphologies were seen on the surface. Columnar oxide mainly consisting of oxygen, sodium, magnesium, silicon, calcium, chromium, manganese, nickel and tin. Whereas clusters oxide is consisting of oxygen, chromium and silicon in major amount and nickel, manganese, calcium and magnesium in minor amount. In case of WC-Co coated T91 steel, it was observed that oxide was delaminated from the surface. Figure 7.5(a) depicts the two different areas of coating. In figure 7.5, Point 1 shown in the image shows the presence of cobalt, tungsten, oxygen, iron and potassium. Whereas, point 2 shown in the figure indicates the existence of chromium, tungsten, iron and oxygen.

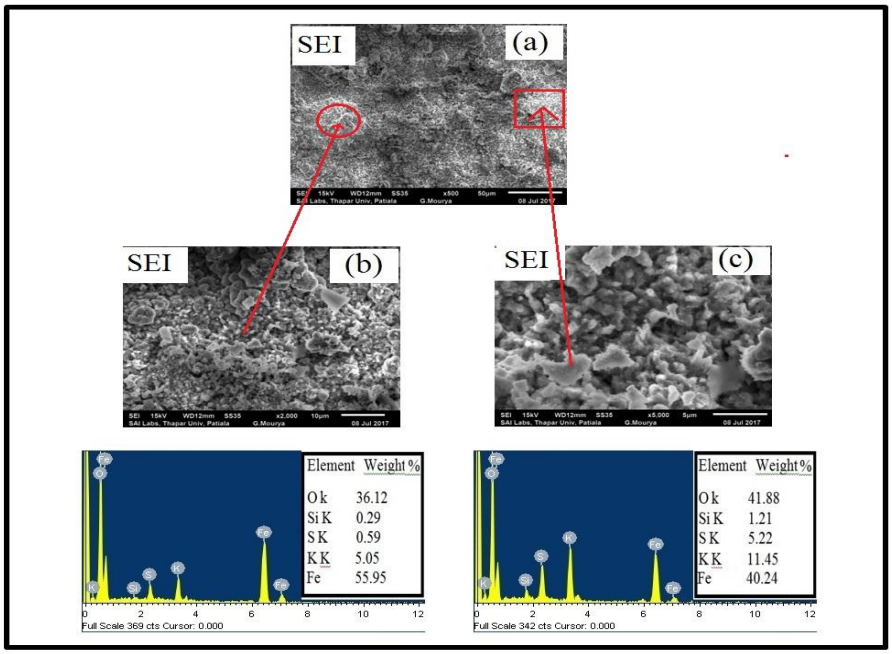

Figure 7.1 SEM micrograph along with EDS spectrum of bare T91 steel after exposed in husk fired boiler for 48h at 750±50°C

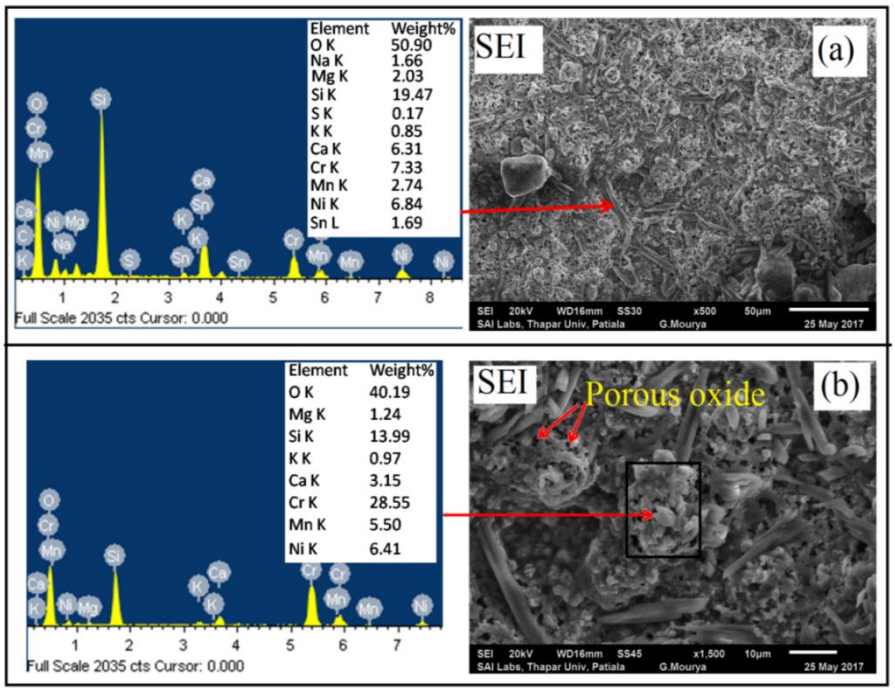

Figure 7.2 SEM micrograph along with EDS spectrum of Cr_2C_3-NiCr coated T91 steel after exposed in husk fired boiler for 48h at 750±50°C

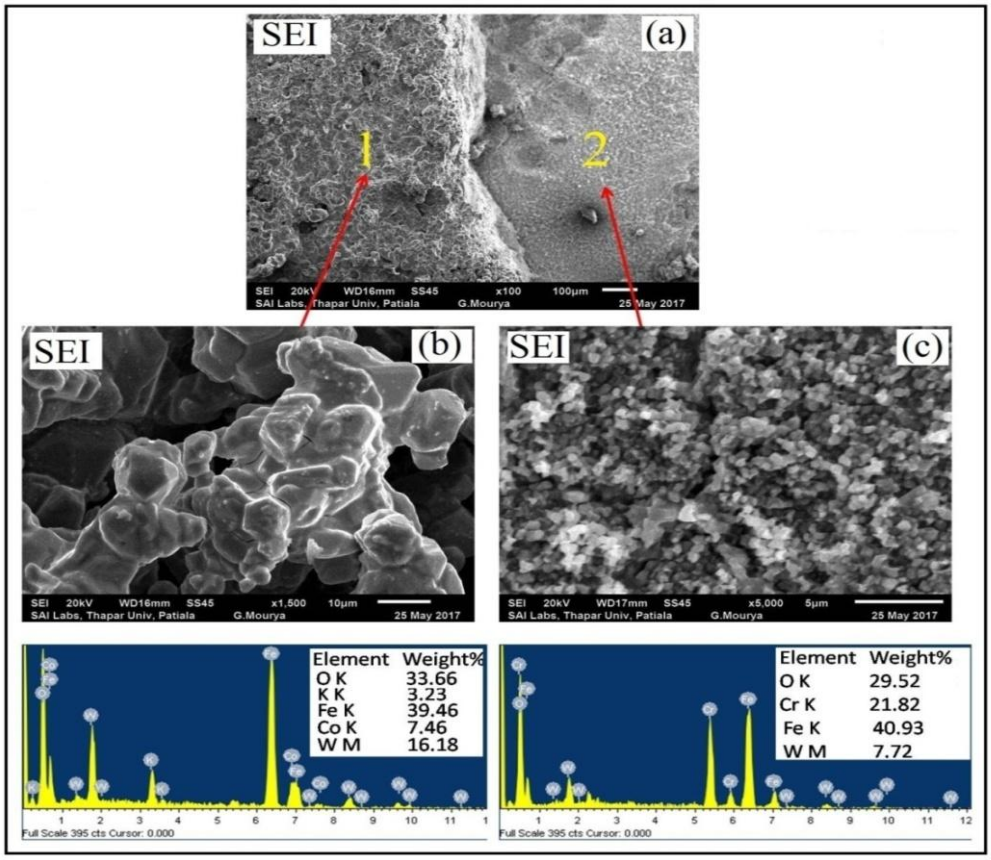

Figure 7.3 SEM micrograph along with EDS spectrum of WC-Co coated T91 steel after exposed in husk fired boiler for 48h at 750±50°C

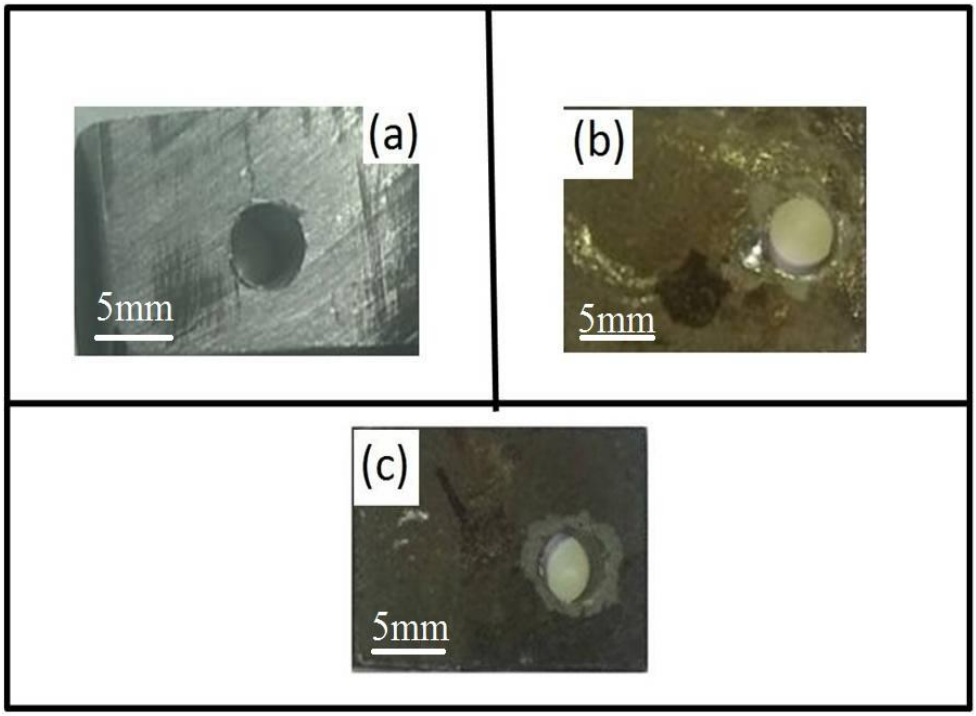

Figure 7.4 Macro photos of uncorroded (a) Bare (b) Cr_3C_2-NiCr and (c) WC-Co coated T91 steel

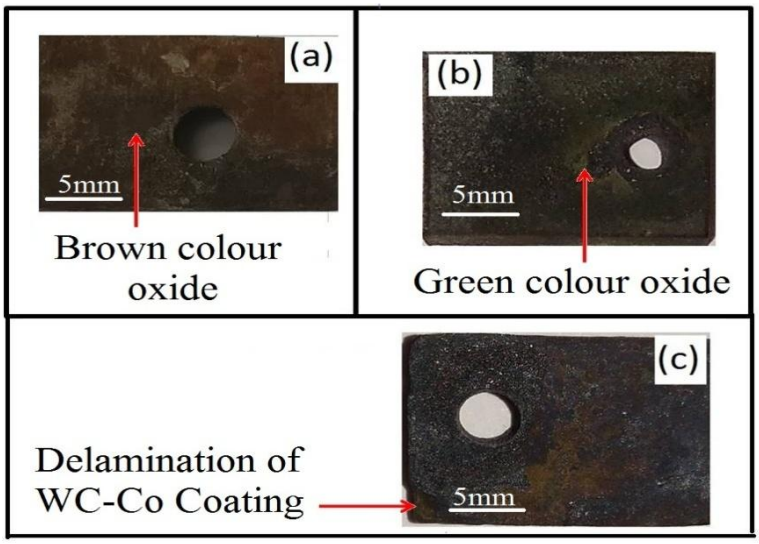

Figure 7.5 Macro photos of corroded (a) Bare (b) Cr_3C_2-NiCr and (c) WC-Co coated T91 steel after subjected to hot corrosion under actual boiler environment for 48 h

7.2.3 XRD analysis

XRD graph has been plotted between Intensity and diffraction angle 2θ to identify the phases present in the scale formed. This can be done by comparing the 'd' value of intensity peaks. X-ray diffractograms of the scale formed on the oxidized steel are shown in figure. 7.6. XRD analysis of Cr_3C_2-NiCr coated T91 steel showed the formation of K_2CrO_4, Mg_2SiO_4, MnO_2, CaO, SiO_2, $CaCr_2O_4$, Ni_2SiO_4 and $NiCr_2O_4$. Whereas WC-Co coated T91 steel, indicated the formation of $NiCr_2O_4$, $CoCr_2O_4$, $CoWO_4$, $FeWO_4$ and Co_3O_4. In case of bare sample formation of oxide are Cr_2O_3, Cr_2S_3, and $FeSiO_3$ was illustrated in the oxide

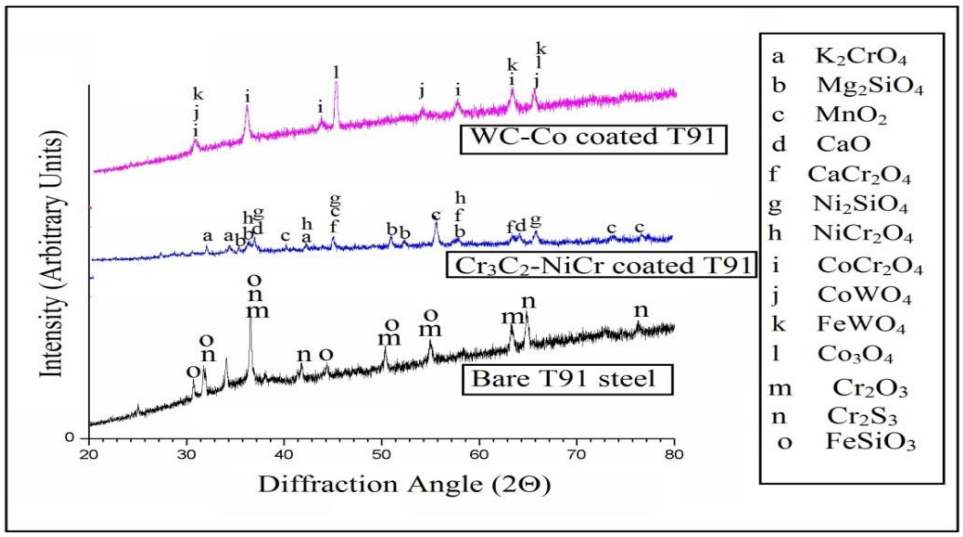

Figure 7.6 XRD analysis of bare, Cr_3C_2-NiCr and WC-Co coated T91 steel after exposed in husk fired boiler for 48h at 750±50°C

7.2.4 Elemental X-Ray Mapping

The elements present in the oxide layer that were found by using x ray mapping, The elements were found in case of bare T91 steel are Fe, Al ,Cr C, and Cl. High presence of Cr and Fe can be seen in metal and oxide region from X-Ray mapping. Formation iron oxide leads to less protective behaviour of bare T91 steel. The XRD analysis also shows the presence of two main phases in bare sample that were Fe_2O_3(non protective) and Cr_2O_3(protective) . However in case of Cr_3C_2-NiCr coating the elements present are C, Fe, Ni, Cr and O. Cr_2O_3 oxide was mainly responsible for providing protection to Cr_3C_2-NiCr coated steel. In case WC-Co coated T91 sample C, O, Cr, W and Fe were found from the X-Ray mapping.

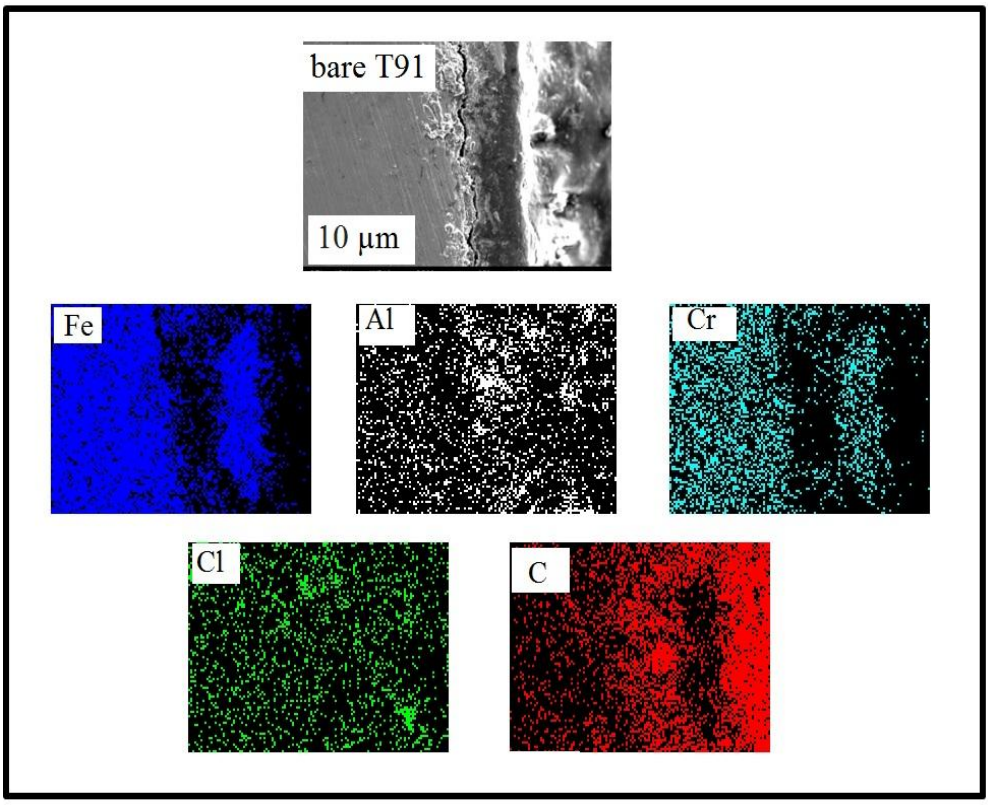

Figure 7.7 X-Ray mapping of bare T91 steel after exposed in husk fired boiler for 48h at 750±50°C

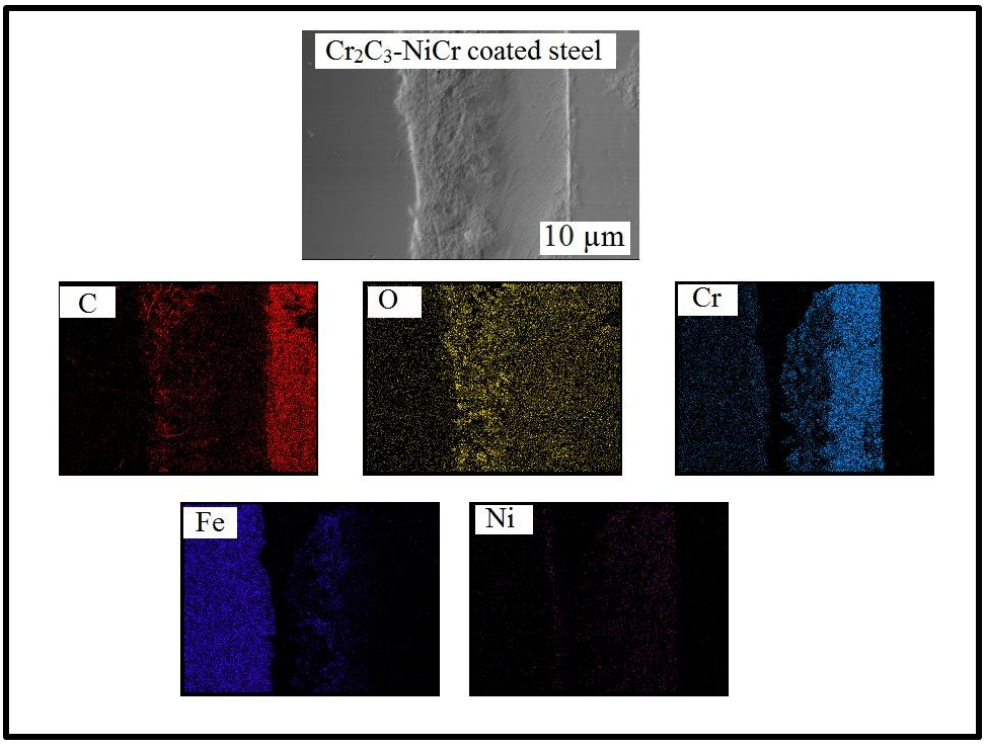

Figure 7.8 X-Ray mapping of Cr_3C_2-NiCr coated T91 steel after exposed in husk fired boiler for 48h at 750±50°C

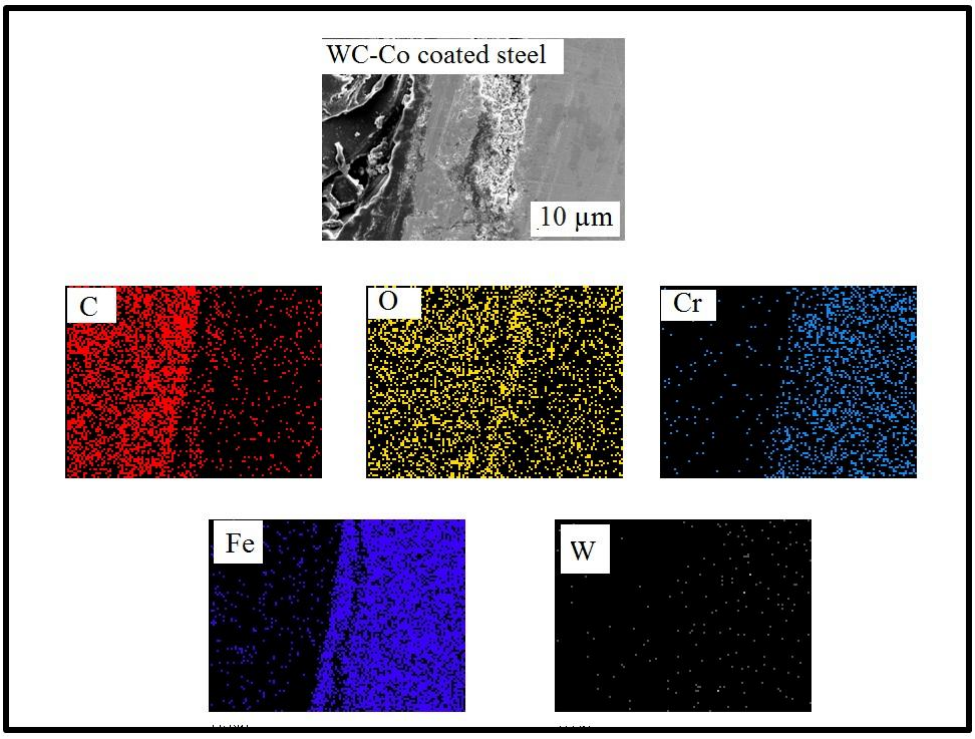

Figure 7.9 X-Ray mapping of WC-Co coated T91 steel after exposed in husk fired boiler for 48h at 750±50°C

7.3 Thickness loss measurements

The thickness loss describe the how much thickness is lost during the experiment.Cr3C2 coated steel experienced less thickness loss is about of 0.39mm.Thickness loss in WC-Co is high is of 0.96mm and in case of bare sample thickness loss is 0.62mm.

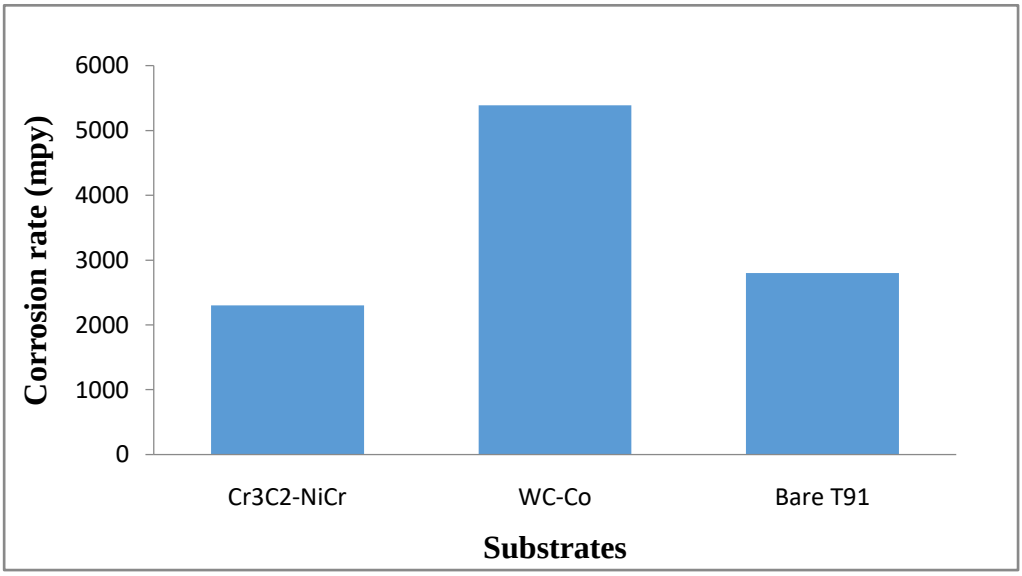

Figure7.10 Thickness loss measurements of Cr_3C_2-NiCr and WC-Co coated T91 steel and bare T91 steel after exposed in husk fired boiler for 48h at 750±50°C

7.4 Discussion

Form visual analysis it was clearly indicated that bare T91 steel suffered for corrosion under the given environment. Whereas, chromium carbide-nickel chromium showed protective behaviour under the husk fired boiler atmosphere. Formation of reddish colour (figure 7.2(a)) oxide clearly depicts the formation iron oxide in case of T91 steel. Whereas existence of green colour oxides shows that the oxide of chromium might have formed on the surface of Cr_3C_2-NiCr coated T91 steel (figure 7.2(b)). WC-Co coated T91 steel does not performed satisfactorily under boiler atmosphere.

SEM analysis of Cr_3C_2-NiCr coated T91 steel shows that the oxide formed on the surface of the coating is porous. Although the coating was protective among all the three substrate. However, the oxide formed on the substrate is unprotective. It id because of the presence of different salt species which combines with protective oxide layer and dissolve it thereby leading to the formation of unprotective porous oxide . WC-Co coated T91 steel shows two

different morphology. Point 1 (figure 7.5) reveals the oxide formed on the coating having tungsten and cobalt. Whereas point 2 (figure) shown porous unprotective oxide formed on the steel substrate after coating delamination showing high amount of iron and tungsten.

XRD analysis shows the formation of K_2CrO_4, Mg_2SiO_4, MnO_2, CaO, SiO_2, $CaCr_2O_4$, Ni_2SiO_4 and $NiCr_2O_4$ in case of Cr_3C_2-NiCr coated T91 steel. K_2CrO_4 might have formed on the outer layer of the Cr_3C_2-NiCr coating. When Cr_3C_2-NiCr coating was exposed at high temperature, chromium oxide was formed by decomposition of chromium carbide into chromium oxide. Also chromium have tendency to formed oxide because of its negative Gibbs free energy at high temperature. Hence when this coating was exposed, Cr_2O_3 was formed on the surface. Also, it was reported that potassium is present in the husk fired boiler in large amount. It may be possible that this Cr_2O_3 reacts with KCl present in boiler environment to form K_2CrO_4 by the following reactions 7.1.

$$Cr_2O_3(s) + 4KCl(s) + (\frac{5}{2})O_2(g) \rightarrow 2K_2CrO_4(s) + 2Cl_2(g) \quad \text{.....(7.1)}$$

Similarly, $NiCr_2O_4$ oxide was formed after solid state reaction between nickel oxide and chromium oxide. Nickel and chromium is present in the coating which when combine with oxygen formed oxide as shown in equation 7.2.

$$NiO + Cr_2O_3 \longrightarrow NiCr_2O_4 \quad \text{.....(7.2)}$$

In case of WC-Co coated T91 steel, $CoCr_2O_4$ oxide was formed on the surface. Cobalt have tendency to form oxide when exposed at high temperature. Co_3O_4 or CoO is generally formed. However, if chromium is also present in the coating or substrate. Then this cobalt oxide combines with the chromium oxide to form spinel as shown in equation 7.3 (Birks *et al.*2006).

$$Cr_2O_3 + CoO \longrightarrow CoCr_2O_4 \quad \text{……(7.3)}$$

The poor resistance of the WC-Co coating in the given environment might be due to the presence of tungsten. As it was reported by (Elliott 2001) that tungsten have tendency to form volatile compounds which can evaporate from the oxide thus leaving the oxide unprotective.

7.4 Conclusions

1. Cr_3C_2-NiCr coated T91 steel showed best corrosion resistance among all the samples.

2. Formation of $NiCr_2O_4$ might have resulted in providing god corrosion resistance to the coated substrate.

3. Presence of tungsten seems to have detrimental effect on coating under the given environment.

4. $CoCr_2O_4$, $CoWO_4$, $FeWO_4$ and Co_3O_4 were formed in case of WC-Co coated T91 steel whereas CaO, SiO_2,and $CaCr_2O_4$ were found to be the major phases in case of Cr_3C_2-NiCr coated T91 steel.

Chapter 8

Conclusion

8.1 Oxidation study

1. T91 steel and Cr_2C_3-NiCr coated steel showed good oxidation resistance while subjected to oxidation in air at 800°C for 50 cycles. However, WC-Co coating was totally delaminated from the substrate.

2. Cr_2O_3 oxide was mainly responsible for providing protection to Cr_3C_2-NiCr coated steel whereas formation of iron oxide leads to less protective behaviour of bare T91 steel. In case of bare T91 steel, major phases indentified were Cr_2O_3, FeO and Fe_2O_3. Whereas in case of Cr_3C_2-NiCr coated T91 steel, main phases identified were Cr_2O_3, $Cr_{23}C_6$ and Cr_7C_3. In case of WC-Co coated T91 steel, peaks of $CoCr_2O_4$, Co_3O_4 , WO_3 and Cr_2O_3 were seen.

3. Formation of WO_3 might have contributed to the poor corrosion resistance of WC-Co coated T91 steel.

4. Based on overall weight gain after exposure of 50 cycles in air environment at 800°C, the oxidation resistance of the bare steel studied in the present investigation has been found to be in the following order:

Cr_3C_2-NiCr Coated steel> bare T91 steel >WC-Co coated T91 steel

8.2 Hot corrosion

1. Based on overall weight gain after 50 cycles in molten salt environment at 800°C for bare and coated T91 steel could be arranged in the following order.

$Na_2SO_4+K_2SO_4+NaCl+KCl$: Cr_3C_2-NiCr Coated steel> bare steel >WC-Co coated T91 steel

2. WC-Co coating got delaminated from the substrate after few cycles whereas Cr_3C_2-NiCr coating remains intact throughout the experiments when subjected to cyclic hot corrosion run under simulated bio-fuel fired environment at 800°C for 50 cycles.

3. The major phases indentified in case of Cr_3C_2-NiCr samples are Cr_2O_3, $CrCl_3$, Na_2SO_4 and Cr_3S_4, Whereas in case of WC-Co the major oxide are Co_3O_4, FeO, Fe_3O_4 and In case of bare sample the formation of oxide are Cr_2O_3 MnO_2 and Mn_3O_4 was formed.

4. Chromium oxide was formed in all the three alloys. Whereas iron oxide was also formed.

5. Chromium oxide is mainly responsible for providing protection to Cr_3C_2-NiCr coating and bare T91 substrate under the aggressive atmosphere.

8.3 Actual enviroment

1. Cr_3C_2-NiCr coated T91 steel showed best corrosion resistance among all the samples.

2. Formation of $NiCr_2O_4$ might have resulted in providing good corrosion resistance to the coated substrate.

3. Presence of tungsten seems to have detrimental effect on coating under the given environment.

4. $CoCr_2O_4$, $CoWO_4$, $FeWO_4$ and Co_3O_4 were formed in case of WC-Co coated T91 steel whereas CaO, SiO_2,and $CaCr_2O_4$ were found to be the major phases in case of Cr_3C_2-NiCr coated T91 steel. Two main phases in bare sample that were Fe_2O_3(non protective) and Cr_2O_3(protective)

From the all samples Cr_3C_2-NiCr coated T91 steel showed excellent corrosion resistant in oxidation test, in hot corrosion test and in actual boiler enviroment whereas WC-Co coated steel showed poor corrosion resistance in all three study. The coating of WC-Co coated steel was delaminated in all studies. In case of bare sample, the specimen showed slight better performance as compared to WC-Co coated steel. The order of performance of corrosion resistance from all the all study is given below.

Cr_3C_2-NiCr Coated steel> bare T91 steel >WC-Co coated T91 steel.

8.4 Future scope

1.Rare earth/Reactive elements addition should be tried into the coating at different concentration to find out the optimum content for obtaining a desired properties.

2.Stepwise corrosion mechanism should be formulated to understand the mechanism of corrosion in incinerators environment.

3.superalloys substrate can be taken instead of steel to assess the protective role of the coatings. More study should be done in actual medical waste incinerator environment for longer durations and actual biomass fuel fired boiler.

4.Study of coating thickness of thermal spray coating process using Taguchi method.

5.Study of nano structured coatings under different environment.

6.Developing hydrophobic and super hydrophobic coating.

References

1. Armesto L., Bahillo, A., Veijonen,K., Cabanillas,A., & Otero, J. (2002). Combustion behaviour of rice husk in a bubbling fluidised bed. Biomass and Bioenergy, 23(3), 171-179.
2. Arbon, I. M. (2002). Worldwide use of biomass in power generation and combined heat and power schemes. Proceedings of the Institution of Mechanical Engineers, Part A: Journal of Power and Energy, 216(1), 41-57.
3. Baddoo, N. R. (2008). Stainless steel in construction: A review of research, applications, challenges and opportunities. Journal of Constructional Steel Research, 64(11), 1199-1206.
4. Benjamin, J.S. (1970). Dispersion strengthened super alloys by mechanical alloying. Metallurgical transactions, 1(10), 2943-2951.
5. Baxter, L. (2005). Biomass-coal co-combustion: opportunity for affordable renewable energy. Fuel, 84(10), 1295-1302.
6. Baxter, L. L., Miles, T. R., Jenkins, B. M., Milne, T., Dayton, D., Bryers, R. W., & Oden, L. L. (1998). The behavior of inorganic material in biomass-fired power boilers: field and laboratory experiences. Fuel processing technology, 54(1), 47-78.
7. Birks, N., Meier, G. H., & Pettit, F. S. (2006). Introduction to the high temperature oxidation of metals.2nd edition, Cambridge University Press, United Kingdom.
8. Chatha, S. S., Sidhu, H. S., & Sidhu, B. S. (2012). High temperature hot corrosion behaviour of NiCr and Cr_3C_2–NiCr coatings on T91 boiler steel in an aggressive environment at 750°C. Surface and Coatings Technology, 206(19), 3839-3850.
9. Chawla, V., Chawla, A., Puri, D., Prakash, S., Gurbuxani, P. G., & Sidhu, B. S. (2011). Hot corrosion & erosion problems in coal based power plants in India and possible solutions–a review. Journal of minerals and materials characterization and Engineering, 10(04), 367.
10. Cha, S. C., & Spiegel, M. (2004). Fundamental Studies on Alkali Chloride Induced Corrosion during Combustion of Biomass. Materials Science Forum, 461-464, 1055–1062.
11. Chattopadhyay, S.(2004). Pressure vessels: design and practice. CRC press,Taylor and Francis group , USA

12. Deshpande, S. V., Gulari, E., Harris, S. J., & Weiner, A. M. (1994). Filament activated chemical vapor deposition of boron carbide coatings. Applied physics letters, 65(14), 1757-1759.
13. Daniel, P. L., Barna, J. L., & Blue, J. D. (1986, June). Furnace-wall corrosion in refuse-fired boilers. In Proc. 1986 Natl. Waste Proc. Conf., Denver, Colorado (p. 221).
14. Demirbas, A. (2005). Potential applications of renewable energy sources, biomass combustion problems in boiler power systems and combustion related environmental issues. Progress in energy and combustion science, 31(2), 171-192.
15. Elliott, P. (2001). Choose Materials for High-Temperature Environments, Chemical Engineering Progress, 97(2), 75-91.
16. Fauchais, P. (2004). Understanding plasma spraying. Journal of Physics D: Applied Physics, 37(9), R86.
17. French, D. (1992). Austenitic stainless steel. The National Board of Boiler and Pressure Vessel Inspectors Bulletin.
18. Gardner, L., Insausti, A., Ng, K. T., & Ashraf, M. (2010). Elevated temperature material properties of stainless steel alloys. Journal of Constructional Steel Research, 66(5), 634-647.
19. Gond, D., Chawla, V., Puri, D., & Prakash, S. (2010). Oxidation Studies of T-91 and T-22 Boiler Steels in Air at 900 C. Journal of Minerals and Materials Characterization and Engineering, 9(08), 749-761.
20. Herman, H., Sampath, S., & McCune, R. (2000). Thermal spray: current status and future trends. MRS bulletin, 25(7), 17-25.
21. Henderson, P. J., Ljung, P., Kallner, P., & Tollin, J. (2000). Fireside corrosion of superheater materials in a wood-fired circulating fluidised bed boiler. In Proceedings of the Euro Corr.
22. Henderson, P., Szakalos, P., Pettersson, R., Andersson, C., & Högberg, J. (2006). Reducing superheater corrosion in wood-fired boilers. Materials and corrosion, 57(2), 128-134.
23. Herman, H., Sampath, S., & McCune, R. (2000). Thermal spray: current status and future trends. MRS bulletin, 25(7), 17-25.
24. Kaiser, J. J., Zurecki, Z., Berger, K. R., Swan, R. B., & Hayduk Jr, E. A. (1994). U.S. Patent No. 5,294,462. Washington, DC: U.S. Patent and Trademark Office.

25. Khan, A. A., De Jong, W., Jansens, P. J., & Spliethoff, H. (2009). Biomass combustion in fluidized bed boilers: potential problems and remedies. Fuel processing technology, 90(1), 21-50.
26. Kumar, S., Mudgal, D., Singh, S., & Prakash, S. (2013). Cyclic oxidation behavior of bare and Cr_3C_2-25 (NiCr) coated super alloy at elevated temperature. Adv. Mater. Lett, 4(10), 754-761.
27. Komai, N., Masuyama, F., & Igarashi, M. (2005). 10-Year Experience With T23 (2.25 Cr-1.6 W) and T122 (12Cr-0.4 Mo-2W) in a Power Boiler. Journal of pressure vessel technology, 127(2), 190-196.
28. Laverde, D., Gomez-Acebo, T., & Castro, F. (2004). Continuous and cyclic oxidation of T91 ferritic steel under steam. Corrosion Science, 46(3), 613-631.
29. Le Page, M. (2016). The great carbon scam, New Scientist, Vol 231(3092), Page 20-21.
30. Lofaj, F., & Kaganovskii, Y. S. (1995). Kinetics of WC-Co oxidation accompanied by swelling. Journal of materials science, 30(7), 1811-1817.
31. Luthra, K.L., Spacil,H.S., (1982). Impurity deposits in gas turbines from fuels containing sodium and vanadium. Journal of the Electrochemical Society, 129(3), 649-656.
32. Matthews, S., James, B., & Hyland, M. (2009). The role of microstructure in the high temperature oxidation mechanism of Cr_3C_2–NiCr composite coatings. Corrosion Science, 51(5), 1172-1180.
33. Masuyama, F. (2001). History of power plants and progress in heat resistant steels. ISIJ international, 41(6), 612-625.
34. Marantz, D. R., Marantz, D. R., & Kowalsky, K. A. (1995). U.S. Patent No. 5,442,153. Washington, DC: U.S. Patent and Trademark Office.
35. Michelsen, H. P., Frandsen, F., Dam-Johansen, K., & Larsen, O. H. (1998). Deposition and high temperature corrosion in a 10 MW straw fired boiler. Fuel Processing Technology, 54(1), 95-108.
36. Miller, P. D., Kravse, H. H., Vaughan, D. A., & Boyd, W. K. (1972). The mechanism in high temperature corrosion in municipal incinerators. Corrosion, 28(7), 274-282.
37. Mudgal, D., Singh, S., & Prakash, S.(2014). Hot Corrosion Behavior of Some Superalloys in a Simulated Incinerator Environment at 900° C. Journal of Materials Engineering & Performance, 23(1).

38. Mudgal, D., Singh, S., & Prakash, S. (2015). Hot Corrosion Behavior of Bare, Cr_3C_2-(NiCr) and Cr_3C_2-(NiCr)+ 0.2 wt.% Zr Coated SuperNi 718 at 900° C. Journal of Materials Engineering and Performance, 24(1), 1-15.
39. Montgomery M., Karlsson A., Larsen O.H., 2000. In situ corrosion experiments at various strawfired power plants in Denmark, Proceedings of the Eurocorr 2000, 10th 14th september 2000, Queen Mary westfield college university of london UK.
40. Nielsen,H. P.Frandsen, F. J., Dam-Johansen, K., & Baxter, L. L. (2000). The implications of chlorine-associated corrosion on the operation of biomass-fired boilers. Progress in energy and combustion science, 26(3), 283-298.
41. Oliveira, M. O., Inocencio, M. C., Ando Junior, O. H., & Bretas, A. S. (2012). Viability Study for Use of Rice Husk in Electricity Generation by Biomass. In International Conference of Renewable Energies and Power Quality, Santiago de Campostela, Spain. March 28th–30th.
42. Pettersson, J., Asteman, H., Svensson, J. E., & Johansson, L. G. (2005). KCl induced corrosion of a 304-type austenitic stainless steel at 600° C; the role of potassium. Oxidation of Metals, 64(1), 23-41.
43. Rapp, R. A. (2002). Hot corrosion of materials: a fluxing mechanism?. Corrosion science, 44(2), 209-221.
44. Riabkina-Fishman, M., Rabkin, E., Levin, P., Frage, N., Dariel, M. P., Weisheit, A., ... & Mordike, B. L. (2001). Laser produced functionally graded tungsten carbide coatings on M2 high-speed tool steel. Materials Science and Engineering: A, 302(1), 106-114.
45. Reichal H.H, 1988. Fireside corrosion in german fossil fuel fired power plants, Appearance, mechanism and causes, Werkstoffe and Korrosion, 39, p 54-63.
46. Richert, M. W., Wawrzyniak, S., & Grzelka, R. (2012). Journal of achievements in materials and manufacturing engg., 55(1), 108–112.
47. Radin, S. R., & Ducheyne, P. (1992). Plasma spraying induced changes of calcium phosphate ceramic characteristics and the effect onin vitro stability. Journal of materials science: Materials in medicine, 3(1), 33-42.
48. Sandberg, J., Karlsson, C., & Fdhila, R. B. (2011). A 7year long measurement period investigating the correlation of corrosion, deposit and fuel in a biomass fired circulated fluidized bed boiler. Applied Energy, 88(1), 99-110.

49. Saravanan, P., Selvarajan, V., Rao, D. S., Joshi, S. V., & Sundararajan, G. (2000). Influence of process variables on the quality of detonation gun sprayed alumina coatings. Surface and Coatings Technology, 123(1), 44-54.
50. Shao, Y., Wang, J., Preto, F., Zhu, J., & Xu, C. (2012). Ash deposition in biomass combustion or co-firing for power/heat generation. Energies, 5(12), 5171-5189.
51. Sidhu, T. S., Agrawal, R. D., & Prakash, S. (2005). Hot corrosion of some superalloys and role of high-velocity oxy-fuel spray coatings—a review. Surface and coatings technology, 198(1), 441-446
52. Skrifvars, B. J., Yrjas, P., Laurén, T., Kinni, J., Tran, H., & Hupa, M. (2005). The fouling behavior of rice husk ash in fluidized-bed combustion. 2. Pilot-scale and full-scale measurements. Energy & fuels, 19(4), 1512-1519.
53. Smith R.J.,Farr N.C.,Baker B.A., (2001) The corrosion resistance of high nickel based alloys in relation to waste incineratore applications, Proceedings of the Eurrcorr 2001, 30 sep-4 oct 2001, Rivadel garda, lake garda , Italy.
54. Spiegel M., Zahs A., Grabke H.J., (2000). Fundamental aspects of chlorine induced corrosion in power plants, Materials at high temperature, 2, p 153-159
55. Uusitalo, M. A., Vuoristo, P. M. J., & Mäntylä, T. A. (2003). High temperature corrosion of coatings and boiler steels in oxidizing chlorine-containing atmosphere. Materials Science and Engineering: A, 346(1), 168-177.
56. Viklund,P., Anders Hjornhede, Pamela Henderson, Annika Stalenheim, Rachel Pettersson, Superheater corrosion in a waste-to energy plant, presented on Impacts of fuel quality on Power Production & Environment, 2010.
57. Viswanathan, R., Coleman, K., & Rao, U. , 2006. Materials for ultra-supercritical coal-fired power plant boilers. International Journal of Pressure Vessels and Piping, 83(11), 778-783.
58. Viswanathan, R., & Bakker, W. (2001). Materials for ultra supercritical coal power plants Boiler materials: Part 1. Journal of Materials Engineering and Performance, 10(1), 81-95.
59. Viklund, R. Pettersson, A. Hjornhede, P. Henderson and P. Sjovall (2009). Effect of sulphur containing additive on initial corrosion of superheater tubes in waste fired boiler. Corrosion Engineering Science and Technology, 44(3), 234–240.
60. Yadav, J. P., & Singh, B. R. (2011). Study on Comparison of Boiler Efficiency Using Husk and Coal as Fuel in Rice Mill. *S-JPSET*, *2*, 1-15.

61. Yoon, S. J., Son, Y. I., Kim, Y. K., & Lee, J. G. (2012). Gasification and power generation characteristics of rice husk and rice husk pellet using a downdraft fixed-bed gasifier. Renewable Energy, 42, 163-167.

Web references

1.Combustion powder thermal spray process flame spray process, http://www.gordonengland.co.uk/cps.htm (Accessed on 10 July 2017).

2. Rotating Equipment Specialists Thermal and Plasma Flame and Arc Spray Coating, https://www.linkedin.com/pulse/rotating-equipment-specialiststhermal-plasma-flame-arc-raci-onelge (Accessed on 10 July 2014).

3. Thermal Spray and Multiphase Flow Laboratories, http://users.encs.concordia.ca/~dolat/Research-TS-Processes.html (Accessed on 10 July 2017).

4. Flame Spray, http://www.kondex.com/flamespray.html (Accessed on 10 July 2017).

5. High Velocity Oxy-fuel flame spray system, http://www.emcpl.in/HVOF.html (Accessed on 10 July 2017).

Appendix

1.Oxidation Process

(a) Weight change in Bare T91 substrate after every cyclic oxidation

WEIGHT OF SAMPLE: 12.044 g					
WEIGHT OF BOAT: 50.231					
WEIGHT OF SAMPLE + BOAT: 62.275					
Cycle	DATE	TIME IN	TIME OUT	WEIGHT (g)	COMMENT
1	30/3	5.13 PM	6:13pm	62.858	Formation of dark Reddish orange oxide with spots of green oxide
2	31/3	10:16am	11:16am	62.277	reddish orange oxide is formed
3	31/3	11:38am	12:38pm	62.276	reddish orange oxide is formed
4	31/3	12:50pm	1:50pm	62.274	reddish colour
5	31/3	2:01pm	3:01pm	62.275	Light grey & dark grey oxide, Reddish orange oxide is formed.
6	31/3	3:25pm	4:25pm	62.277	Spallation &sputtering is observed
7	31/3	4:50pm	5:50pm	62.275	Spallation &sputtering continuous
8	31/3	6:25pm	7:25pm	62.276	dark grey colour oxide with spallation &sputtering

9	1/4	8:44am	9:44pm	62.277	dark grey colour oxide & dark green oxide with increased in spallation
10	1/4	10:15am	11:15pm	62.277	dark grey colour oxide with spallation & green colour oxide
11	1/4	11:45am	12:45pm	62.279	Spallation &sputtering has increased
12	01-Apr	1:20pm	2:22pm	62.275	Dark grey and green colour oxide with increase in spallation and sputtering
13	01-Apr	3:00pm	4:00pm	62.276	Dark grey and green colour oxide with increase in spallation and sputtering
14	01-Apr	4:35pm	5:35pm	62.278	Dark grey and green colour oxide with increase in spallation and sputtering
15	01-Apr	6:00pm	7:00pm	62.279	Dark grey and green colour oxide with increase in spallation and sputtering
16	03-Apr	9:00am	10.00am	62.275	sputtering and spallation increased
17	03-Apr	10:25	11:25	62.277	sputtering and spallation increased
18	03-Apr	12:00	1:00	62.280	no more sputtering and spallation
19	03-Apr	1:35	2:35	62.280	no more sputtering and spallation
20	03-Apr	3:05	4:05	62.270	no more sputtering and spallation
21	03-Apr	4:32	5:32	62.275	no more sputtering and spallation
22	03-Apr	6:00	7:00	62.277	no more sputtering and spallation

23	03-Apr	7:35	8:35	62.278	no more sputtering and spallation
24	04-Apr	8:40am	9:40am	62.279	more sputtering and spallation
25	04-Apr	10:00	11:00	62.276	dark brown & grey colour oxide with more sputtering &spallation
26	04-Apr	11:30	12:30	62.275	dark brown & grey colour oxide with more sputtering &spallation
27	04-Apr	1:00	2:00	62.275	dark green oxide, some spots of grey colour oxide
28	04-Apr	2:25	3:25	62.276	grey colour oxide & green with more sputtering& colour spallation
29	04-Apr	4:00	5:00	62.274	grey colour oxide & green with more sputtering& colour spallation
30	04-Apr	5:30	06:30	62.276	grey colour oxide & green with more sputtering& colour spallation
31	04-Apr	7:00	8:00	62.277	grey colour oxide & green with more sputtering& colour spallation
32	05-Apr	09:00am	10:00am	62.277	grey colour oxide & green with more sputtering& colour spallation
33	05-Apr	10:30	11:30	62.278	grey colour oxide & green with more sputtering& colour spallation
34	05-Apr	12:00	1:00	62.279	grey colour oxide & green with more sputtering & colour spallation
35	05-Apr	1:30	2:30	62.279	grey colour oxide & green with more sputtering& colour spallation

36	05-Apr	3:00	4:00	62.279	grey colour oxide & green with more sputtering& colour spallation
37	05-Apr	4:30	5:30	62.279	grey colour oxide & green with more sputtering& colour spallation
38	05-Apr	6:00	7:00	62.279	grey colour oxide & green with more sputtering& colour spallation
39	06-Apr	8:25am	9:25am	62.276	grey colour oxide & green with more sputtering& colour spallation
40	06-Apr	9:55am	10:55	62.279	grey colour oxide & green with more sputtering& colour spallation
41	06-Apr	11:30	12:30	58.432	grey colour oxide & green with more sputtering& colour spallation
42	06-Apr	1:00	2:00	58.435	grey colour oxide & green with more sputtering& colour spallation
43	06-Apr	2:30	3:30	58.434	grey colour oxide & green with more sputtering& colour spallation
44	06-Apr	4:00	5:00	58.435	grey colour oxide & green with more sputtering& colour spallation
45	06-Apr	5:30	6:30	58.435	grey colour oxide & green with more sputtering& colour spallation
46	07-Apr	9:00am	10:00am	58.433	grey colour oxide & green with more sputtering& colour spallation
47	07-Apr	10:30	11:30	58.434	grey colour oxide & green with more sputtering& colour spallation

48	07-Apr	12:00	1:00	58.432	grey colour oxide & green with more sputtering& colour spallation
49	07-Apr	1:30	2:30	58.431	grey colour oxide & green with more sputtering& colour spallation
50	07-Apr	3:00	4:00	58.433	grey colour oxide & green with more sputtering& colour spallation

(b) Weight change of Cr_3C_2-NiCr T91 substrate after every cyclic oxidation					
WEIGHT OF SAMPLE: 13.168 g					
WEIGHT OF BOAT: 48.671					
WEIGHT OF SAMPLE + BOAT: 61.839					
Cycle	DATE	TIME IN	TIME OUT	WEIGHT (g)	COMMENT
1	30/3	5.13 PM	6:13pm	61.845	Formation of dark Reddish orange oxide with spots of green oxide
2	31/3	10:16am	11:16am	61.846	reddish orange oxide is formed
3	31/3	11:38am	12:38pm	61.848	reddish orange oxide is formed
4	31/3	12:50pm	1:50pm	61.847	reddish orange, grey brown colour oxide is formed ; spallation is also observed.
5	31/3	2:01pm	3:01pm	61.848	Light grey & dark grey oxide, Reddish orange oxide is formed. Spallation is also observed.

6	31/3	3:25pm	4:25pm	61.850	Spallation &sputtering is observed. Dark brown & grey colour oxide is observed.
7	31/3	4:50pm	5:50pm	61.848	dark grey colour oxide with spots of brown colour oxide. Spallation &sputtering continuous
8	31/3	6:25pm	7:25pm	61.844	dark grey colour oxide with spallation &sputtering
9	1/4	8:44am	9:44pm	61.847	dark grey colour oxide & dark green oxide with increased in spallation
10	1/4	10:15am	11:15pm	61.847	dark grey colour oxide with spallation & green colour oxide
11	1/4	11:45am	12:45pm	61.847	Spallation &sputtering has increased
12	01-Apr	1:20pm	2:22pm	61.847	increase in spallation and sputtering
13	01-Apr	3:00pm	4:00pm	61.845	spallation and sputtering
14	01-Apr	4:35pm	5:35pm	61.848	Dark grey and green colour oxide with increase in spallation and sputtering
15	01-Apr	6:00pm	7:00pm	61.849	Dark grey and green colour oxide with increase in spallation and sputtering
16	03-Apr	9:00am	10.00am	61.846	sputtering and spallation increased
17	03-Apr	10:25	11:25	61.848	sputtering and spallation increased
18	03-Apr	12:00	1:00	61.848	no more sputtering and spallation

19	03-Apr	1:35	2:35	61.848	no more sputtering and spallation
20	03-Apr	3:05	4:05	61.847	no more sputtering and spallation
21	03-Apr	4:32	5:32	61.848	no more sputtering and spallation
22	03-Apr	6:00	7:00	61.849	no more sputtering and spallation
23	03-Apr	7:35	8:35	61.848	no more sputtering and spallation
24	04-Apr	8:40am	9:40am	61.847	more sputtering and spallation
25	04-Apr	10:00	11:00	61.843	dark brown & grey colour oxide with more sputtering &spallation
26	04-Apr	11:30	12:30	61.842	dark brown & grey colour oxide with more sputtering &spallation
27	04-Apr	1:00	2:00	61.844	dark green oxide, some spots of grey colour oxide
28	04-Apr	2:25	3:25	61.846	grey colour oxide & green with more sputtering& colour spallation
29	04-Apr	4:00	5:00	61.845	grey colour oxide & green with more sputtering& colour spallation
30	04-Apr	5:30	06:30	61.846	grey colour oxide & green with more sputtering& colour spallation
31	04-Apr	7:00	8:00	61.848	grey colour oxide & green with more sputtering& colour spallation

32	05-Apr	09:00am	10:00am	61.847	grey colour oxide & green with more sputtering& colour spallation
33	05-Apr	10:30	11:30	61.847	grey colour oxide & green with more sputtering& colour spallation
34	05-Apr	12:00	1:00	61.848	grey colour oxide & green with more sputtering & colour spallation
35	05-Apr	1:30	2:30	61.848	grey colour oxide & green with more sputtering& colour spallation
36	05-Apr	3:00	4:00	61.849	grey colour oxide & green with more sputtering& colour spallation
37	05-Apr	4:30	5:30	61.849	grey colour oxide & green with more sputtering& colour spallation
38	05-Apr	6:00	7:00	61.849	grey colour oxide & green with more sputtering& colour spallation
39	06-Apr	8:25am	9:25am	61.846	grey colour oxide & green with more sputtering& colour spallation
40	06-Apr	9:55am	10:55	61.850	grey colour oxide & green with more sputtering& colour spallation
41	06-Apr	11:30	12:30	61.847	grey colour oxide & green with more sputtering& colour spallation
42	06-Apr	1:00	2:00	61.850	grey colour oxide & green with more sputtering& colour spallation
43	06-Apr	2:30	3:30	61.851	grey colour oxide & green with more sputtering& colour spallation

44	06-Apr	4:00	5:00	61.849	grey colour oxide & green with more sputtering& colour spallation
45	06-Apr	5:30	6:30	61.852	grey colour oxide & green with more sputtering& colour spallation
46	07-Apr	9:00am	10:00am	61.847	grey colour oxide & green with more sputtering& colour spallation
47	07-Apr	10:30	11:30	61.847	grey colour oxide & green with more sputtering& colour spallation
48	07-Apr	12:00	1:00	61.847	grey colour oxide & green with more sputtering& colour spallation
49	07-Apr	1:30	2:30	61.848	grey colour oxide & green with more sputtering& colour spallation
50	07-Apr	3:00	4:00	61.848	grey colour oxide & green with more sputtering& colour spallation

(c) Weight change in WC-Co coated T91 substrate after every cyclic oxidation

WEIGHT OF SAMPLE: 15.405 g					
WEIGHT OF BOAT: 42.180					
WEIGHT OF SAMPLE + BOAT: 57.584					
Cycle	DATE	TIME IN	TIME OUT	WEIGHT (g)	COMMENT
1	30/3	5.13 PM	6:13pm	57.855	Formation of dark Reddish orange oxide with spots of green oxide

2	31/3	10:16am	11:16am	57.952	reddish orange oxide is formed
3	31/3	11:38am	12:38pm	58.059	reddish orange oxide is formed
4	31/3	12:50pm	1:50pm	58.138	reddish colour
5	31/3	2:01pm	3:01pm	58.190	Light grey & dark grey oxide, Reddish orange oxide is formed.
6	31/3	3:25pm	4:25pm	58.172	Spallation &sputtering is observed
7	31/3	4:50pm	5:50pm	58.149	Spallation &sputtering continuous
8	31/3	6:25pm	7:25pm	58.137	dark grey colour oxide with spallation &sputtering
9	1/4	8:44am	9:44pm	58.144	dark grey colour oxide & dark green oxide with increased in spallation
10	1/4	10:15am	11:15pm	58.144	dark grey colour oxide with spallation & green colour oxide
11	1/4	11:45am	12:45pm	58.145	Spallation &sputtering has increased
12	01-Apr	1:20pm	2:22pm	58.143	Dark grey and green colour oxide with increase in spallation and sputtering
13	01-Apr	3:00pm	4:00pm	58.141	Dark grey and green colour oxide with increase in spallation and sputtering
14	01-Apr	4:35pm	5:35pm	58.144	Dark grey and green colour oxide with increase in spallation and sputtering

15	01-Apr	6:00pm	7:00pm	58.144	Dark grey and green colour oxide with increase in spallation and sputtering
16	03-Apr	9:00am	10.00am	58.136	sputtering and spallation increased
17	03-Apr	10:25	11:25	58.117	sputtering and spallation increased
18	03-Apr	12:00	1:00	58.119	no more sputtering and spallation
19	03-Apr	1:35	2:35	58.119	no more sputtering and spallation
20	03-Apr	3:05	4:05	58.118	no more sputtering and spallation
21	03-Apr	4:32	5:32	58.119	no more sputtering and spallation
22	03-Apr	6:00	7:00	58.109	no more sputtering and spallation
23	03-Apr	7:35	8:35	58.017	no more sputtering and spallation
24	04-Apr	8:40am	9:40am	58.018	more sputtering and spallation
25	04-Apr	10:00	11:00	58.016	dark brown & grey colour oxide with more sputtering &spallation
26	04-Apr	11:30	12:30	58.016	dark brown & grey colour oxide with more sputtering &spallation
27	04-Apr	1:00	2:00	58.005	dark green oxide, some spots of grey colour oxide
28	04-Apr	2:25	3:25	58.007	grey colour oxide & green with more sputtering& colour spallation

29	04-Apr	4:00	5:00	57.972	grey colour oxide & green with more sputtering& colour spallation
30	04-Apr	5:30	06:30	57.974	grey colour oxide & green with more sputtering& colour spallation
31	04-Apr	7:00	8:00	57.972	grey colour oxide & green with more sputtering& colour spallation
32	05-Apr	09:00am	10:00am	57.972	grey colour oxide & green with more sputtering& colour spallation
33	05-Apr	10:30	11:30	57.973	grey colour oxide & green with more sputtering& colour spallation
34	05-Apr	12:00	1:00	57.975	grey colour oxide & green with more sputtering & colour spallation
35	05-Apr	1:30	2:30	57.976	grey colour oxide & green with more sputtering& colour spallation
36	05-Apr	3:00	4:00	57.976	grey colour oxide & green with more sputtering& colour spallation
37	05-Apr	4:30	5:30	57.976	grey colour oxide & green with more sputtering& colour spallation
38	05-Apr	6:00	7:00	57.976	grey colour oxide & green with more sputtering& colour spallation
39	06-Apr	8:25am	9:25am	57.974	grey colour oxide & green with more sputtering& colour spallation
40	06-Apr	9:55am	10:55	57.976	grey colour oxide & green with more sputtering& colour spallation

41	06-Apr	11:30	12:30	57.973	grey colour oxide & green with more sputtering& colour spallation
42	06-Apr	1:00	2:00	57.979	grey colour oxide & green with more sputtering& colour spallation
43	06-Apr	2:30	3:30	57.976	grey colour oxide & green with more sputtering& colour spallation
44	06-Apr	4:00	5:00	57.977	grey colour oxide & green with more sputtering& colour spallation
45	06-Apr	5:30	6:30	57.978	grey colour oxide & green with more sputtering& colour spallation
46	07-Apr	9:00am	10:00am	57.976	grey colour oxide & green with more sputtering& colour spallation
47	07-Apr	10:30	11:30	57.976	grey colour oxide & green with more sputtering& colour spallation
48	07-Apr	12:00	1:00	57.975	grey colour oxide & green with more sputtering& colour spallation
49	07-Apr	1:30	2:30	57.976	grey colour oxide & green with more sputtering& colour spallation
50	07-Apr	3:00	4:00	57.978	grey colour oxide & green with more sputtering& colour spallation

2 HOT CORROSION

(a) Weight change of bare T91 substrate after every cyclic hot corrosion

WEIGHT OF SAMPLE: 12.044 g					
WEIGHT OF BOAT: 50.231					
WEIGHT OF SAMPLE + BOAT: 62.275					
Cycle	DATE	TIME IN	TIME OUT	WEIGHT (g)	COMMENT
1	10 Apr	3:37 PM	4:37pm	58.524	Formation of dark Reddish orange oxide with spots of green oxide
2	11 Apr	9:16am	10:16am	58.529	reddish orange oxide is formed
3	11 Apr	10:45am	11:45pm	58.535	reddish orange oxide is formed
4	11 Apr	12:20pm	1:20pm	58.541	reddish orange, grey brown colour oxide is formed ; spallation is also observed.
5	11 Apr	1:50pm	2:50pm	58.544	Light grey & dark grey oxide, Reddish orange oxide is formed. Spallation is also observed.
6	11 Apr	3:25pm	4:25pm	58.548	Spallation &sputtering is observed. Dark brown & grey colour oxide is observed.
7	11 Apr	4:50pm	5:50pm	58.549	dark grey colour oxide with spots of brown colour oxide. Spallation &sputteringcontinuous
8	11 Apr	6:25pm	7:25pm	58.553	dark grey colour oxide with spallation &sputtering
9	12 Apr	9:05am	10:05pm	58.555	dark grey colour oxide & dark green oxide with increased in spallation

10	12 Apr	10:30am	11:30pm	58.556	dark grey colour oxide with spallation & green colour oxide
11	12 Apr	12:00am	1:00pm	58.556	Spallation &sputtering has increased
12	12-Apr	1:30pm	2:30pm	58.556	Dark grey and green colour oxide with increase in spallation and sputtering
13	12-Apr	3:00pm	4:00pm	58.555	Dark grey and green colour oxide with increase in spallation and sputtering
14	12-Apr	4:35pm	5:35pm	58.557	Dark grey and green colour oxide with increase in spallation and sputtering
15	12-Apr	6:00pm	7:00pm	58.556	Dark grey and green colour oxide with increase in spallation and sputtering
16	13-Apr	9:00am	10.00am	58.556	sputtering and spallation increased
17	13-Apr	9:15	10:15	58.562	sputtering and spallation increased
18	13-Apr	10:45	11:45	58.562	no more sputtering and spallation
19	13-Apr	12:10	1:10	58.562	no more sputtering and spallation
20	13-Apr	1:45	2:45	58.563	no more sputtering and spallation
21	13-Apr	3:20	4:20	58.564	no more sputtering and spallation
22	13-Apr	4:45	5:45	58.561	no more sputtering and spallation
23	14-Apr	9:35	10:35	58.566	no more sputtering and spallation

24	14-Apr	11:00am	12:00am	58.564	more sputtering and spallation
25	14-Apr	12:30	1:30	58.565	dark brown & grey colour oxide with more sputtering &spallation
26	14-Apr	2:00	3:00	58.564	dark brown & grey colour oxide with more sputtering &spallation
27	14-Apr	3:30	4:30	58.558	dark green oxide, some spots of grey colour oxide
28	14-Apr	5:00	6:00	58.567	grey colour oxide & green with more sputtering& colour spallation
29	14-Apr	4:00	5:00	58.565	grey colour oxide & green with more sputtering& colour spallation
30	14-Apr	6:30	7:30	58.574	grey colour oxide & green with more sputtering& colour spallation
31	15-Apr	9:20	10:20	58.578	grey colour oxide & green with more sputtering& colour spallation
32	15-Apr	10:50am	11:50am	58.579	grey colour oxide & green with more sputtering& colour spallation
33	15-Apr	12:20	1:20	58.579	grey colour oxide & green with more sputtering& colour spallation
34	15-Apr	1:45	2:45	58.579	grey colour oxide & green with more sputtering & colour spallation
35	15-Apr	3:30	4:30	58.579	grey colour oxide & green with more sputtering& colour spallation

36	15-Apr	5:00	6:00	58.580	grey colour oxide & green with more sputtering& colour spallation
37	17-Apr	9:10	10:10	58.582	grey colour oxide & green with more sputtering& colour spallation
38	17-Apr	10:40	11:40	58.583	grey colour oxide & green with more sputtering& colour spallation
39	17-Apr	11:05am	1:05pm	58.584	grey colour oxide & green with more sputtering& colour spallation
40	17-Apr	1:30am	2:30	58.584	grey colour oxide & green with more sputtering& colour spallation
41	17-Apr	3:00	4:00	58.580	grey colour oxide & green with more sputtering& colour spallation
42	17-Apr	4:30	5:30	58.577	grey colour oxide & green with more sputtering& colour spallation
43	17-Apr	6:00	7:00	58.578	grey colour oxide & green with more sputtering& colour spallation
44	18-Apr	9:40	10:40	58.581	grey colour oxide & green with more sputtering& colour spallation
45	18-Apr	11:10	12:10	58.435	grey colour oxide & green with more sputtering& colour spallation
46	18-Apr	12:40am	1:40am	58.583	grey colour oxide & green with more sputtering& colour spallation
47	18-Apr	2:10	3:10	58.585	grey colour oxide & green with more sputtering& colour spallation

48	18-Apr	3:40	4:40	58.586	grey colour oxide & green with more sputtering& colour spallation
49	18-Apr	5:10	6:10	58.586	grey colour oxide & green with more sputtering& colour spallation
50	18-Apr	6:40	7:40	58.586	grey colour oxide & green with more sputtering& colour spallation

(b) Weight change ofCr_3C_2- NiCr substrate after every cyclic hot corrosion.

WEIGHT OF SAMPLE: 13.2806 g					
WEIGHT OF BOAT: 48.4107 g					
WEIGHT OF SAMPLE + BOAT: 61.691					
Cycle	DATE	TIME IN	TIME OUT	WEIGHT (g)	COMMENT
1	10 Apr	3:37 PM	4:37pm	61.713	Formation of dark Reddish orange oxide with spots of green oxide
2	11 Apr	9:16am	10:16am	61.711	reddish orange oxide is formed
3	11 Apr	10:45am	11:45pm	61.712	reddish orange oxide is formed
4	11 Apr	12:20pm	1:20pm	61.715	reddish orange, grey brown colour oxide is formed
5	11 Apr	1:50pm	2:50pm	61.713	Light grey & dark grey oxide, Reddish orange oxide is formed.

6	11 Apr	3:25pm	4:25pm	61.714	Dark brown & grey colour.
7	11 Apr	4:50pm	5:50pm	61.714	dark grey colour oxide with spots of brown colour oxide.
8	11 Apr	6:25pm	7:25pm	61.715	dark grey colour oxide with spallation &sputtering
9	12 Apr	9:05am	10:05pm	61.716	dark grey colour oxide
10	12 Apr	10:30am	11:30pm	61.716	dark grey colour oxide with spallation & green colour oxide
11	12 Apr	12:00am	1:00pm	61.714	Spallation &sputtering has increased
12	12-Apr	1:30pm	2:30pm	61.714	Dark grey and green colour oxide with increase in spallation and sputtering
13	12-Apr	3:00pm	4:00pm	61.714	Dark grey and green colour oxide with increase in spallation and sputtering
14	12-Apr	4:35pm	5:35pm	61.714	Dark grey and green colour oxide with increase in spallation and sputtering
15	12-Apr	6:00pm	7:00pm	61.714	Dark grey and green colour oxide with increase in spallation and sputtering
16	13-Apr	9:00am	10.00am	61.718	sputtering and spallation increased
17	13-Apr	9:15	10:15	61.718	sputtering and spallation increased
18	13-Apr	10:45	11:45	61.718	no more sputtering and spallation

19	13-Apr	12:10	1:10	61.717	no more sputtering and spallation
20	13-Apr	1:45	2:45	61.714	no more sputtering and spallation
21	13-Apr	3:20	4:20	64.714	no more sputtering and spallation
22	13-Apr	4:45	5:45	61.715	no more sputtering and spallation
23	14-Apr	9:35	10:35	61.716	no more sputtering and spallation
24	14-Apr	11:00am	12:00am	61.716	more sputtering and spallation
25	14-Apr	12:30	1:30	61.716	dark brown & grey colour oxide with more sputtering &spallation
26	14-Apr	2:00	3:00	61.716	dark brown & grey colour oxide with more sputtering &spallation
27	14-Apr	3:30	4:30	61.714	dark green oxide, some spots of grey colour oxide
28	14-Apr	5:00	6:00	61.719	grey colour oxide & green with more sputtering& colour spallation
29	14-Apr	4:00	5:00	61.718	grey colour oxide & green with more sputtering& colour spallation
30	14-Apr	6:30	7:30	61.719	grey colour oxide & green with more sputtering& colour spallation
31	15-Apr	9:20	10:20	61.722	grey colour oxide & green with more sputtering& colour spallation

32	15-Apr	10:50am	11:50am	61.773	grey colour oxide & green with more sputtering& colour spallation
33	15-Apr	12:20	1:20	61.774	grey colour oxide & green with more sputtering& colour spallation
34	15-Apr	1:45	2:45	61.776	grey colour oxide & green with more sputtering & colour spallation
35	15-Apr	3:30	4:30	61.776	grey colour oxide & green with more sputtering& colour spallation
36	15-Apr	5:00	6:00	61.776	grey colour oxide & green with more sputtering& colour spallation
37	17-Apr	9:10	10:10	61.774	grey colour oxide & green with more sputtering& colour spallation
38	17-Apr	10:40	11:40	61.775	grey colour oxide & green with more sputtering& colour spallation
39	17-Apr	11:05am	1:05pm	61.774	grey colour oxide & green with more sputtering& colour spallation
40	17-Apr	1:30am	2:30	61.775	grey colour oxide & green with more sputtering& colour spallation
41	17-Apr	3:00	4:00	61.775	grey colour oxide & green with more sputtering& colour spallation
42	17-Apr	4:30	5:30	61.772	grey colour oxide & green with more sputtering& colour spallation
43	17-Apr	6:00	7:00	61.773	grey colour oxide & green with more sputtering& colour spallation

44	18-Apr	9:40	10:40	61.769	grey colour oxide & green with more sputtering& colour spallation
45	18-Apr	11:10	12:10	61.764	grey colour oxide & green with more sputtering& colour spallation
46	18-Apr	12:40am	1:40am	61.764	grey colour oxide & green with more sputtering& colour spallation
47	18-Apr	2:10	3:10	61.766	grey colour oxide & green with more sputtering& colour spallation
48	18-Apr	3:40	4:40	61.766	grey colour oxide & green with more sputtering& colour spallation
49	18-Apr	5:10	6:10	61.765	grey colour oxide & green with more sputtering& colour spallation
50	18-Apr	6:40	7:40	61.765	grey colour oxide & green with more sputtering& colour spallation

(c) Weight change of WC-Co coated substrate after every cyclic hot corrosion

WEIGHT OF SAMPLE: 14.665 g					
WEIGHT OF BOAT: 48.670 g					
WEIGHT OF SAMPLE + BOAT: 63.335 g					
Cycle	DATE	TIME IN	TIME OUT	WEIGHT (g)	COMMENT
1	10 Apr	3:37 PM	4:37pm	63.395	Formation of dark Reddish orange oxide with spots of green oxide

2	11 Apr	9:16am	10:16am	63.402	reddish orange oxide is formed
3	11 Apr	10:45am	11:45pm	63.407	reddish orange oxide is formed
4	11 Apr	12:20pm	1:20pm	63.465	reddish orange, grey brown colour oxide is formed ; spallation is also observed.
5	11 Apr	1:50pm	2:50pm	63.509	Light grey & dark grey oxide, Reddish orange oxide is formed. Spallation is also observed.
6	11 Apr	3:25pm	4:25pm	63.592	Spallation &sputtering is observed. Dark brown & grey colour oxide is observed.
7	11 Apr	4:50pm	5:50pm	63.631	dark grey colour oxide with spots of brown colour oxide. Spallation &sputtering continuous
8	11 Apr	6:25pm	7:25pm	63.661	dark grey colour oxide with spallation &sputtering
9	12 Apr	9:05am	10:05pm	63.685	dark grey colour oxide & dark green oxide with increased in spallation
10	12 Apr	10:30am	11:30pm	63.701	dark grey colour oxide with spallation & green colour oxide
11	12 Apr	12:00am	1:00pm	63.704	Spallation &sputtering has increased
12	12-Apr	1:30pm	2:30pm	63.703	Dark grey and green colour oxide with increase in spallation and sputtering
13	12-Apr	3:00pm	4:00pm	63.705	Dark grey and green colour oxide with increase in spallation and sputtering

14	12-Apr	4:35pm	5:35pm	63.706	Dark grey and green colour oxide with increase in spallation and sputtering
15	12-Apr	6:00pm	7:00pm	63.716	Dark grey and green colour oxide with increase in spallation and sputtering
16	13-Apr	9:00am	10.00am	63.705	sputtering and spallation increased
17	13-Apr	9:15	10:15	63.718	sputtering and spallation increased
18	13-Apr	10:45	11:45	63.700	no more sputtering and spallation
19	13-Apr	12:10	1:10	63.616	no more sputtering and spallation
20	13-Apr	1:45	2:45	63.611	no more sputtering and spallation
21	13-Apr	3:20	4:20	63.607	no more sputtering and spallation
22	13-Apr	4:45	5:45	63.612	no more sputtering and spallation
23	14-Apr	9:35	10:35	63.617	no more sputtering and spallation
24	14-Apr	11:00am	12:00am	63.618	more sputtering and spallation
25	14-Apr	12:30	1:30	63.618	dark brown & grey colour oxide with more sputtering &spallation
26	14-Apr	2:00	3:00	63.220	dark brown & grey colour oxide with more sputtering &spallation
27	14-Apr	3:30	4:30	63.620	dark green oxide, some spots of grey colour oxide

28	14-Apr	5:00	6:00	63.625	grey colour oxide & green with more sputtering& colour spallation
29	14-Apr	4:00	5:00	63.226	grey colour oxide & green with more sputtering& colour spallation
30	14-Apr	6:30	7:30	63.641	grey colour oxide & green with more sputtering& colour spallation
31	15-Apr	9:20	10:20	63.642	grey colour oxide & green with more sputtering& colour spallation
32	15-Apr	10:50am	11:50am	63.643	grey colour oxide & green with more sputtering& colour spallation
33	15-Apr	12:20	1:20	63.643	grey colour oxide & green with more sputtering& colour spallation
34	15-Apr	1:45	2:45	63.635	grey colour oxide & green with more sputtering & colour spallation
35	15-Apr	3:30	4:30	63.636	grey colour oxide & green with more sputtering& colour spallation
36	15-Apr	5:00	6:00	63.637	grey colour oxide & green with more sputtering& colour spallation
37	17-Apr	9:10	10:10	63.639	grey colour oxide & green with more sputtering& colour spallation
38	17-Apr	10:40	11:40	63.640	grey colour oxide & green with more sputtering& colour spallation
39	17-Apr	11:05am	1:05pm	63.641	grey colour oxide & green with more sputtering& colour spallation

40	17-Apr	1:30am	2:30	63.641	grey colour oxide & green with more sputtering& colour spallation
41	17-Apr	3:00	4:00	63.640	grey colour oxide & green with more sputtering& colour spallation
42	17-Apr	4:30	5:30	63.636	grey colour oxide & green with more sputtering& colour spallation
43	17-Apr	6:00	7:00	63.637	grey colour oxide & green with more sputtering& colour spallation
44	18-Apr	9:40	10:40	63.621	grey colour oxide & green with more sputtering& colour spallation
45	18-Apr	11:10	12:10	63.619	grey colour oxide & green with more sputtering& colour spallation
46	18-Apr	12:40am	1:40am	63.618	grey colour oxide & green with more sputtering& colour spallation
47	18-Apr	2:10	3:10	63.620	grey colour oxide & green with more sputtering& colour spallation
48	18-Apr	3:40	4:40	63.625	grey colour oxide & green with more sputtering& colour spallation
49	18-Apr	5:10	6:10	63.626	grey colour oxide & green with more sputtering& colour spallation
50	18-Apr	6:40	7:40	63.626	grey colour oxide & green with more sputtering& colour spallation